Involvement of CFTR in Prostatitis and Prostate Cancer Development

XIE, Chen

A Thesis Submitted in Partial Fulfillment
Of the Requirements for the Degree of
Doctor of Philosophy
In
Physiology

The Chinese University of Hong Kong
September 2010

ProQuest LLC
789 East Eisenhower Parkway
P.O. Box 1346
Ann Arbor, MI 48106-1346

Thesis/Assessment Committee

Professor WH Yung (Chair)

Professor HC Chan (Thesis Supervisor)

Professor SB Yu (Committee Member)

Professor XY Guan (External Examiner)

This thesis is dedicated to my beloved grandmother and parents.

Everyday and every moment, I feel your forever love to me.

I love you forever !

本論文獻給我最愛的外婆和爸爸媽媽

每天每刻，我都能感受到您們無盡的愛

我永遠愛您們！

Acknowledgements

The last four years in Epithelial Cell Biology Research Center, The Chinese University of Hong Kong was an important period in my life. First I'd like to express my most sincere and deepest appreciation to my supervisor, Professor Chan Hsiao Chang for her inspiration, patience, generosity and love to me. I always feel so lucky that she gave me such a chance to study here. In my eyes, she is not only my best teacher but also like my beloved mother and true friend. I am especially grateful for her support to my wonderful study trip to Professor Jiang WenGuo lab in Cardiff University, UK.

My great appreciation goes to Dr. Jiang Xiao Hua for her helpful discussion and valuable suggestions in my study and spending her precious time and great patience in revision of my thesis.

It is also a pleasure to convey my gratitude to Professor Jiang WenGuo, Dr Andrew J and Dr Ye Lin in Metastasis and Angiogenesis Research Group, Department of Surgery, Cardiff University, UK for their guideness and help in the part of my study on clinical samples; Professor Lan HuiYao and Dr Huang XiaoRu in Department of Medicine and Therapeutics and Li Ka Shing Institute of Health Sciences, Chinese University of Hong Kong, HK for their help in ultrasound microbubble technique.

My special recognition goes to Miss Tsang Lai Ling and Mr. Chung Yiu Wa for their powerful technical supports and great helps in my studies. I would like to thank every member in ECBRC and my friends for their friendship and support during these years. I enjoyed so many happy hours with them. I am thankful to Chen Hui for giving her time and expertise proofreading my thesis draft.

Words fail me to express my special and deep gratitude to my beloved grandmother and my parents. Their love, support and understanding is warmly appreciated in my whole life. Last but not the least, I would like to give my deep thanks to my husband Mr Wang ZhiJun for his great love and care, advice and encouragement to me.

Abstract

The cystic fibrosis transmembrane conductance regulator (CFTR) is an anion channel conducting both Cl^- and HCO_3^-. It is expressed in epithelial cells of a wide variety of tissues. CFTR is also known to be expressed in human prostate, however, the physiological role of CFTR in the prostate and related diseases remains largely unknown This thesis explored the biological roles of CFTR in prostatitis and cancer development

In the first part of the study, the possible role and a bacterial killing mechanism involving CFTR-mediated bicarbonate secretion in prostatitis were investigated in a rat prostate model. CFTR was found to be expressed in the epithelium of rat ventral prostate Experiments using cultured rat primary prostate epithelial cells demonstrated that CFTR was involved in mediating bicarbonate extrusion across the prostate epithelium. The expression of CFTR and carbonic anhydrase II (CAII), a key enzyme involved in cellular HCO_3 production, along with several pro-inflammatory cytokines including IL-6, IL-1β, TNF-α, was significantly up-regulated in the primary culture of rat prostate epithelial cells upon *E coli*-LPS challenge. Inhibition of CFTR function *in vitro* or *in vivo* resulted in reduced bacterial killing by prostate epithelial cells or the prostate High HCO_3^- content (>50mM), rather than alkaline pH, was found to be responsible for bacterial killing. The direct action of HCO_3^- on bacterial killing was confirmed by its ability to suppress bacterial initiation factors in *E coli*. The relevance of the CFTR-mediated HCO_3^- secretion in human was demonstrated by the upregulated expression of CFTR and CAII in human prostatitis tissues. The present results have demonstrated that CFTR plays a previously undefined role in prostatitis and could be up-regulated during the inflammation in prostate as a host defense mechanism to increase bicarbonate

secretion for bacterial killing.

In the second part of the study, the possible role of CFTR in prostate cancer development and the underlying mechanisms were investigated. Our results showed that the expression of CFTR and CAII in prostate was remarkably decreased in aged rat prostate. We observed that testosterone could up-regulate the expression of CFTR and CAII *in vitro* and *in vivo*, indicating that the declined male hormones during aging may be responsible for the observed age-dependent expression of CFTR. In the present study, we found that inhibition of CFTR enhanced cell proliferation/anti-apoptosis in the prostate primary epithelial cells. CFTR was detected in all examined prostate cell lines, but with relatively higher expression levels in immortalized cell lines (PZ-HPV-7, PNT1A, PNT2C2) than in cancer cell lines (PC-3, DU-145, LNCaP). Immunohistological studies showed that the expression of CFTR was dramatically reduced in prostate cancer specimens as compared to that in normal prostate tissues. Furthermore, our gain and loss of function studies showed that knockdown of CFTR profoundly enhanced cell proliferation, cell adhesion, invasion and migration, while inhibited apoptosis in prostate cancer cell lines, overexpression of CFTR dramatically suppressed tumorigenic phenotype of cancer cells. Soft agar anchorage-independent growth assay showed that knockdown of CFTR in prostate cancer cells increased the number of colonies formed in soft agar. More importantly, we demonstrated that CFTR knockdown promoted the tumor growth *in vivo* and forced overexpression of CFTR in prostate cancer cells and ultrasound-mediated gene transfer of CFTR inhibited xenograft tumor growth *in vivo*. Mechanistically, multiple mechanisms were identified to contribute to the CFTR- mediated tumor suppressive effects. Firstly, CFTR chloride

channel function was implicated in the regulation of apoptosis in prostate cancer cells. Secondly, CFTR up-regulated the transcription level of miR-34a and miR-193b, both of which have been indicated as tumor suppressors in multiple cancers. Thirdly, 11 cancer-related genes were found to be up- or down-regulated by CFTR using PCR-array. These data demonstrated that CFTR may play an important role in prostate cancer development by acting as a tumor suppressor.

In summary, the present findings have demonstrated the important roles of CFTR in prostatitis and cancer development, which may provide new insight into the understanding of the prostate in health and disease. The present findings may also have potential application in diagnosis and prognosis of cancer.

中文摘要

囊性纖維變性跨膜電導調節器（CFTR）是一種轉運氯離子和碳酸氫根離子的陰離子通道，廣泛表達在機體不同組織的上皮細胞上。据報道人前列腺上也具有CFTR的表達，然而，CFTR在前列腺以及前列腺相關疾病的生理學意義並不清楚。本論文研究了CFTR在前列腺炎和前列腺癌發展中發揮的生物學作用。

實驗的第一部分用大鼠前列腺模型研究了CFTR在前列腺炎中發揮的作用及其介導的碳酸氫根離子分泌在前列腺炎中的殺菌機理。CFTR在培養的大鼠原代上皮細胞以及大鼠腹側前列腺上都有表達，並介導前列腺上皮細胞碳酸氫根離子的分泌。在大腸杆菌LPS的刺激下，大鼠前列腺上皮細胞上CFTR和碳酸酐酶II (CAII), 一種參與細胞內碳酸氫根产生的酶，以及多種炎性細胞因子包括IL-6, IL-1β, TNF-α的表達都有明顯上調。在體內體外實驗中抑制CFTR的功能可導致前列腺上皮細胞或前列腺的殺菌能力降低。高濃度碳酸氫根離子(>50mM) 本身，而不是鹼性pH具有殺菌能力。碳酸氫根離子是通過抑制大腸杆菌起始因子起到直接殺菌的作用。在人前列腺上CFTR介導的碳酸氫根離子分泌的作用通過CFTR和CAII在前列腺炎病人前列腺上表達的上調得到驗證。目前結果闡明了CFTR在前列腺炎中以前未曾闡明的作用以及它在前列腺炎中的上調從而引起碳酸氫根離子分泌的增加在宿主防禦中的殺菌機理。

實驗的第二部分研究了CFTR在前列腺癌發展中可能發揮的作用和機理。結果顯示CFTR和CAII在老齡老鼠的前列腺上表達明顯降低。在體內和體外實驗中，我們觀察到睾丸激素能够上調CFTR和CAII的表達，表明了隨著年齡的增加男性激素

的減少可能會導致觀察到的CFTR年齡依賴性表達。目前的實驗我們發現如果抑制大鼠前列腺上皮細胞CFTR的功能，細胞增殖/抗凋亡能力將會增加。CFTR在所檢測的幾株前列腺細胞上都有表達，但在前列腺正常永生細胞株 (PZ-HPV-7, PNT1A, PNT2C2) 的表達要比前列腺腫瘤細胞株 (PC-3, DU-145, LNCaP) 的表達高。免疫組化實驗表明前列癌病理標本中CFTR的表達要比正常前列腺組織有明顯降低。進一步通過对腫瘤細胞CFTR功能獲得或丢失，顯示在前列腺腫瘤細胞株上敲減CFTR可以顯著增加細胞增殖，粘附，侵襲和遷移能力並抑制細胞凋亡。而超表達CFTR可以顯著抑制腫瘤細胞致瘤性的表型。軟膠（soft agar）非錨定生長實驗表明在前列腺腫瘤細胞株上敲減CFTR可以增加細胞在軟膠上克隆形成的數量。更重要的是，我們證明了敲減CFTR可以促進體內腫瘤的生長，而超表達CFTR以及利用超聲介導CFTR基因的轉入可以抑制體內腫瘤的生長。機理研究表明，CFTR介導的腫瘤抑制作用是通過多種機理途徑完成的。首先，CFTR作爲氯離子通道參與調節前列腺腫瘤細胞的調亡。其次，CFTR可以上調miR-34a和 miR-193b轉錄水平的表達，這兩種miRNAs在多種腫瘤中可以作爲抑癌基因。第三，利用PCR array的方法，CFTR可以上調或下調11個与腫瘤相關的基因。以上結果表明了CFTR作爲抑癌基因在前列腺癌發展過程中發揮重要作用。

綜上所述，本論文的發現證明了CFTR在前列腺炎和前列腺癌上的重要作用，对理解CFTR在前列腺健康和疾病中的作用提供了新的認識。同時目前的發現对癌症診斷和預後也提供了潛在應用。

List of Publications

1. **XIE C** [#], JIANG XH[#], SUN TT, ZHANG JT, SANDERS AJ, DIAO RY, TSANG LL, YU MK, FOK KL, ZHANG XH, CHUNG YW, YE L, ZHAO MY, DONG JD, GUO JH, XIAO ZJ, LAN HY, NG CF,CAI ZM, JIANG WG*, CHAN HC*. CFTR as a tumor suppressor and prognostic predictor. *(Submitted to Nature).* [#]Co-first author publication *Co- correspondence author

2. **XIE C**, TANG XX, XU WM, DIAO RY, CAI ZM, CHAN HC. A host defense mechanism involving CFTR-mediated bicarbonate secretion in prostatitis. *(Submitted to PLos One)*

3. **XIE C**, WANG XF, QI XJ, LU LL, CHAN HC. Effect of Huoxiang-zhengqi liquid on HCO3- secretion by intact porcine distal airway epithelium. *Acta Physiologica Sinica,* February 25, 2008, 60 (1): 90-96

4. CHAN HC, RUAN YC, HE Q, CHEN MH, CHEN H, XU WM, CHEN WY, **XIE C**, Zhang XH, Zhou Z. The cystic fibrosis transmembrane conductance regulator in reproductive health and disease. *J Physiol.* 2009 May 15; 587(Pt 10):2187-95. Epub 2008 Nov 17. Review.

Conference Abstract

1. **XIE C**, CHAN HC. The age-dependent expression of CFTR and carbonic anhydrase II in rat prostate. International symposium on frontiers in life sciences:From basic research to translational medicine. *Cell Biol Int* (2008) S46
2. **XIE C**, LU LL, ZANG CB, WANG XF, CHAN HC. Huoxiang-Zhengqi liquid stimuliates cAMP-independent HCO_3^- secretion in porcine distal airway epithelium. International symposium on frontiers in life sciences:From basic research to translational medicine. *Cell Biol Int* (2008) S46
3. **XIE C**, CHAN HC. The expression of CFTR and SLC26A6 in cultured prostate epithelial cells of rats and their involvement of pH regulation. Physiology 2008, Proc Physiol, Soc 11 PC160

Declaration

I hereby declare that this thesis represents my own work, except where due acknowledgement is made, and that it has not been previously included in a thesis, dissertation or report submitted to this University or to any other institution for a degree, diploma or other qualification.

Signature

XIE Chen

List of Figures

List of Tables

List of Abbreviations

ABC	ATP-binding cassette
APS	Ammonium persulfate
bp	base pair
BSA	Bovine serum albumin
$CaCl_2$	calcium Chloride
CAII	Carbonic Anhydrase II
cAMP	Adenosine-3',5'-cyclicmonophosphate
CF	cystic fibrosis
CFTR	Cystic Fibrosis Transmembrane Conductance Regulator
C.F.U	colony-forming unit
CO_2	Carbon Dioxide
DAPI	4',6-diamidino-2-phenylindole
DEPC	Diethyl pyrocarbonate
dH_2O	Deionized water
DNA	Deoxyribonucleoic acid
DNase	Deoxyribonuclease
dNTPs	Deoxynucleoside triphosphate
DTT	DL-Dithiothreitol
ECM	extracellular matrix
ECL	Chemiluminescence
EDTA	Ethylene-diamine-tetraacetic acid
E. coli	*Escherichia coli*
EPS	Expressed prostate secretion
FACS	Flow analyisis cytometry system
FBS	Fetal Bovin Serum
FITC	Fluorescein-5-isothiocyanate
G1/S	Checkpoint between G1 (Gap 1) phase and S (DNA synthesis) phase in a cell cycle
G2/M	Checkpoint between G2 (Gap 2) phase and M (mitosis) phase in a cell cycle
G418	Geneticin
H&E	Hemotoxylin and Eosin
HCl	Hydrochloric acid
hr	hour
HRP	Horse-radish peroxidase-linked antibody
IgG	Immunoglobin G
IL	Interleukins
Kb	Kilobase-pair
LPS	lipopolysaccharide

min	minute
miRNA	micro RNA
M-MLV	Moloney Murine Leukemia Virus
MTS	3-(4,5-dimethylthiazol-2-yl)-5-(3-carboxymethoxyphenyl)-2- (4-sulfophenyl)-2H-tetrazolium)
NP40	Nonidet-P40
PBS	Phosphate buffer saline
PCNA	Proliferating Cell Nuclear Antigen
PCR	Polymerase Chain Reaction
PMSF	Phenylmethylsulfonyl fluoride
PAGE	Poly-acrylamide gel electrophoresis
P/S	penicillin/streptomycin
PSA	Prostate specific antigen
RIPA	Radioimmunoprepicitation
RNA	Ribonucleic acid
rpm	rotation per minute
RT-QPCR	Reverse transcription quantitative polymerase chain reaction
RIPA	Radioimmunoprecipitation Assay
SDS-PAGE	Sodium dodecyl suphate – polyacrylamide gel electrophoresis
sAC	Soluble Adenylyl Cyclase
TBS	Tris- buffered saline
TBST	Tris-buffered saline Tween
TEMED	Tetramethylethylenediamine
TNF-α	Tumor Necrosis Factor alpha
Tris-HCl	2-amino-2-(hydroxymethyl) propane-1, 3-diol-hydrochloroic acid
uPA	urokinase plasminogen activator
UV	Ultra Violet
SEM	standard error of the mean

Chapter 1
Introduction

1. 1 Structure and functions of the prostate

1. 1.1 Structure and functions of the human prostate

The prostate is a small, but important organ (or gland) found only in the male reproductive system. It lies below the bladder in front of the rectum. In general, the developed prostate could be divided into the peripheral, central and transitional zones (McNeal JE, 1981) (Figure 1.1). The peripheral zone represents about 70% of the prostate in volume and is the most common site of prostatic intraepithelial neoplasia (PIN) and carcinoma. The central zone comprises about 25% of the volume of the prostate. The ratio of epithelium to stroma is higher in the central zone than the rest of the prostate. The transitional zone represents the smallest region in the whole prostate gland-about 5% in volume. With the increasing age, the transitional zones increase in size due to benign prostatic hyperplasia (BPH) whilst the central zone atrophies and the peripheral zone remains static. (Grant M. Baxter).

The prostate is an exocrine gland which secrete through ducts to the outside of the body. The main function of the prostate is to store and secrete slightly acidic fluid (pH 6.2-6.6) that constitutes 30% of the volume of the seminal fluid (Blacklock NJ, 1974). The prostate also contains some smooth muscles that help expel semen during ejaculation. The gland is also responsible for liquefying sperm immediately after ejaculation by prostate specific antigen (PSA). In addition, the prostate also plays a role

in controlling the flow of urine. Acute urinary retention is one of the long-term outcomes resulting from BPH.

1.1.2 Features of the rat prostate

It is necessary to describe a few features of the rat prostate here as a background since the rat is the most often used animal model in the study of prostate physiology. Generally, the rat prostate is divided into ventral, dorsal, lateral and anterior lobes (Figure 1.2). In our present study, we used the rat ventral prostate lobe since this lobe is representative of the entire prostate gland. The ventral prostate is known to be the most androgen-dependent part of the prostate gland in rodents, so the lobe is generally used to elucidate how hormone such as testosterone or estrogen influence prostate proliferation and cell death (Kurita T, 2001). Of note, the apoptotic cell death is specific to the ventral lobe in prostate after castration (Banerjee PP, 1995). Except for the structure, the functional roles and the underlying mechanisms of rat prostate are similar to that in humans.

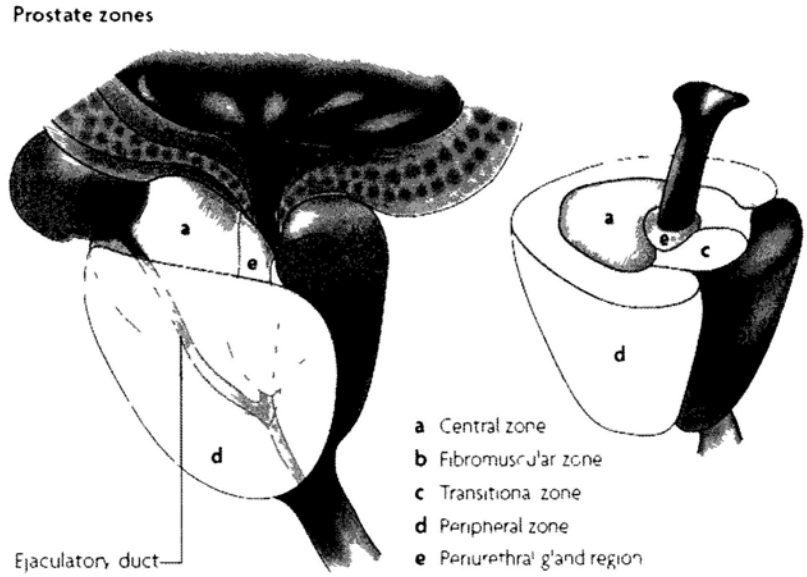

Figure 1.1 Anatomical depiction of the zonal anatomy of the human prostate gland. *(Adopted from De Marzo AM, 2007)*

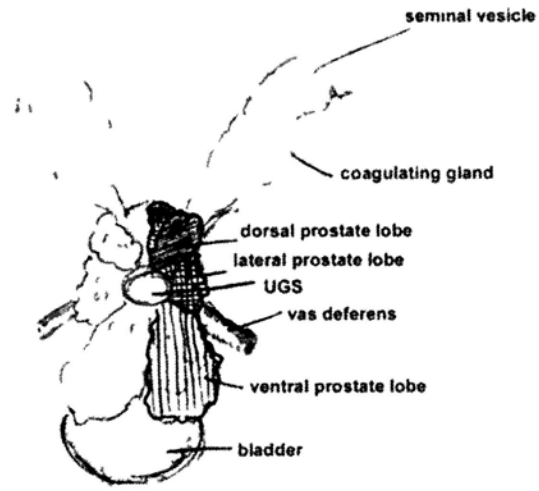

Figure 1.2 Diagram of rat prostate. *(Drawing by Oliver Putz, University of Illinois at Chicago)*

1.1.3 Compartments of Prostate

The prostate epithelium in the prostate is composed mainly of two major cell types, the epithelial cells and stromal cells. The interaction between these two cells plays an important role in maintaining the homeostasis of the normal prostate.

1.1.3.1 Epithelial compartment

The prostate epithelial compartment consists of luminal secretory epithelial cells, basal epithelial cells, neuroendocrine cells, stem cell and transit-amplifying cells.

Luminal secretory cells are the most common cell types in the prostate epithelium. They are terminally differentiated and have a low proliferative index. They express cytokeratins 8 and 18 as well as high level of androgen receptor (AR) (Wernert N, 1987). The growth and survival of these cells are androgen dependent. Interspaced among these secretory epithelial cells are neuroendocrine cells and transit-amplifying cells. In comparison to the secretory epithelial cells, the basal cells are the main proliferating population. They express a distinct cytokeratins 5, 14 and 15 (Xue Y, 1998) and they are origins of various disease process and target of neoplastic agents. In prostate, the basal cells are the likely source of the epithelial stem cells (Foster CS, 2002).

1.1.3.2 Stromal cells

The noncellular stroma and connective tissue of the prostate make up what is termed the ground substance and the extracellular matrix. Smooth muscle cells, fibroblasts and endothelial are basic cell types which make up the stromal compartment of the prostate, all embedded within an extracellular matrix. Many peptide growth factors in the prostate are synthesized by the smooth muscle cells, some of which have been implicated in the

regulation of the growth and differentiation of the prostate epithelial cells. (Wong YC, 2000).

The smooth muscle cells and the fibroblasts are in close approximation to the basement membrane (BM). The BM is composed of laminins, collagen type V and IV and other molecules. The layer forms an interface to the stomal compartment that provides structural support for the secretory epithelium, basal cells, stem cells and transit-amplifying cells. It consists of an extracellular matrix, ground substance and a variety of stromal cells.

1.1.4 Prostate secretion

The prostate secretes various substances including PSA, prostatic acid phosphatase (PAP), citrate acid and zinc etc. The prostate has the highest concentration of citrate of any tissue in the human body. The relationship between prostatic inflammatory disease and citric acid has been investigated. (Chen J, 2007). Zinc is also found in the prostate at high concentrations. Zinc levels are elevated or stable in BPH, whereas there is a marked decrease in zinc content associated with prostate adenocarcinoma. The important role for zinc in prostate secretion has been studied which suggest the direct role of zinc as a prostatic antibacterial factor (Fair WRl, 1976). Human PSA has been proved to be a clinically important marker for diagnosis and prognosis of prostate cancer; however PSA is an organ-specific but not a cancer-specific marker. The elevated PSA levels could be found in benign prostatic hyperplasia (BPH) and prostatitis patients (Stamey TA, 1987). A limitation of PSA as a tumor marker is demonstrated in the substantial overlap in

values between benign and malignant prostate diseases (Partin AW, 1990). The acid phosphatase activity is more than 200 times in the prostate than in any other tissues and is the source of the high levels of acid phosphatase in ejaculation. The biologic function of this enzyme in the prostate remains largely unclear.

1.1.5 Control of prostate growth by endocrine and paracrine pathways

1.1.5.1 Endocrine control of prostate growth

Like other sex accessory tissues, the prostate is stimulated for its growth, maintenance and secretory function by certain hormones and growth factors. The major androgen in the serum of human is testosterone, which is synthesized in the Leydig cells of the testis. The testosterone is converted within the prostate into the more active androgen dihydrotestosterone (DHT) by 5α-reductase or converted into estrogens by aromatase. Both processes are irreversible. Testosterone appears to function as a prohormone in that the most active form of the androgen in the prostate is not testosterone but rather DHT (Bruchovsky N, 1968) which is 1.5 to 2.5 times more active than testosterone. DHT or testosterone bind to androgen receptors in the cytoplasma and activated the receptors to regulate a variety of cellular processes and it is the major androgen regulating the cellular events of growth, differentiation and other biological function in the prostate.

In the plasma of young human males, estrogens are derived from the peripheral conversion of androstenedione and testosterone to estrone and estradiol through the aromatase reaction. Up to 75% to 90% of the estrogen is derived in this fashion. The fact

that the age-related decrease in the plasma free testosterone level whiles the free estradiol level is maintained produces about 40% increase in the ratio of free estradiol/free testosterone. Estrogen is known to have two opposite effects on prostate growth, one is positive and the other one is negative. The physiologic levels of estrogens do not block androgen-induced growth of the prostate cells but rather synergize androgen effect and the latter result comes from the inhibition of LH secretion. Nevertheless, how estrogen exerts its various effects on prostatic growth remains to be further clarified.

1.1.5.2 Paracrine control of prostate growth

Stroma cells in the prostate could produce different kinds of growth factors and regulatory peptide such as KGF, EGF, TGF-β, IGF-1, which have been suggested to play an important role in stromal-epithelial interactions. These growth factors have been implicated in the regulation of the growth and differentiation of the prostate.

1.1.6 Prostate related diseases

There are three main prostate related diseases including benign prostate hyperplasia (BPH), prostatitis and prostate cancer. BPH is the non-cancerous enlargement of the prostate gland in middle-aged and elderly men. If the prostate becomes enlarged, it can place pressure on the bladder and urethra which would cause symptoms that affect urination. Prostatitis is referring to the inflammation or infection of the prostate gland. Prostate cancer is the second leading cause of cancer death in men, exceeded only by

lung cancer. In this study, we focused on two major diseases of prostate, namely prostatitis and prostate cancer.

1.2 Prostatitis

Prostatitis is defined as an increased number of inflammatory cells within the prostatic parenchyma (Figure 1.3). The most common pattern of inflammation is a lymphocytic infiltration in the stroma immediately adjacent to the prostatic acini (Kohnen PW, 1979). Prostatitis is the most common urologic diagnosis in men younger than 50 years and the third most common urologic diagnosis in men older than 50 years (McNaughton-Collins M, 1998). Prostatitis affects men of all ages, unlike BPH and prostate cancer, which are predominant diseases of older men.

1.2.1 Classification of prostatitis syndromes

Category I: Acute Bacterial Prostatitis

Acute bacterial prostatitis is an acute bacterial infection of the prostate gland which is a generalized infection of the prostate. Approximately 5% of patients with acute bacterial prostatitis may progress to chronic bacterial prostatitis.

Category II: Chronic bacterial prostatitis

Chronic bacterial prostatitis is a recurrent infection of the prostate which is associated with recurrent lower UTIs (i.e., cystitis). The prevalence of bacterial prostatitis ranges from 5% to 15% of prostatitis cases.

Category III: Chronic nonbacterial Prostatitis/Chronic Pelvic Pain Syndrome (CP/CPPS)

Chronic nonbacterial Prostatitis/Chronic Pelvic Pain Syndrome (CP/CPPS), accounting for 90%-95% of prostatitis diagnoses when there is no demonstrable infection.

IIIA CPPS: inflammatory

IIIB CPPS: non-inflammatory

Category IV: Asymptomatic inflammatory prostatitis

Asymptomatic inflammatory prostatitis when there are no subjective symptoms, but leukocytosis is found in the prostate secretions. The patients present with BPH, an elevated PSA level, prostate cancer, or infertility.

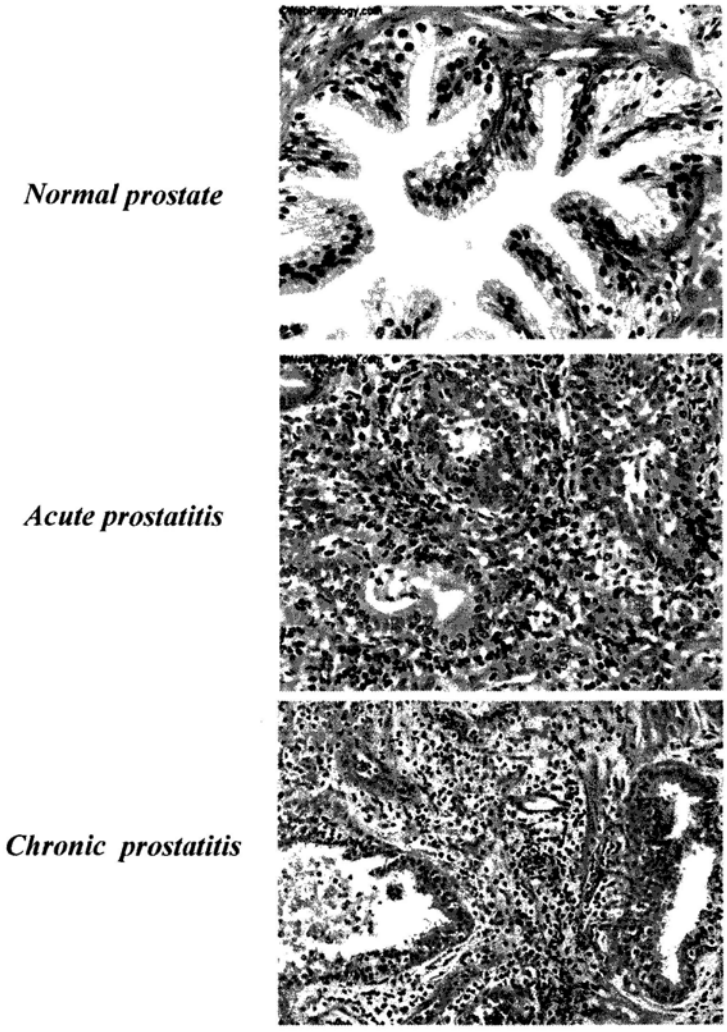

Figure 1.3 H&E staining for prostatitis. *(Adopted from Nickel JC, 2003)*

1.2.2 Causes of prostatic inflammation

1.2.2.1 Infectious agents

1.2.2.1.1 Gram-Negative and Gram-Positive bacteria

A wide range of pathogenic organisms have been observed to induce an inflammatory response in the prostate. The most common cause of bacterial prostatitis is gram-negative bacteria such as *Escherichia coli* (*E.coli*), which is responsible for approximately 50% to 80% of infection cases in human (Mitsumori K, 1999). *Pseudomonas aeruginosa, Klebsiella* species, *Serratia* species, and *Enterobacter aerogenes* are identified in a further 10% to 15%. Among the gram-positive bacteria, *Enterococci* are believed to account for 5% to 10% of documented prostate infections.

1.2.2.1.2 Other microbiologic and viruses infections

Anaerobic bacteria, corynebacterium infection, chlamydia infection, ureaplasma infection and other microorganisms are also responsible for some cases of the 'nonbacterial' form. Viruses such as human papillomavirus (HPV), human herpes simplex virus type 2 (HSV2), cytomegalovirus (CMV) and human herpes virus type 8 (HHV8) can also infect the prostate (De Marzo AM, 2007).

1.2.2.2 Altered composition of prostate secretion

Secretory dysfunction of the prostate characterized by an alteration in the composition of prostatic secretions can be diagnostic of patients with prostatitis. In prostatitis, the levels of fructose; citric acid; acid phosphatase; the cations zinc, calcium and magnesium; and the zinc-containing prostatic antibacterial factor are decreased,

whereas pH, inflammatory proteins such as ceruloplasmin are increased (Anderson RU, 1976). Normal human prostatic secretions are remarkably rich in citrate, which is considered the most useful marker for determining prostate secretory function. The alterations in the prostate secretory function will impair the normal antibacterial capacity. It is not known whether these compositional changes are a cause or a consequence of inflammation.

1.2.2.3 Other possible causes of prostate inflammation

Hormonal alterations, dysfunctional voiding, intraprostatic ductal reflux, immunologic alterations, chemically induced inflammation, neural dysregulation, interstitial cystitis-like cause, psychological cause and dietary factors have been postulated as the possible causes involved in the pathogenesis of chronic bacterial and nonbacterial prostatic inflammation (Figure 1.4).

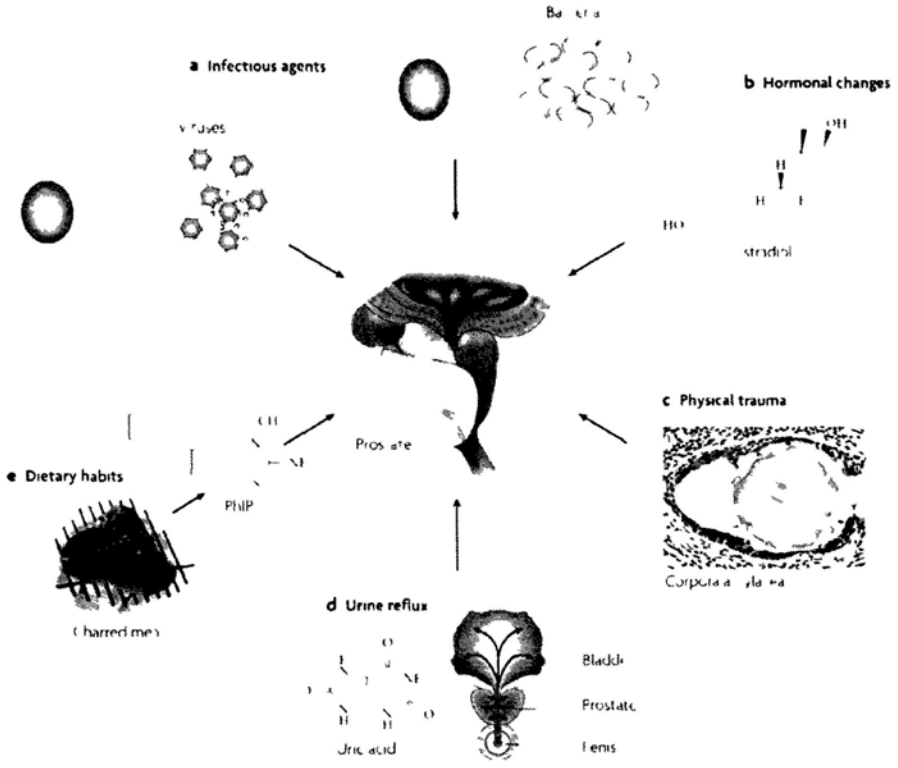

Figure 1.4 Possible causes of prostate inflammation. a | Infection. Chronic bacterial prostatitis is a rare recurring infection in which pathogenic bacteria are cultured from prostatic fluid. Viruses, fungi, mycobacteria and parasites can also infect the prostate and incite inflammation. The figure represents two prostate cells infected either by bacteria or viruses. **b** | Hormones. Hormonal alterations such as oestrogen exposure at crucial developmental junctures can result in architectural alterations in the prostate that produce an inflammatory response. **c** | Physical trauma. Corpora amylacea can traumatize the prostate on a microscopic level. The figure shows a corpora within a prostatic acinus in which its edges appear to be eroding the epithelium, resulting in an increase in expression of the stress enzyme cyclooxygenase 2 (PTGS2). **d** | Urine reflux. Urine that travels up back towards the bladder ('retrograde' movement) can penetrate the ducts and acini of the prostate. Some compounds, such as crystalline uric acid, can directly activate innate inflammatory cells. Although these compounds would not be expected to traverse the prostate epithelium, if the epithelium was already damaged this would facilitate the leakage of these compounds into the stromal space where they would readily activate inflammatory cells. **e** | Dietary habits. Ingested carcinogens (for example 2-amino-1-methyl-6-phenylimidazo[4,5-b]pyridine (PhIP), which derives from charred meat) can reach the prostate through the bloodstream or by urine reflux and cause DNA damage and mutations, and result in an influx of inflammatory cells.
(Adopted from De Marzo AM, 2007)

1.2.3 The association of prostatitis with pH increase and possible reasons behind

It was shown that in humans, normal human prostatic fluid has a pH value between 6.2-6.6, the pH would increase in inflammation which often rises to above 8.0. The pH change appears to accompany with the inflammatory response of the prostate whether this be bacterial or not (Pfau A, 1978; Blacklock NJ, 1974; Weidner W, 1992; White MA, 1975), however, the pH of expressed prostate secretion (EPS) in bacterial prostatitis is significantly higher than the nonbacterial prostatitis (Chandiok S, 1992). The pH varies according to the intensity of the inflammation reaction and in general the greater this reaction, the more elevated the pH (White MA, 1975).

Under the circumstances of inflammation, the secretory function of the prostate is impaired to different degrees and the level of citric acid, which is thought to maintain the osmotic pressure and pH of the prostate fluid, has been reported to decrease correspondingly (Chen J, 2007). However, whether the increase in pH of the expressed prostatic secretion seen with bacterial infection is simply due to a decrease in the relative level of citric acid is not clear.

1.2.4 The diagnostic and therapeutic implications of the characteristic pH increase in prostatitis

Prostate epithelium appears to be a barrier to the passage of antibiotics and antibacterial agents from the plasma to the prostatic fluid. Antibiotics therapy is the most commonly prescribed for the prostatitis syndromes. The diffusion of an antibiotic into the prostate site of inflammation is an important factor in determining its effectiveness in

treatment (Heinert G, 1993). In general, the pH of fluid in the prostate acini and ducts was lower than in the plasma. In order to diffuse into the site of prostatic infection, an antibiotic must nonionized in plasma and be able to ionize in the relatively acidic environment of the prostatic fluid (Bjerklund Johansen TE, 1998). However, it was shown that in inflammation, whether this is of bacterial origin or not, the pH of the prostate fluid would be higher than plasma (White MA, 1975). The increased alkalinity of the pH of expressed prostatic secretions is one of the reasons for poor results of antibiotic therapy (Weidner W, 1992). The pH of the prostatic fluid is not only significant to the antibiotic concentration in the prostate but also is important for its influence on the biological activity of the antibiotic; slight variation in pH may considerably alter its therapeutic effect.

The pH of expressed prostate secretion (EPS) could both serve as an indicator for diagnosis of the presence of prostatitis and have significance in antibiotic treatment of prostatitis.

1.3 Prostate cancer

1.3.1 Risk factors for prostate cancer

For men in the United States, the incidence of prostate cancer has recently undergone dramatic changes. The strongest risk factors for prostate cancer are age, race and family history, among which age is the most significant risk factor for prostate cancer development. It has been reported that about 85% of prostate cancer patients are diagnosed at the age of 65 (Boyle, P, 1996). The African American men have the highest

incidence of prostate cancer in the world, while the lowest is found in Japanese and Chinese. Studies on the familial linkage in prostate cancer revealed that the risk for the cancer elevated in brothers or sons of prostate cancer patient (Narod, SA, 1995). Hormone profiles and diet are other potential risk factors.

1.3.2 Pathology of prostate neoplasia

1.3.2.1 Prostatic intraepithelial neoplasia

Prostatic intraepithelial neoplasia (PIN) is a premalignant proliferation arising within the prostate. It is a collection of irregular, atypical epithelial cells and is classified into low grade and high grade. The architecture of the glands and ducts remains normal. The epithelial cells proliferate and crowd, resulting in a pseudo-multilayer appearance. It tends to occur in the peripheral zone of the prostate. In prostate cancer, the abnormal cells spread beyond the boundaries of the acinus and form clusters without basal cells. In PIN, the basal cell layer is disrupted but present. The high-grade PIN is a precursor to some prostate carcinomas.

1.3.2.2 Prostate adenocarinoma

There are numerous grading systems to evaluate the prostatic adenocarcinoma, among which Gleason grading system is the most widely accepted. The Gleason system is based on the glandular pattern of the tumor. The tumor patterns were divided into grade 1 to 5, with 1 being the most differentiated and 5 being the least differentiated (Figure 1.5). It is important to recognize Gleason pattern 4 tumor because tumors with this pattern have a significantly worse prognosis than those with pure Gleason pattern 3.

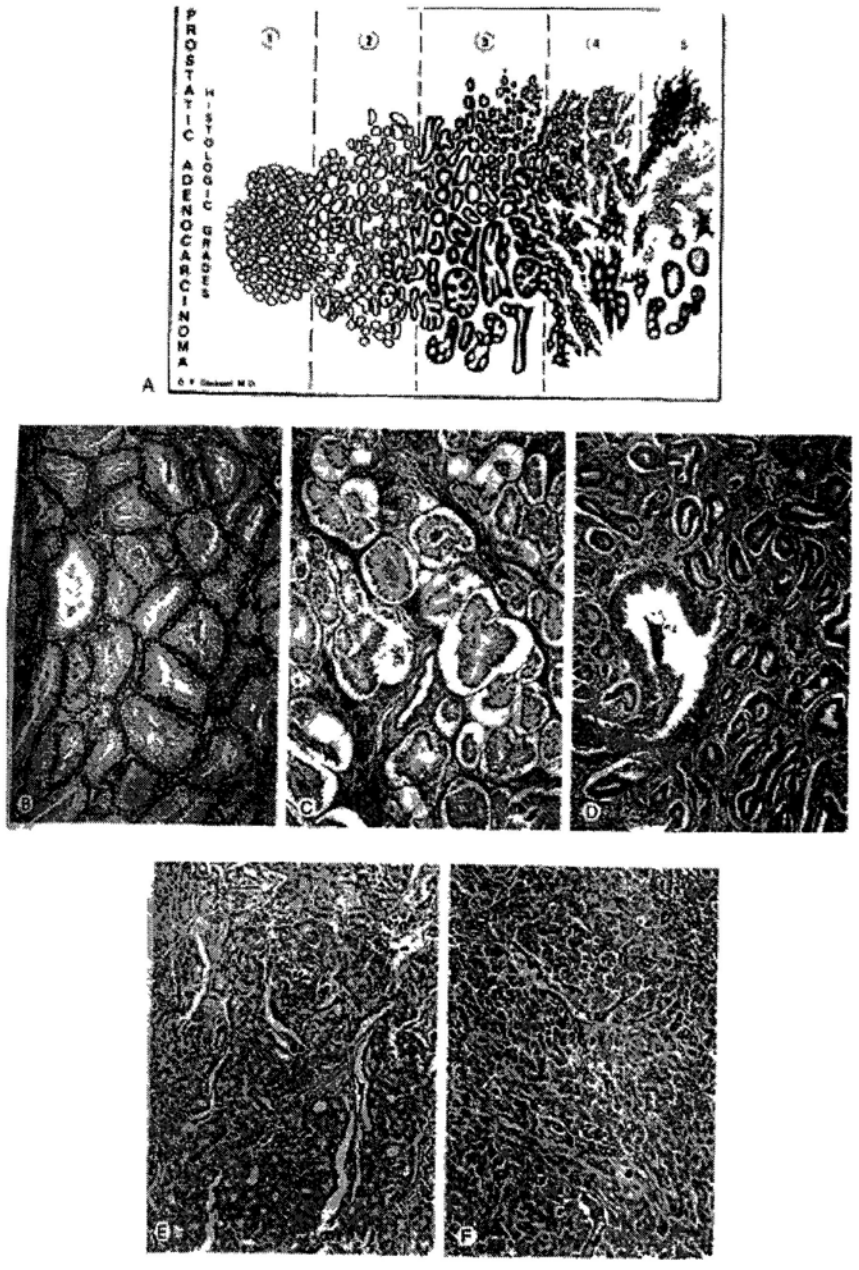

Figure 1.5 The Gleason grading system. B-F represents Gleason patterns from 1 to 5. *(Adopted from Campbell-Walsh Urology, Ninth edition)*

1.3.3 Ion channel and prostate cancer

Enhanced proliferation, aberrant differentiation and resistance to death are the main reasons for abnormal tissue growth, which eventually develop into uncontrolled expansion and invasion. These transformations often go together with changes in ion channel expression. Prostate cancer cells express a variety of plasma membrane ion channels. Some ions in the prostate cancer epithelial cells play a key role in apoptosis and differentiation-related events (Prevarskaya N, 2007).

1.3.3.1 Potassium channels

Potassium channels are involved in the maintenance of resting potential and regulation of cell volume. Androgen sensitivity prostate cancer epithelial cells display relatively weak metastatic potential and are generally characterized by higher voltage-gated K^+ current (I_k) compared with the highly metastatic, androgen-insensitive cells. The high I_k would promote proliferation but more prone to apoptosis. The decrease in I_k could make the cell shift to a 'more excitable' phenotype of their plasma membrane. The lower I_k and K^+-channel expression in androgen-insensitive cells contribute to their apoptotic resistance although reducing the proliferative activity (Prevarskaya N, 2007, Rybalchenko V, 2001; Laniado ME, 2001).

1.3.3.2 Chloride channels

Maintaining relative volume constancy in cells is a major prerequisite for cell survival. The disordered or altered cell volume regulation is associated with apoptosis. One of the mechanisms for cells to restore their volume following hypo-osmotic stress is to activate the chloride current by specialized volume-regulated anion channels (VRACs)

in response to cell swelling ($I_{cl,swell}$). It has been shown that the endowed powerful $I_{cl,swell}$ in LNcap cells provide an effective regulatory volume decrease (RVD) under hypo-osmotic stress with cell transition to androgen-independence and increased survival (Lemonnier L, 2004).

The chloride channel also has the ability to regulate the intracellular pH. Calcium-sensitive chloride channel 2 (mCLCA2) in the mammary epithelial cells could promote either apoptosis or senescence by reducing intracellular pH (Elble RC, 2001).

1.3.3.3 Voltage-gated sodium channels, store-operated calcium entry and TRP channels

In several prostate cancer cells, the voltage-gated Na^+ channels (VGSCs) activity can enhance the metastatic behavior of cells including the proliferation characters. Ca^{2+} signaling is involved in the appearance of cell proliferation, differentiation, apoptosis and cellular activities. In prostate cancer cells, Ca^{2+} entry from extracellular space is mainly supported by 'store-operated calcium entry' (SOCE) (Parekh AB, 2005). It is very important to identify the activation or regulation of SOC in these cells because the SOC activity seems to play a major role in the establishment of androgen-independent apoptosis-resistant phenotype of prostate cancer.

TRPM8 is one of the transient receptor potential (TRP) members. It has recently been considered as an important player in normal and pathological development of the prostate. It is expressed not only in the plasma membrane, but also in the ER membrane to operate as an ER Ca^{2+} release channel (Thebault S, 2005). Due to its different expression pattern in malignant tissue specimens, TRPM8 has been proposed as a

potential competitor in prostate cancer diagnosis and staging comparable to the currently used marker PSA (Fuessel S, 2003). Some other TRP channels such as TRPC1, TRPC4, and TRPV6 are also involved in the controlling prostate cancer cells proliferation.

1.3.4 Etiology and molecular genetics of prostate cancer

1.3.4.1 The influence of hormones

Many studies have suggested that androgen might be associated with prostate cancer development. Absence of androgen to the prostate appears to cause prostate cancer to regress. In normal prostate cells, epithelial cell growth by androgen stimulation is indirect which is mediated by a paracrine influence from the stroma. However in prostate cancer, androgens play a direct autocrine role in supporting epithelial cell proliferation. In addition to androgen, estrogen has been shown to play positive role in prostate cancer development (Noble RL, 1980). The age-related prostatic disease parallels increases in serum estrogen levels (Zumoff B, 1982).

1.3.4.2 Inflammation in prostate carcinogenesis

About 20% of all human cancers in adults result from chronic inflammatory. Most regions that contain acute or chronic inflammatory infiltration in the prostate are associated with atrophic epithelium and there is an increased fraction of epithelial cells. The term of proliferative inflammatory atrophy (PIA) is described for these highly proliferative lesions. Some findings support the association between prostatitis and prostate cancer (De Marzo AM, 1999). Several key genes involved in prostate cancer

were showed to be altered in PIA. For example three tumor-suppressor genes *NKX3.1, CDKN1B* and *PTEN* are all downregulated in atrophy lesion. Some genes involved in inflammatory pathways are also candidates for determinants of prostate cancer risk such as RNASEL, MSR1, Toll-like receptor, MIC1 and IL1RN (De Marzo AM, 2007).

1.3.4.3 Somatic gene alterations in prostate cancer

1.3.4.3.1 Oncogenes

Oncogenes are originated from proto-oncogenes by means of genetic changes including mutation, amplification, overexpression or translocation. They have been implicated in the carcinogenic development of diverse types of human malignancies. Some oncogenes play roles in the development of prostate cancer such as Ras, c-myc, Bcl-2, c-met, HER2, Id-1 et al. Among them, alterations in c-myc, HER2 and Bcl-2 have been observed in advanced and hormone-refractory prostate cancer but not commonly in lower state cancers (Gurumurthy S, 2001).

1.3.4.3.2 Tumor suppressor genes

Tumor suppressor genes are the protective genes that normally limit the growth of tumors. The function of tumor suppressor genes is to suppress the proliferation of tumor cells by inhibiting cell cycling, activation of apoptosis. Inactivation of them by mutation or methylation or chromosomal deletion is an important step in the development of most cancers. Mutation or loss of NKX3.1, p53, RB, PTEN and p16 genes has been detected in prostate cancer (Gonzalgo ML, 2003) which could contribute to the progression of prostate cancer.

1.3.4.4 Epigenetic changes in prostate cancer

1.3.4.4.1 DNA methylation and histone modifications

Epigenetic changes, defined as heritable changes in gene expression that occur without altering the sequence of DNA, appear to contribute to the malignant transformation and progression of prostate cancer. DNA methylation and histone modifications are two important mechanisms in the area of epigenetics (Gonzalgo ML, 2003). A variety of genes implicated in prostate cancer initiation and progression are affected by these processes (Table 1.1).

Table 1.1 A list of genes affected by epigenetic aberrations in prostate cancer

Epigenetic aberration	Gene symbol
DNA hypermethylation	
Hormonal response	AR, ESR1, ESR2, RARB, RARRES1
Cell cycle control	CCND2, CDKN2A
Tumor cell invasion/tumor architecture	APC, CAV1, CD44, CDH1, CDH13, LAMA3, LAMB3, LAMC2
Repair of DNA damage	GSTP1, MGMT
Signal transduction	DAB2IP, DAPK1, EDNRB, RASSF1
Inflammatory response	PTGS2
Others	HIC1, MDR1, PXMP4
DNA hypomethylation	CAGE, HPSE, PLAU
Histone hypoacetylation	CAR, CPA3, RARB, VDR
Histone methylation	GSTP1, PSA

(The data was from *Li LC, 2005*. All gene symbols are official gene symbols (or names) from HUGO Gene Nomenclature Committee.)

1.3.4.4.2 MicroRNA (miRNA) and prostate cancer

miRNAs are a class of naturally occurring, small non-coding RNAs that negatively regulate expression of protein-coding genes at the post-transcriptional level. The procedure for biogenesis of miRNA is described in Figure 1.6, miRNAs regulate gene

expression by resulting in direct cleavage of the targeted mRNAs or inhibiting translation through perfect complementarity to the 3' untranslated regions (UTRs) of the target transcripts (De Moor CH, 2005).

Aberrant expression of several miRNAs has been found in prostate cancer cells. It was reported that three miRNAs (miR-184, miR-361 and miR-424) were significantly upregulated and eight miRNAs (miR-19b, miR-29b, miR146b, miR-146a, miR-221, miR-222 and miR-663) were down-regulated in androgen independent cell lines compared with androgen dependent cell lines (Lin SL, 2008). Most prostate cancer cell lines had increased expression of miR-125b, miR-191, miR-92, miR-106a, miR-21 and miR-145 than the normal prostate cells. The miRNAs expression profile is different among the human prostate cancer tissues, benign prostatic hyperplasia tissues using global miRNA microarray profiling technology (Porkka KP, 2007).

The formation or development of cancer is the combined interaction of both cancer inducers and tumor suppressors. Recent studies suggest that miRNAs are involved in human tumourigenes as oncogenes or tumor suppressors as described in Table 1.2.

Table 1.2 Targets of prostate cancer-related miRNAs and their function

CaP-related miRNA	Function	Targets and function
miR-20a	oncomiRNA	E2F1-3:cell cycle regulator, pro-apoptosis
miR-125b	oncomiRNA	Bak1: pro-apoptotic regulator
miR-126	ts-miRNA	SLC45A3: related to prostate malignancy
miR-146a	ts-miRNA	ROCK1:myosin phosphorylation; PI3K activatin
miR-221/222	oncomiRNA	$P27^{Kip1}$: inhibition of cell cycle

oncomiRNA, oncogenic miRNA; ts-miRNA, tumor-suppressor miRNA (Shi XB, 2008)

Limited information is available about the regulation of the expression of miRNAs. It has been reported that epigenetic silencing such as DNA methylation and histone modifications serves as one of the mechanisms to regulate miRNA in cancer cells (Saito Y, 2006). The transcription factors involved in mRNA transcription also contribute to miRNA transcriptional regulation (Raver-Shapira N, 2007). The enzymes including RNA Pol II and two nuclear RNases (Dorsha and Dicer) could regulate the expression of miRNAs (Lee Y, 2004). In addition, several lines of evidence suggest that the androgen-androgen receptor (AR) signaling may be involved in the regulation of the expression of miRNAs in LNcap cells (Shi XB, 2007).

Therefore, prostate cancer related miRNAs might be the potential novel biomarkers for clinical prostate cancer.

1.3.5 pH and carbonic anhydrases (CAs) in cancers

Tumor growth involves complex interactions between cells and their unique microenviroment which is characterized by low acidic pH and altered hydrostatic and oxygen delivery (Helmlinger G, 1997). Hypoxia and acidosis in the tumor microenviroment are critical in driving tumor growth and metastasis. The hypoxia-inducible factor-1(HIF-1) is active under hypoxia conditions and regulates pH homeostasis by enhancing expression of membrane located transporters, exchangers, pumps and ecto-enzymes (Brahimi-Horn MC, 2007). Carbonic anhydrase (CA) are zinc metalloenzymes that convert CO_2 and H_2O in to H^+ and HCO_3^- which is widely expressed in a variety of tissues. CAs participates in a variety of physiological processes, including ureagenesis, gluconeogenesis, lipogenesis and brain metabolism (Chegwidden

WR, 2000). The possible relationship between the expression of CAs and cancer has also been reported. CAIX and CAXII are membrane-associated carbonic anhydrase. Both of them are overexpressed in a large number of solid tumors including breast cancer, colon cancer, lung cancer and other malignancies (Chia SK, 2001; Kivela A., 2000; Vermylen P, 1999) which could be a biomarker for cancers. Recently it was shown that cancer-associated carbonic anhydrases (CA IX and CAXII) are key regulatory molecules for countering acidosis during hypoxia and maintain extracellular acidity in tumors (Chiche J, 2009). The net effect of CA IX/XII is to trap acid extracellularly, lowering extracellular pH (pHe) (~6.9-7.0) and maintaining normal intracellular pH (pHi) (~7.2) with HCO_3^- recycled back into the cell (Swietach P, 2009). Among the various CA isozymes, CAI and CAII are located in cytosol of cells. It was reported that the cytosolic CAI and CAII are significantly less expressed in non-small cell lung cancer (NSCLC) (Chiang WL, 2002) and colorectal tumors (Mori M, 1993), but overexpressed in nervous system tumors (Parkkila AK, 1995) and pancreatic tumors (Parkkila S, 1995). Therefore, the clear-cut relationship between the expressions of CA isozymes in normal and malignant cells needs to be further investigated.

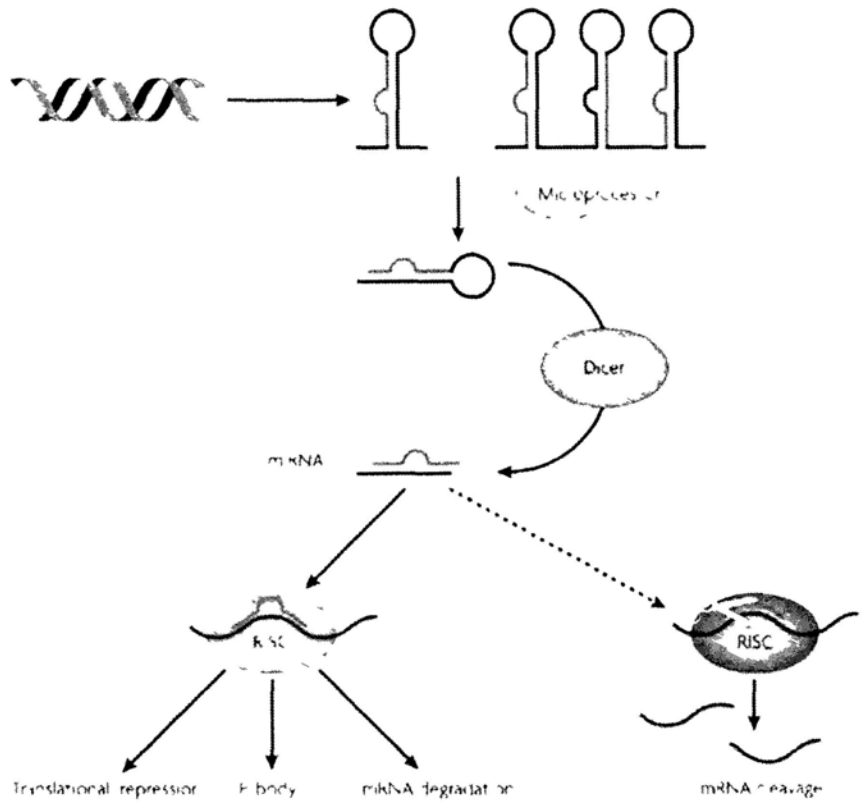

Figure 1.6 Current model of miRNA biogenesis and post-transcriptional silencing. Nascent transcripts of microRNA (miRNA) genes are processed by microprocessor into a stem-loop precursor, which is further processed by Dicer into a mature miRNA duplex, which often displays imperfect base-pairing. One strand of the miRNA duplex gets incorporated into the effector complex RISC (RNA-induced silencing complex), which recognizes specific targets through imperfect base-pairing and induces post-transcriptional gene silencing. Several mechanisms have been proposed for this mode of regulation: miRNAs can induce the repression of translation initiation, mark target mRNAs for degradation by deadenylation, or sequester targets into the cytoplasmic P-body.
(Adopted from He L. 2007)

1.4 Structure and functions of CFTR

1.4.1 The structure of CFTR

Cystic fibrosis transmembrane conductance regulator (CFTR) is a member of the ATP-binding cassette (ABC) transporter family. CFTR is expressed in a wide variety of epithelial tissues including the lung, liver, pancreas, intestine, reproductive tracts and sweet glands (Chan HC, 2006; Hug MJ, 2003; Strong TV, 1994; Cohn JA, 1991). CFTR mutations lead to cystic fibrosis (CF), the No.1 lethal genetic disease found among Caucasian (Boat TF, 1989). CFTR gene encodes a 1480 amino acid protein, functioning as a cAMP-dependent Cl^- ion channel, and is composed of two structurally homologus halves: the membrane-spanning domain (MSD-1 and -2) and the nucleotide binding domain (NBD1 and 2), both of which are linked together by a regulatory (R) domain. The MSDs contribute to the formation of the anion pore, while the NBDs bind and hydrolyse ATP to regulate channel gating, and the R domain can be phosphorylated by PKA and PKC to control channel activity. About 70% of this common lethal genetic disease, cystic fibrosis (CF), is caused by a mutation in a single gene deletion of phenylalanine amino acid (ΔF508) at NBD1. ΔF508 gene mutation gives rise to defective protein trafficking and defective channel regulation of CFTR (Figure 1.7).

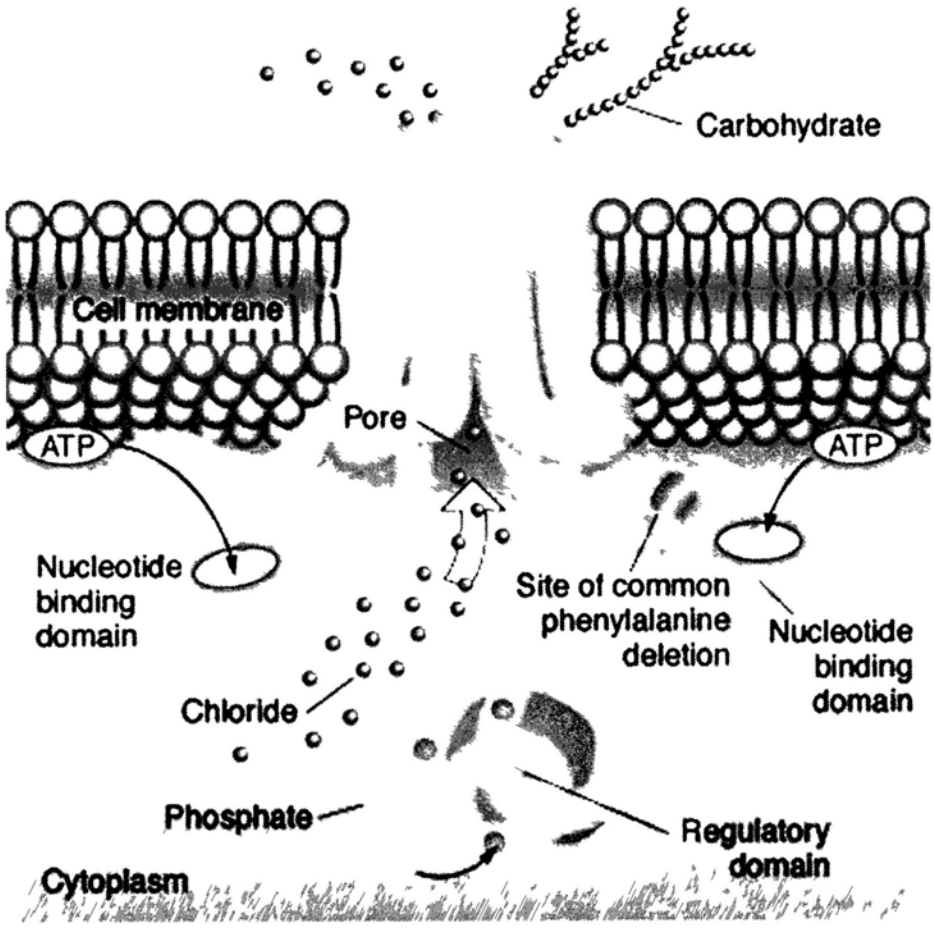

Figure 1.7 Schematic representation of proposed CFTR structure. CFTR is made up of five domains: two membrane-spanning domains that form the chloride ion channel, two nucleotide-binding domains that bind and hydrolyze ATP and a regulatory domain. From www.cfgenetherapy.org.uk/cysticfibrosismore.htm

1.4.2 Functions of CFTR

CFTR is a channel that regulates the secretion of Cl^- ions on apical surfaces of most epithelia (Crawford I., 1991; Welsh MJ, 1993). CFTR chloride channel activation depends on phosphorylation by cAMP-dependent protein kinase, PKA, and ATP binding and hydrolysis. A variety of cAMP-evoking hormones and neurotransmitters, such as adrenalin, prostaglandin E2 and F2α are known to activate CFTR (Scheckenbach KL, 2010).

Besides Cl^- ions, CFTR also conducts HCO_3^- (Poulsen JH, 1994). Although CFTR in a number of tissues including the airway, pancreas and intestine has been shown to conduct HCO_3^- (Hug MJ, 2003), the seemingly low permeability of CFTR to HCO_3^- raises doubt in its ability to secrete sufficient amount of HCO_3^- to be considered physiologically significant. However, a recent study has demonstrated that the anion selectivity of glutamate-activated CFTR in the human sweat duct could undergo a dynamic shift from primarily Cl^- conducting to primarily HCO_3^- conducting by a process involving ATP hydrolysis (Reddy MM, 2003). The duct cells from patients with ΔF508 mutant CFTR showed no glutamate/ATP activated Cl^- or HCO_3^- conductance, suggesting that the loss of this uniquely regulated HCO_3^- conductance may be most probably responsible for the more severe forms of CF pathology.

1.4.3 Interaction between CFTR and other proteins

CFTR is also known to function as a regulatory protein interacting with a wide array of proteins including ion channels and transporters, such as ENaC, inwardly rectifying K^+ channel and water channel (Guggino WB, 2004).

In fact, structural study indicates that CFTR contains one PDZ-interacting domain in the C terminus. PDZ domains are one of the most common modules that are found in mammalian proteins. Previous studies have shown that they mediate protein–protein interactions, cluster and colocalize transporters, channels and signalling proteins in specific subcellular domains, determine the polarized localization of many proteins, control channel and transporter function and regulate endocytic trafficking.

Recent studies have also demonstrated a molecular mechanism for interaction between CFTR and other HCO_3^- transporters and this interaction has been shown to be defective due to mutations of CFTR (Choi JY, 2001; Ko SB., 2002; Ko SB., 2004). It was reported that CFTR could interact with SLC26 transporters such as SLC26A6 and SLC26A3, both of which are electrogenic Cl^-/ HCO_3^- exchangers. The studies showed that SLC26A6 functions as a $1Cl^-/2HCO_3^-$- exchanger, while SLC26A3 functions as a $2Cl^-/HCO_3^-$ exchanger. Another significant feature of these two SLC26 transporters is the mutual activation of the SLC26 transporters and CFTR, which is mediated by the CFTR R domain and the SLC26 transporters STAS domain (Ko SB, 2004), suggesting that the SLC26 transporters participate in and regulate epithelia Cl^- absorption and HCO_3^-secretion.

Taken together, the evidences suggest that CFTR may be directly or indirectly involved in mediating HCO_3^- transport, aberrance of which may contribute to CF pathogenesis.

1.4.4 CFTR gene mutation types

About 70% of CF is caused by a mutation in a single amino acid deletion (ΔF508) at NBD1. Since the discovery of CFTR, more than 1500 additional mutations have been detected (The Cystic Fibrosis Genetic Analysis Consortium; http://www.genet.sickkids.on.ca/cftr). In general, according to their functional properties, CFTR mutations can be divided into five classes (Zielenski J, 1995). Class 1 ('no synthesis') mutations abolish the synthesis of full length, normal CFTR polypeptide. About half of the known CFTR mutations belong to this class of non-sense, frameshift or aberrant splicing mutations. Class 2 ('block in processing') mutations affect protein maturation. The most common mutation ΔF508 belongs to this class. Because of improper folding, the ΔF508 protein is mislocalized in the epithelial cell and fails to gain a protease-resistant, mature conformation in the endoplasmic reticulum. Class 3 ('block in regulation') mutations affect Cl^- channel regulation and represent the third class of typical 'severe' CF mutations. Both classes 4 ('altered conductance') mutations, affecting Cl^- channel conductance or gating, and 5 ('reduced synthesis') mutations, reducing normal, functional CFTR protein, are often seen in patients with 'mild' or atypical forms of CF.

1.4.5 Regulation of CFTR

The expression of CFTR gene appears to be under hormonal regulation in both males and females (McCarthy VA, 2005). In reproductive system, expression of CFTR in rodents occurs in round spermatids (spermatogenic stages V-X), and may be necessary for a reduction in cytoplasmic volume and subsequent correct elongation of these cells. In the female uterine, CFTR expression is correlated with the estrous cycle, with the

highest level seen in the grandular epithelium during proestrous (Trezise AE, 1993). This cyclic expression pattern is proposed to attribute to the estrogen level changes. The up-regulation of CFTR levels could be seen in uterine epithelium and the oviductal mucosa of immature females and ovariectomized mature females after treatment with estrogen (Ajonuma LC, 2005).

The studies showed that CREB (cAMP response element binding protein) binds to the CRE element in the CFTR gene with high affinity in vitro. When placed upstream of a heterologous basal promoter, this element was capable of driving cAMP mediated expression, suggesting that CFTR expression is also regulated by intracellular cAMP levels (Matthews RP, 1996).

The CFTR gene promoter is clearly important for maintaining levels of CFTR gene expression. Cytokines such as interleukin 1 beta (IL-1β) are potent modulators of CFTR (Cafferata EG, 2000). IL-1β could activated the NF-κB protein, enabling it to enter the nucleus and bind to the κB-like response element at position -1103 to -1093 in the CFTR 5'-regulatory region and a subsequent increase in CFTR promoter activity, resulting in increased CFTR mRNA(Brouillard F, 2001).

Multiple CFTR transcription start sites have been reported and variation in the transcription start site could provide a level of tissue-specific regulation of CFTR expression, while the use of alternative 5' exons may provide developmental regulation of CFTR in the lung (McCarthy VA, 2005). Removal of an inverted CCAAT element (Y box) located between nucleotide positions -132 to 119 upstream of the translational start sites has been reported to reduce CFTR transcript levels (Pittman N, 1995).

1.5 Hypotheses and aims of study

CFTR has been reported to be expressed in human prostate, however, the physiological role of CFTR in the prostate related diseases such as prostatitis and prostate cancer remains largely unknown.

Therefore, two hypotheses were made:

I. CFTR may play a key role in host defense of the prostate by mediating bicarbonate secretion, which may be enhanced in prostatitis for bacterial killing.

II. CFTR may play an important role in prostate cancer development.

For hypotheses I, four objectives were proposed:

1. To examine the expression of CFTR in rat prostate and its involvement in mediating bicarbonate extrusion in prostate epithelial cells.

2. To study the expression of CFTR and CAII in prostate epithelial cells challenged by LPS and in clinical human prostate samples with prostatitis.

3. To investigate the involvement of CFTR on the bacterial killing activities in the prostate *in vitro* and *in vivo*.

4. To investigate the physiological significance of the HCO_3^- secretion on anti-bacterial activities and the possible underlying mechanism.

For hypotheses II, four objectives were proposed:

1. To study the expression pattern of CFTR in rat prostate at different developmental stages.

2. To study the expression profile of CFTR in prostate cancer cells and human prostate cancer specimen.

3. To investigate the biological functions of CFTR in prostate cancer cells, including cell cycle regulation, apoptosis, adhesion, motility, invasion and tumor growth.

4. To investigate the potential mechanisms underlying tumor suppressive effects of CFTR in cancer development.

Chapter 2
General Methods

2.1 Materials

2.1.1 Cell culture materials

Dulbecco's Modified Eagle's Medium with nutrient mixture F-12 (DMEM/F12), RPMI-1640, McCoy's 5A, antibiotics penicillin-streptomycin, trypsin, collagenase I (catalog no: C0130), Insulin(catalog no: I6634), EGF (catalog no: E4127), transferring (catalog no: T8158), cholera toxin (catalog no: C8052) were purchased from Sigma-Aldrich Co. (St. Louis, MO, USA); while phosphate-buffered solution (PBS), Hanks' Balanced Salt Solution (HBSS), fetal bovine serum (FBS) were purchased from Gibco Invitrogen (Grand Island, New York, USA). Transwell-Col Permeable Supports (24mm diameter, 0.45μm pore) were from Corning Incorporated (Corning, NY, USA). Bovine pituitary extract (catalog no: 354123), Matrigel basement membrane matrix, 100-μm mesh cell strainer (catalog no: 352360) and transwell-Col Permeable Supports (6.5mm diameter, 8μm pore) were from BD biosciences (Franklin Lakes, NJ, USA).

2.1.2 Chemicals and reagents

D-(+) glucose anhydrous, Sodium gluconate (2,3,4,5,6-pentahydroxycaproic acid), Calcium gluconate (2,3,4,5,6-pentahydroxycapproic acid), Potassium gluconate (2,3,4,5,6-pentahydroxycaproic acid), Disodium hydrogen phosphate (Na2HPO4), Sodium dihydrogen phosphate (NaH2PO4), Sodium azide (NaN3), Acetic acid (glacial), Agar, Ammonium Bromophenol blue, Chloroform, Citric acid, Deoxyribonulease I (DNase I), Diethyl pyrocarbonate (DEPC), 4',6-diamidino-2-phenylindole (DAPI), 4-

Dimethylaminoazobenzene (DAB), *N,N*-dimethyl sulfoxide (DMSO), Dithiothreitol (DTT), Eosin Y, Ethidium bromide, Formaldehyde, Formamide, Glycerol, Glycine, Hematoxylin, Chlortetracycline, L-cysteine, Hydrochloric acid, Hydrogen peroxide, Isopropyl alcohol, Poly-L-lysine, Luria broth, 2-mercaptoethanol, Nonidet-40 (NP-40), Pepstatin A, Ethylenediaminetetraacetic acid (EDTA), N-2-hydroxyethylpiperazine-N'-2-ethanesulfonic acid (HEPES), Tris base, Bovine serum albumin (BSA), Triton X-100, Polyoxyethylene sorbitan monolaurate (Tween-20), *N,N,N',N'*-Tetramethylethylenediamine (TEMED), Phenylmethyl sulfonyl fluoride (PMSF), Sodium diodecyl sulfate (SDS), Ammonium persulfate (APS), Triton X-100, Propidium iodide (PI), Proteinase K, Rubidium chloride, Sodium Acetate, Sodium azide, 2-mercaptoethanol, Dimethyl sulfoxide (DMSO), Formaldehyde and Accustain Harris hematoxylin/eosin solution sets were purchased from Sigma-Aldrich Co. (St. Louis, MO, USA).

Agarose, DNA marker, Lipofectamine 2000, Opti-MEMR I Reduced Serum Medium, Prestained protein marker, RNase inhibitor, Tris base, TRIZOL Reagent were purchase from GIBCO BRL/ Invitrogen (USA).

Sodium chloride (NaCl), Magnesium chloride ($MgCl_2$), Potassium chloride (KCl), Calcium chloride dehydrate ($CaCl_2.2H_2O$), Magnesium sulphate heptahydrate ($MgSO_4$), Potassium dihydrogen phosphate (KH_2PO_4) and Sodium hydrogen carbonate ($NaHCO_3$), Ethanol, Methanol and Xylene were purchased from Merck & Co., Inc (Whitehouse station, NJ, USA).

Biotinylated secondary antibody and Streptavidin-HRP antibody were purchased from Vector Labs (USA). Bicinchoninic acid (BCA) protein assay system was obtained

from Pierce (USA). Super RX x-ray film was purchased from Fuji (Japan). Ampicillin, Karnamycin, dNTPs, ECL Western Blot Detection Reagent, Hybond-ECL nitrocellulose membranes were from Amersham Biosciences. MMLV reverse transcriptase and RNase Inhibitor were purchased from Promega (USA). Acrylamide, Bis N-N'-methylene-bis-acrylamide, Coomassie blue R250 were obtained from Bio-Rad laboratories (USA). Primers used for all polymerase chain reactions in the present study were purchased from Invitrogen (USA). FITC labeled goat anti-rabbit secondary antibody, QIAquick Gel Extraction Kit, were purchased from Qiagen (Germany). Forskolin , acetazolamide , CFTRinh-172, 5-Nitro-2-(3-phenylpropylamino) benzoic acid (NPPB) and LPS from Escherichia coli 055:B5 were purchased from Sigma-Aldrich Co. (St. Louis, MO, USA). For luminal surface pH measurements, the pH-sensitive fluorescent dye 2', 7'-bis-2(2-carbosyethyl)-5-(and-6)-carboxyfluorescence, acetoxymethyl ester (BCECF) was purchased from Molecular Probes (Eugene, OR, USA).

Anesthetic ketamine (10%) and xylazine (2%) were purchased from Alfasan International BV (Woerden, Holland).

2.1.3 Antibodies

Antibodies used for immunoblotting (Western blot) in the present study are listed in Appendix A.

2.1.4 Animals

Male 4-week-old and 12-week-old SD rats and female 4-6-week-old nude mice were provided by Laboratory Animal Service Center of the faculty of medicine, the Chinese University of Hong Kong (CUHK). The animals handling protocol was approved by the

Animal Research Ethics Committee of the university. Animals were maintained in an air-conditioned room with controlled temperature of 24 ± 2 °C and humidity of 55 ± 15%, on a 12-h light/dark cycle. Animals were housed singly in polycarbonate cages with a bedding of pine shavings, and they had free access to food and water.

2.2 Cell culture

2.2.1 Culture medium preparation

2.2.1.1 DMEM/F12 medium

Dulbecco's modified Eagle's medium with nutrient mixture F-12 (DMEM/F12) in power form was kept stirring in a 1L beaker with 800 ml Nano-pure water inside. Then 1.2 g $NaHCO_3$ was added into the solution. The pH value was adjusted to 7.2, a little bit lower than the desired value 7.4 because there will be a 0.2~0.3 rise in pH value after filtering. The solution was made up to 1L. The medium was filtered into two 500 ml bottles through the sterilized filter unit. Each 500 ml growth medium was supplemented with 100 IU/ml penicillin and 100 μg/ml streptomycin, and 10% FBS. The completed growth medium was kept refrigerated.

2.2.1.2 RPMI-1640 medium

RPMI-1640 in powder form was dissolved as described above and 2 g $NaHCO_3$ was added into the solution. After filter sterilization, 100 IU/ml penicillin, 100 μg/ml streptomycin and 10% FBS was added.

2.2.1.3 McCoy'5A medium

McCoy's 5A (Sigma, catalog no: M4892) medium containing 5% FBS, 10ug/mL Insulin,10ug/mL EGF, 5ug/ml transferring, 10ng/ml cholera toxin, 25ug/mL Bovine

pituitary extract, 100 U/ml penicillin and 100 μg/ml streptomycin was prepared for further study.

2.2.2 Maintenance of cells

Cells were grown in culture medium in a humidified incubator at 37°C, in 5% CO2. The cells were routinely sub-cultured upon reaching 80 – 90% confluence and washed with Hanks' (GibcoBRL, USA) and trypsinized with 1 ml of trypsin-EDTA for 2 minutes. The Balanced Salt Solution (HBSS) digestion was neutralized by DMEM/F12 medium. The cell suspension was transferred to a 15-ml centrifuge tube and centrifuged at 1000 rpm in a CR412 desktop centrifuge (Jouan, USA) at room temperature for 5 minutes. The cell pellet was resuspended with fresh medium and transferred to new culture flasks. The subcultivation ratio of 1:3 to 1:5 was commonly adopted.

2.2.3 Preparation of cell stock

Semi-confluent cells on a $75cm^3$ culture flask were washed with HBSS solution and trypsinized as described above. After centrifugation, the cell pellet was resuspended in 1ml of DMEM /F12 supplemented with 10% v/v FBS and 5% DMSO. The resuspended cells were transferred to a cryotubes™ vial (Nuncbrand Demark). The vial was put in a freezing pot (Stratagene, CA) and the pot was put into a -80°C freezer so that the cell stock was frozen at a constant rate of about 1°C/min. Cell stocks were stored at liquid nitrogen.

2.2.4 Revival of cells from liquid nitrogen

The required cell stock was taken out from the liquid nitrogen tank and thawed rapidly in a water bath at 37°C. Once thawed, the outside of the cryotube was cleaned thoroughly with a sterile swab. To remove the DMSO, the cell stock was diluted into 10 ml of pre-warmed DMEM /F12 medium with 10% v/v FBS. The cell suspension was centrifuged as described above and the supernatant was discarded. The cell pellet was then resuspended in 10 ml culture medium and placed into a fresh $25cm^3$ tissue culture flask and incubated as above. Medium was changed one day after recovery of the cells. Cells were used for experiments after one or two passages.

2.3 Molecular biological studies

2.3.1Total RNA extraction

For tissue sample, tissue samples were homogenized in 1 ml of TRIZOL Reagent (Invitrogen USA) per 50-100 mg of sample using Tissue-Tearor™ (BioSpec Products, USA). For cultured cells, cells were lysed directly in a culture dish using TRIZOL Reagent (1 ml per 10 cm^2). To complete dissociate nucleoprotein complex, the samples were incubate at room temperature for 5 minutes. 0.2 ml per 1 ml of TRIZOL Reagent of chloroform was added to lysates and tubes were shaken vigorously by hand for 15 seconds. After centrifuged at 12,000 rpm for 10 minutes at 4°C, the upper aqueous phase was transferred to a 1.5-ml microcentrifuge. To precipitate the RNA, 0.5 ml per 1 ml of TRIZOL Reagent of isopropyl alcohol was added to the aqueous phase and the samples were incubated at room temperature for 10 minutes. The RNA was pelleted by centrifuging at 12,000 rpm for 10 minutes at 4°C and washed once with 1ml 75% ethanol. The RNA was dissolved in DEPC-treated dH_2O after air-dried at room

temperature for 10 minutes. DEPC water was used in RNA isolation to reduce the effects of any RNases that may be present. DEPC is a histidine specific alkylating agent and inhibits the action of RNases which rely on histidine active sites for their activity. The RNA concentration was measured by NanoVue UV/Vis Spectrophotometer (GE healthcare) at a ratio of A260 and A280. RNA sample was stored at -70°C for no more than a month for RT-PCR analysis.

2.3.2 RT-PCR

2.3.2.1 Reverse transcription

In a 0.2-ml PCR tube, 5 µg of total RNA were mixed with 1 µl of oligo (dT) primers (0.5 µg/µl) and final volume was adjusted to 12ul with DEPC treated water. The secondary structure of RNA was denatured by heat at 70°C for 5 minutes and chilled on ice. The RT mix was prepared by combining the follows: 1×PCR buffer, 2mM $MgCl_2$, 8mM DTT, 0.25 mM deoxynucleoside 5'-triphosphate (dNTP) solution, the reaction mixture was then added to the RNA/primer mixture and incubated at 42°C for 5 min. After this, 1 µl MMLV reverse transcriptase (200 U/µl) was added and incubated at 42°C for 50 min and 70°C for 15 min. Finally, any contamination of sample with RNAase was removed by incubating the sample with 1 µl RNAase H at 37°C for 20 min. The resulting first strand cDNA sample was used for polymerase chain reaction (PCR).

2.3.2.2 Polymerase chain reaction

The Taq DNA polymerase (Amersham Biosciences, USA) was used for common DNA amplification. The template cDNA (1 µl) was mixed with PCR mix [1×PCR buffer;

0.25 μM Forward primer; 0.25 μM Forward primer ; 0.20 μM dNTP solution, 2.5-3 units of Taq polymerase]; then the volume was brought to 25 μl by autoclaved DEPC-treated water. Thermal cyclic reactions were done by the GeneAmp PCR System 2700 (Perkin Elmer, USA). The reaction profile was 94°C for 5 minutes, 26-35 cycles (cycles varied for different primers) of 94°C for 30 seconds, 55°C for 30 seconds (annealing temperature varied for different primers), 72°C for 1 minute (elongation time varied depending on the size of DNA to be amplified), followed by 72°C for 7 minutes and 4°C for infinity.

2.3.2.3 Gel electrophoresis

DNA gel (1.5%) was prepared by mixing 0.75 g agarose with 50 ml 1× TAE and boiling to dissolve agarose. About 15μl ethidium bromide (1 mg/ml) was added to the mixture before the solidification of the gel. The gel was set in a 12 well setter. Then it was put in a gel tank containing sufficient 1× TAE running buffer. Total 25 μl DNA samples were mixed with 5 μl dye and at least 10 μl mixtures were added to gel wells. 1 μg of DNA ladder (100 bp) were used as a molecular weight marker. The gel tank was connected to the power supply. DNA nucleotide, like RNA nucleotide, carried negative charges would migrate to the anode in the presence of electrical field. When two bands of dye were separated by a reasonable distance, the power was turned off. The bands were visualized under an ultraviolet transilluminator (Alphalnnotech).

2.3.3 Western blot analysis

2.3.3.1 Protein extraction

For tissue samples, prostates of rats were cut into very small pieces and diced by razor blade in radioimmunoprecipitation assay (RIPA) lysis buffer to lyse the cells. For cell samples, the cells were harvested at 90% confluence from the plate and resuspended in 1ml PBS. The suspension was transferred into a microcentrifuge tube and centrifuged at 13,000 rpm in a desktop centrifuge (Eppendorf, Germany) for 30 seconds. The supernatant was discarded. The cell pellet was resuspended with three pellet-volumes of RIPA lysis buffer containing 50 μg/ml PMSF and proteinase inhibitors or other buffers as indicated. The lysates were incubated on ice for 30 minutes. To get rid of the cell debris, the resuspension was centrifuged at 13,000 rpm for 30 minutes at 4°C. The supernatant was collected and transferred to a new microcentrifuge tube. The protein concentration of the lysate was measured as described below. For confirmation of expression of expected proteins, the lysate was analyzed by SDS-PAGE followed by immunoblotting.

2.3.3.2 Protein concentration determination

Bradford protein assay system (Bio-Rad, USA) was used to determine the protein concentration of cell lysates. To measure protein concentration, protein sample (1 μl) was mixed with the mixture of 200 μl diluted dye reagent (1:5 dilution with distilled water) and incubated at room temperature for at least 5 minutes. Color development was measured at OD595. The readings of the serially diluted BSA standards were plotted with linear regression as a reference, and the concentration of the sample was deduced by referring the reading of the protein sample to the BSA reference.

2.3.3.3 SDS-PAGE gel electrophoresis

Proteins in SDS-sample buffer were separated, typically on 5%, 8%, 10% or 12% polyacrylamide gels. The pre mixed separating gel mix (5 ml) was mixed with 25 µl of 10% w/v Ammonium persulfate (APS) and 2.5 µl of TEMED, and allowed to polymerize at room temperature for about 30min. To set up the stacking gel, 2 ml of stacker solution was mixed with 20 µl of 10% w/v APS and 2 µl of TEMED. The stacking gel mixture was then loaded on top of the polymerized separating gel, and a comb of 10 wells was inserted into the stacking gel. The comb was removed after the stacker was polymerized.

2.3.3.4 Immunoblotting (Western blot)

Trans-Blot® SD Semi-Dry Electrophoretic Transfer Cell (BioRad, USA) was used to transfer proteins from polyacrylamide gels to Hybond-ECL nitrocellulose membranes (Amersham Biosciences, USA). Proteins were separated by 5%, 8%, 10% or 12% SDS-PAGE. Protein samples were mixed in SDS loading buffer and heat denatured at 95 °C for 5 min. Rainbow Marker (Invitrogen) was used as size standard marker. A stack of six pieces of 3MM paper (Whatman, UK) was soaked in protein transfer buffer and placed into the bottom part of the apparatus. A nitrocellulose membrane of the same size as the polyacrylamide gel was soaked with protein transfer buffer and placed on top of the 3MM paper stack. This was followed by the polyacrylamide gel and another stack of six pieces of 3MM paper soaked with protein transfer buffer, respectively. The upper part of the apparatus was assembled and 0.8 mA/cm^2 current was applied for 1 to 1.5 hours. After the transfer, the membrane was incubated in 4% milk in Tris Buffered Saline-Tween 20 (TBST) for 1 hour for blocking of non-specific protein-binding sites. The membrane was then incubated in 2% milk in TBST containing the primary antibody at

the appropriate dilution. After incubation at 4°C with shaking overnight, the membrane was washed four to five times with TBST for 5 minutes each. The membrane was then incubated in 2% milk in TBST containing the secondary antibody conjugated with horse reddish peroxidase (Amersham Biosciences, USA) at the appropriate concentration at room temperature for 2 hours. The membrane was then washed five to six times with TBST for 5 minutes each, incubated in 1ml ECL Western Blot Detection Reagent (Amersham Biosciences, USA) for 1 minute or Enhanced Chemiluminescence (ECL) system plus (Amersham, UK) reagent for 5 minutes, wrap with cling wrap, and exposed to light sensitive films (Fuji, Japan). The exact exposure time varied depending on the intensity of the signals. For all Western blots, representative examples of at least three independent experiments are shown.

2.4 Histological and morphological studies

2.4.1Tissue section

Paraffin section: The rat prostates were fixed in 4% paraformaldehyde (PFA) at 4 °C overnight, and then wash with tap water to eliminate the residue of PFA. The blocks of tissue were dehydrated by transferring sequentially to 30%, 50%, 70%, 80%, 90%, 95%, and 100% alcohols for about two hours each in Shandon Pathcentre® Tissue Processor (Thermo, USA). After dehydration, the tissues were embedded in paraffin. Then the blocks were cut at 5 microns on a microtome and float on a 40°C water bath containing distilled water. The sections were transferred onto a Superfrost Plus slides and dried overnight.

2.4.2 Hematoxylin and eosin staining

The paraffin sections were deparaffinized in xylene (2×3 minutes) and rehydrated by transferring sequentially to 100% ethanol (2×3 minutes), 95% ethanol (1×3 minute), 80% ethanol (1×3 minute) and deionized water (1×3 minute). After rehydrated, the sections were stained in hematoxylin solution for 1 minute and developed in Tap water for 5 minutes. Then the sections were stained in eosin solution for 30 seconds. After passed through 95% ethanol (2×3 minute), 100% ethanol (2×3 minutes) and xylene (2×3 minutes), the sections were mounted using Permount (Fisher, USA).

2.4.3 Immunohistochemistry

After deparaffining and rehydrating, endogenous peroxidase activity was quenched using 3% hydrogen peroxide incubation for 30 min and then rinsed with PBS (3×5 minutes). Then the slides were placed in 10mM sodium citrate buffer (pH 6) by boiling for antigen retrieval. The sections were rinsed with PBS (3×5 minutes), and then incubated in 10% normal goat serum blocking solution in a humidified box at room temperature for 1 hour. After blocking, the primary antibody at appropriate dilution in PBS-T solution was added and the sections were incubated in a humidified box at 4°C overnight. The sections were rinsed with PBS (3×5 minutes) to wash the primary antibody. The universal biotinylated secondary antibody in UltraVision One HRP Polymer detection kit (Thermo Fisher Scientific) was applied to the sections, and incubated at room temperature for 1 hour in dark room according to the manufacture's instructions. After rinsed with PBS (3×5 minutes), the staining was visualized using DAB Plus Chromogen, followed by counterstained with hematoxylin. The sections were

rinsed in tap water to stop the reaction. After dehydrated with 95% and 100% ethanol and cleared in xylene, the sections were covered with permanent mounting medium and observed in light microscope.

2.4.4 Immunofluorescence staining

For adherent cells, the cells were seeded in cover slip, and the density was about 50-80% confluent at the time of stain. After washed with PBS (2×5 minutes), the cells were fixed in 4% paraformaldehyde (PFA) for 10 minutes. The sections were rinsed with PBS (3×5 minutes) and then cells were permeabilized in PBS containing 0.5% Triton X-100 for 10 min. After washing three times with PBS for 15 min, cells were blocked by 10% normal goat serum for 30min at room temperature to block non-specific binding sites, followed by appropriate diluted primary antibody in a humidified box at 4°C overnight. Cells were washed with PBS three times and incubated with secondary antibody (1:500, Alex 488-conjugated IgG (Molecular Probes) in dark room for 30 minutes at room temperature. Unbounded antibody was removed by washing with PBS three times for 5 min each and then counterstained with DAPI (Sigma) for 5 min. Finally, cells were washed and the slides were mounted to observe under Nikon eclipse 80i microscope with Nikon intensilight C-HGF1 Fluorenscence transmitter. Negative controls were performed by omission of primary antibodies and replacing it with PBS.

2.5 Functional studies

2.5.1 Measurement of intracellular pH in prostate epithelial cells

The technology of measurement of pH_i for many kinds of cells has been described previously (Wang et al., 2002). The measurement of pH_i was achieved by an inverted fluorescent microscope IX-70 (Nikon Eclipse Ti) equipped with a CCD camera (Figure 1), together with a specially designed miniature Ussing chamber (Zoophysioloical Laboratory A, August Krogh Institute, University of Copenhagen, Denmark), which allows bathing solutions to perfuse in apical and basolateral compartment separately. The bottom of chamber was water-sealed by adhering a 29mm diameter glass coverslip onto it with melted dental sticky wax.

The cells were seeded onto each filter membrane, which was made of Matrigel basement membrane matrix (1:8 in PBS) pre-coated clear Transwell-Col membranes with pores of 0.45μm as described in Figure 2.1 through the metal ring. After 24 hours, the metal rings and glass supports were removed from the wells and culture medium were replaced. Due to the transparent properties of the filter, the confluence of cells could be monitored under a conventional inverted microscope. After incubation at 37°C in 5% CO_2 for about 5-6 days, the epithelial cells would form a confluent monolayer. For intracellular pH (pHi) measurement, 5μM 2', 7'-bis-2(2-carbosyethyl)-5-(and-6)-carboxyfluorescence, acetoxymethyl ester (BCECF) was added for 30 min at 37°C. The sample was then mounted into the miniature Ussing chamber attached to the stage of the inverted fluorescence microscope IX-70 (Nikon Eclipse Ti) (Figure 2.2). Samples were superfused with preheated experimental solutions. The fluorescence changes were recorded on a CCD camera used in continuous acquisition mode. Using an excitation wavelength of 490/440 nm and an emission of 530 nm, a radiometric analysis of

fluorescence data was performed using Metafluor software. The ratio (490:440) of two signals is directly proportional to the pH.

The calibration curve for pHi was made according to the method of Thomas et al (Thomas JA, 1979). In brief, cells were exposed to Hepes-buffered solution containing 140 mM K^+ and 20 μM nigericin, and solution pH was adjusted at the different levels (from 6.0 to 8.0) with KOH. The calibration buffer is as followed Table 2.4.

2.5.2 Solutions

The normal Krebs-Henseleit (KH) solution, HCO_3^- free K-H solution and HCO_3^- &Cl^- -free K-H solution were used as bathing solutions in the intracellular pH measurement. Tables 2.1, 2.2 and 2.3 show the compositions and final concentrations of these solutions. The pH of the bathing solutions was maintained at 7.4 when gassed with 5% CO_2/95% O_2.

2.6 Statistical analysis

In pH measurement, the rate of pH recovery was expressed as ΔpH/min, which was obtained from the ratio of two wavelengths (490/440) in the initial 100-200 sec of pH change.

Results were expressed as means ± S.E.M, and Student's unpaired *t*-test was used for 2 groups of statistical analysis. Statistical analyses were performed by Prizm 5.0 software. A p value < 0.05 was considered statistically significant.

Table 2.1 Compositions and concentrations of normal Krebs-Henseleit (K-H) solution

Chemicals	Final concentration (mM)
NaCl	117.0
$NaHCO_3$	24.8
KCl	4.7
$MgCl_2$	1.2
$CaCl_2$	2.56
KH_2PO_4	1.2
Glucose	11.1

The pH value of the normal K-H solution was maintained at 7.4 when gassed with 5% CO_2/95% O_2.

Table 2.2 Compositions and concentrations of HCO_3^- free solution

Chemicals	Final concentration (mM)
NaCl	141.8
KCl	5.9
$MgSO_4$	1.2
HEPES	10.0
Tris	5.6
$CaCl_2$	2.56
Glucose	11.1

The pH value of the HCO_3^- free solution was maintained at 7.4 with 1 M Tris when gassed with 100% O_2.

Table 2.3 Compositions and concentrations of HCO_3^- & Cl^- free solution

Chemicals	Final concentration (mM)
Na-gluconate	117.0
K-gluconate	4.7
$MgSO_4 \cdot 7H_2O$	1.2
KH_2PO_4	1.2
HEPES	10.0
Tris	5.6
D-mannitol	25.0
Ca-gluconate	2.56
Glucose	11.1

The pH value of the HCO_3^- free solution was maintained at 7.4 with 1 M Tris when gassed with 100% O_2.

Table 2.4 High K^+ solution (for calibration)

Chemicals	Final concentration (mM)
KCl	140.0
$MgSO_4.7H_2O$	1.2
KH_2PO4	1.2
$CaCl_2.2H_2O$	1.3
Glucose	11.7
HEPES	10.0

The pH value of the KCl-calibration solution was titrated to different extracellular pH between 6.0 and 8.0 with HCl or KOH.

A)

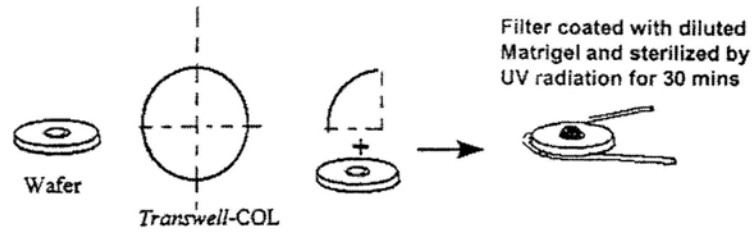

B)

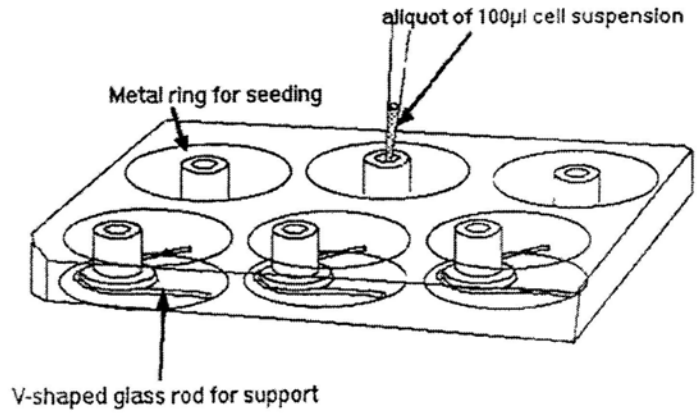

Figure 2.1 Diagrammatic illustration of preparation of permeable support for intracellular pH measurement. A) Transwells-Col membrane was cut into four smaller pieces and carefully stuck onto a wafer. The assembled wafers were then coated with Matrigel and irradiated under UV light for sterilization. B) V-shaped glass rod was used to support the wafer in the culture medium, with metal ring to confine the area for seeding. Cell suspension was added onto each wafer. The metal ring and glass rod were removed and culture media were replaced in each well after 24 hrs.

A)

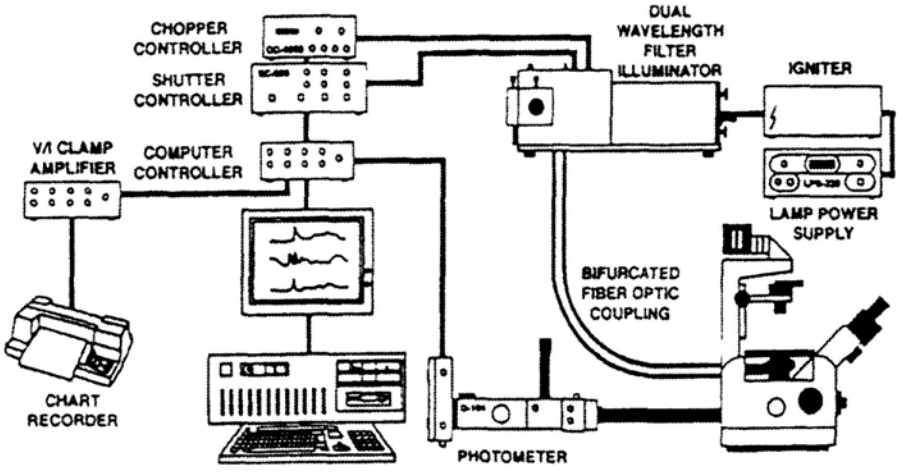

B)

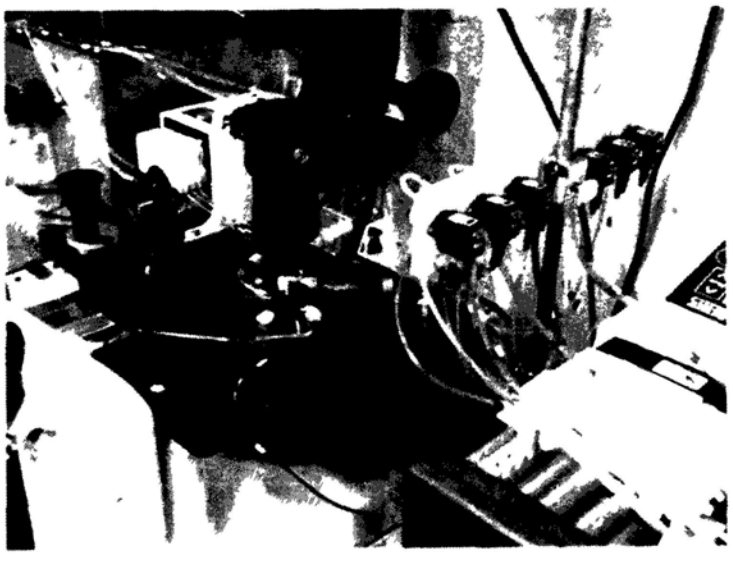

Figure 2.2 Setup of microspectrofluorimetry for luminal surface pH measurement. A) Schematic diagram showing experimental setup of microspectrofluorimetry for intracellular pH measurement. B) A picture showing perfusing chamber on the stage of the inverted microscope.

Appendix A Antibodies used for immunoblotting in the present study

NAME	SIZE (kDa)	TYPE	CAT#	HOST	VENDORS	CROSS REACT
CFTR	160,180	Monoclonal	804-214	Mouse	Alexis	Human, Mouse, Rat
	160	Polyclonal	ACL-006	Rabbit	Almone labs	Human, Rat, Pig
CAII	29	Polyclonal	Sc-25596	Rabbit	Santa Cruz	Human, Mouse and Rat
β-tubulin	55	Polyclonal	SC-9104	Rabbit	Santa Cruz	Human,Rat and Mouse
cytokeratin 5 & 8	40~68	Monoclonal	MA1-06314	Mouse	Research Diagnostic	Human, Mouse, rat, canine, rabbit, hamster and porcine
Bcl2	26	Polyclonal	sc-492	Rabbit	Santa Cruz	Mouse, Rat and Human
PCNA	34	Monoclonal	sc-56	Mouse	Santa Cruz	Mouse, Rat, Human, Insect and *S.pombe*
Cleaved Caspase3	17, 19	Polyclonal	9661	Rabbit	Cell signaling	Human, Mouse, Rabbit and Monkey

Appendix B

PCR reaction

Template	1µl
Primer F (2.5µM)	2.5 µl
Primer R (2.5µM)	2.5 µl
dNTPs (10 µM)	0.5 µl
Go Taq	0.2 µl
10 X PCR buffer	2.5 µl
ddH_2O	15.8 µl

Buffer recipe

RIPA buffer

NaCl	150 mM
Tris-Cl, pH 8.0	50 mM
NP-40	1%
Deoxycholic acid	0.5%
SDS	0.1%
PI mix	1X
PMSF	0.5 mM

Sample buffer

Tris-Cl, pH 6.8	0.35 M
Glycerol	30%
SDS	10.3%
DTT	0.6 M
Bromophenol Blue	0.05%-0.1%

Protein transfer buffer

Tris base	25 mM
Glycine	0.192 M
SDS	0.1%
Methanol	20%

Running buffer

Tris base	25 mM
Glycine	0.192 M
SDS	0.1%

TBST

Tris-Cl, pH 8.0	10 mM
NaCl	150 mM
Tween 20	0.5%

SDS-PAGE stacking gel

30% polycarylamide	0.375ml
ddH_2O	2.2 ml
Tris-Cl 1.0M pH 6.8	0.375 ml
10% SDS	15 µl
10% APS	15 µl
TEMED	3 µl

Separating gel (example 12.5%)

30% polycarylamide	3.2 ml
ddH_2O	1.5 ml
Tris-Cl 1.0M pH 8.8	2.8 ml
10% SDS	37.5 µl
10% APS	37.5 µl
TEMED	7.5 µl

PBS

NaCl	137 mM
KCl	2.7 mM
Na_2HPO_4	4.3 mM
KH_2PO_4	1.4 mM

Chapter 3

A bacterial killing mechanism involving CFTR-mediated bicarbonate secretion in prostatitis

3.1 Summary

Prostatitis is one the most common urological disorders in men, which is associated with a characteristic increase in prostatic fluid pH; however, the cellular mechanism underlying this pH increase and its physiological significance have not been elucidated. Here we report the involvement of CFTR, a cAMP-activated anion channel conducting both Cl^- and HCO_3^-, in mediating prostate HCO_3^- secretion and its possible role in bacterial killing. Upon *Escherichia coli* (*E coli*) LPS challenge, the expression of CFTR and carbonic anhydrase II (CA II), a key enzyme involved in cellular HCO_3^- production, along with several pro-inflammatory cytokines including IL-6, IL-1β, TNF-α, was upregulated in the primary culture of rat prostate epithelial cells. Inhibiting CFTR function *in vitro* or *in vivo* resulted in reduced bacterial killing by prostate epithelial cells or the prostate. High HCO_3^- content (>50 mM), rather than alkaline pH, was found to be responsible for bacterial killing. The direct action of HCO_3^- on bacterial killing was confirmed by its ability to increase cAMP production and suppress bacterial initiation factors in *E coli*. The relevance of the CFTR-mediated HCO_3^- secretion in humans was demonstrated by the upregulated expression of CFTR and CAII in human prostatitis tissues. The present results have revealed a previously undefined role of CFTR in prostatitis and in host defense against bacterial infection in the prostate.

3.2 Introduction

Prostatitis is one the most common urological disorders in men and up to half of the male population may suffer from prostatitis at some time in their lives (Snow DC, 2010). Prostatitis usually presents with irritative or obstructive voiding symptoms, genitourinary, pelvic or rectal pain, and is sometimes associated with sexual dysfunction and infertility (Lipsky BA, 2010; Giamarellou H, 1984; Wolff H, 1991; Leib Z, 1994; Cunningham KA, 2008). According to the recent consensus definition by the National Institute of Health (NIH), prostatitis can be classified into 4 categories. The first 2 categories include prostatitis with bacterial infection, acute bacterial prostatitis (Category I) and chronic bacterial prostatitis (Category II). Chronic nonbacterial prostatitis/chronic pelvic pain syndrome belongs to category III and asymptomatic inflammatory prostatitis belongs to category IV. Clinically, only 5-10% of the prostatitis cases are diagnosed with bacterial infection (category I and II), of which 50-80% is caused by *E coli* (Mitsumori K, 1999), while nonbacterial prostatitis accounts for more than 90-95% of the clinical cases (Snow DC, 2010; De la Rosette JJ, 1993). Irregardless the types of prostatitis, with bacterial infection or not, the common feature in most cases is the inflammation of the prostate gland with the presence of white blood cells or elevated levels of cytokines, especially IL-1β and TNF-α, in the expressed prostate secretion (EPS) or post-prostate-message urine (Alexander RB, 1998; Jang TL, 2003; He L, 2010).

Another hallmark of prostatitis is an alkaline shift in pH consistently found in the expressed prostate secretion (EPS), which appears to accompany with the inflammatory response of the prostate with or without bacterial infection (Fair WR, 1978, Pfau A,

1978; Blacklock NJ, 1974; Weidner W, 1992; White MA, 1975; Chen J, 2007, Lipsky BA, 2010). The pH value of the prostate fluid appears to reflect the intensity of inflammation reaction and in general, the more serious inflammation as reflected by larger number of white blood cells, the more alkaline of the pH value (White MA, 1975, Thin RN, 1991). It has also been reported that the pH of EPS in bacterial prostatitis is significantly higher than that in nonbacterial prostatitis (Chandiok S, 1992). While the marked increase in the pH of EPS has been considered of diagnostic value (Blacklock NJ, 1974; White MA 1975; Chen J, 2007), it is also thought to be one of the reasons for poor results of antibiotic therapy (Weidner W, 1992). Normal human prostatic fluid has a pH value between 6.2-6.6, which is significantly lower than that of the plasma value of 7.4 (Blacklock NJ, 1974; Chen J, 2007). This pH gradient allows electrically neutral molecules, e.g. drugs and antibiotics, to penetrate into the prostate, become ionized and be trapped or concentrated in the prostate fluid (Winnigham DG, 1968; Bjerklund Johansen TE, 1998; Lipsky BA, 2010). However, upon inflammation, the prostate fluid may become markedly alkaline (> pH 8.0), which may affect the concentration of drugs or antibiotics in the prostate (Blacklock NJ, 1974; Lipsky BA, 2010). The variation in pH in prostatitis may also considerably alter the therapeutic efficacy of antibiotics, apart from their reduced concentrations in the prostate (lipsky BA, 2010).

Despite the diagnostic and therapeutic implications of the pH in the EPS, the molecular mechanism governing the pH regulation of the prostate fluid in normal and inflammatory state remains large unknown. The glandular epithelium of the prostate is known to secrete citric acid, which is thought to maintain the osmotic pressure and pH of the prostate fluid. The pH increase observed in prostatitis has been proposed to be due

to impaired secretory function of the prostate (i.e. reduction in citric acid level) upon inflammation (Chen J, 2007). However, whether the increase in pH seen in prostatitis is simply due to a decrease in the relative level of citric acid, or an increase in the secretion of alkaline substances or ions, such as bicarbonate, is not clear. More importantly, the question as to whether the characteristic increase in prostatic fluid pH in prostatitis is of any physiological significance has not been addressed.

The cystic fibrosis transmembrane conductance regulator (CFTR) is a cAMP-activated ion channel which is found in a wide variety of epithelial tissues including the lung, liver, pancreas, intestine, reproductive tracts and sweet glands (Chan HC,2006; Hug MJ,2003; Strong TV,1994; Cohn JA,1991). Mutations in the CFTR gene are known to cause cystic fibrosis (CF), a lethal genetic disease found among Caucasian, which is characterized by defective Cl^- and HCO_3^- secretion (Kopelman H 1988; Devor DC, 1999). CFTR may conduct HCO_3^- directly as an anion channel with measured HCO_3^- permeability (Poulsen JH, 1994) or indirectly as a Cl^- channel working in parallel with Cl^-/ HCO_3^- exchangers to provide a recycling pathway (Lee, M G., 1999; Ishiguro H, 2007; Chen WY, 2009). In fact, our previous studies have demonstrated the involvement of CFTR in mediating uterine and oviductal HCO_3^- secretion, which are vital to the fertilizing capacity of sperm and emebryo development (Wang XF, 2003; Chan HC, 2009; Chen MH, 2010). Since CFTR is also known to be expressed in the human prostate (Walker J, 1995; Hihnala S, 2006; Qiao D, 2008), it may also play a role in prostatic HCO_3^- secretion as well although the physiological role of CFTR in the prostate has not been elucidated.

It has been reported that under the circumstances of inflammation, or upon bacterial infection, the increased release of inflammatory cytokines such as IL-1β and TNF-α have potent effect on up-regulation of CFTR in epithelial cells (Cafferate EG, 2000; Ajonuma LC, 2008). Since increased levels of inflammatory cytokines including IL-1β and TNF-α are also found in prostatitis, with or without bacterial infection, they may also up regulate CFTR in the prostate, thereby enhancing HCO_3^- secretion and leading to the characteristic pH increase in prostatitis. Interestingly, recent studies have indicated the possible involvement of defective CFTR-mediated HCO_3^- secretion in the pathogenesis of CF (Choi JY, 2001. Quinton PM, 2001; Wang XF, 2003). There seems to be a link between defective HCO_3^- secretion and higher risk of infection in CF. Most CF patients, about 95%, die from lung infection with airway acidification found (Tate S, 2002). It has been reported that the acidity in CF airways may be due to defective HCO_3^- ion transport (Coakley RD, 2003), although the exactly role of HCO_3^- in CF pathogenesis is still not fully understood. Of note, HCO_3^- has been implicated in bacterial killing, however whether its action is direct or indirect remains unclear (Corral LG, 1988; Thompson, KD, 1993; Drake, DR ,1995; Craig, SB , 1999; Jarvis GN , 2001). Recently it has been reported that in the presence of carbonate, the susceptibility of bacteria to antimicrobial peptides may be increased since carbonate may induce global changes in the structure and gene expression of bacteria (Dorschner RA, 2006). Thus, the increased pH observed in prostatitis would be of physiological significance for host defense against bacterial infection and the pH increase should be due to enhanced prostatic HCO_3^- secretion.

Taken together, we hypothesized that CFTR might be involved in prostatic HCO_3^- secretion, its upregulation by inflammatory cytokines and thus enhanced HCO_3^- secretion might be responsible for the hallmark increase in pH observed in prostatitis. We further hypothesized that the enhanced CFTR-mediated HCO_3^- secretion in prostatitis might be an important host defense mechanism of the prostate against bacterial infection. We undertook the present study to test these hypotheses using a primary culture of rat prostatic epithelial cells and a rat prostatitis model. We demonstrated the expression of CFTR in rat prostatic epithelium and its involvement in prostatic bicarbonate secretion. The results showed that CFTR as well as carbonic anhydrase II (CAII), which is a key enzyme responsible for conversion of HCO_3^- from CO_2, could be up-regulated during prostate inflammation in the animal model and human prostatic tissues with inflammation. The role of CFTR in host defense of the prostate was demonstrated by impaired bacterial killing activity upon interfering with CFTR function *in vitro* and *in vivo*. The direct effect of HCO_3^- on bacterial killing and possible underlying mechanism were also investigated. The present results have provided the molecular mechanism underlying the long observed pH increase in prostatitis and demonstrated a previously unsuspected role of CFTR in the host defense of the prostate.

3.3 Materials and Methods

3.3.1 Animals

Male 4-week-old and 12-week-old SD rats were kept in the Laboratory Animal Service Center of the Chinese University of Hong Kong. Ethics committee approval was

obtained prior to the study and the animal experiment was conducted in accordance with the Laboratory Animals Service Center's guidelines.

3.3.2 Primary culture of prostate epithelial cells from immature SD rats

The 4-week-old SD rats were killed by placing them in a CO_2-gassed chamber for about 3 minutes. The prostate epithelial cells were enzymatically isolated from the rat prostate according to the method described by Shigeo Taketa (Shigeo Taketa et al, 1990) with some modifications. In brief, the ventral prostates of 4-week-old rats were removed and placed into a Petri dish containing sterile HBSS. After washing with HBSS and the prostates were sliced into small pieces. The sliced tissue were placed in RIPM 1640 medium containing 0.1% collagenase I (Sigma) and incubated at 35°C for 45min with constant shaking. After enzyme digestion, the supernatant fraction was passed through a 100-μm mesh cell strainer (BD Falcon™). The filtrate was centrifuged at 1000rpm for 5 min. The tissue pieces remaining in the tube were subjected to digest twice as before and the final supernatant was pooled with the first fraction after sieving. The combined cells were collected by centrifugation at 1000rpm for 5min and then washed twice with RIPM 1640 medium. The cells were finally suspended in 10ml RIPM 1640 medium containing 10% FBS and incubated at 37°C in a humidified atmosphere containing 5% CO_2 overnight to remove fibroblasts. The cell supernatant was collected and cultured in a new culture flask with McCoy's 5A (Sigma) medium containing 5% FBS, 10ug/mL Insulin(Sigma),10ug/mL EGF (Sigma), 5ug/ml transferring (Sigma), 10ng/ml cholera toxin (Sigma), 25ug/mL Bovine pituitary extract (BD), 100 U/ml penicillin, 100 μg/ml streptomycin for further study (Taketa S, 1990).

3.3.3 RT-PCR

RT-PCR for cultured prostate epithelial cells was performed as described in chapter 2 section 2.3.2.

The RNA of *E.coli DH5α* in different concentration of bicarbonate and pH were extracted using Trizol Bacterial isolation kit (Invitrogen). The reverse transcription and PCR was performed as described in chapter 2 section 2.3.2.

3.3.4 Western blot

Western blot for cultured prostate epithelial cells were performed as described in chapter 2 section 2.3.3.

3.3.5 Immunohistochemistry and Immunofluorescent Staining

Immunohistochemistry staining for rat and human prostate and immunofluorescent staining for cultured prostate epithelial cells were performed as described in chapter 2 section 2.4.3 and 2.4.4.

3.3.6 Measurement of intracellular pH in primary prostate epithelial cells

To establish a cell culture system of polarized prostate primary epithelial cells with both apical and basolateral compartment, the isolated cells were seeded at a density of about 2×10^5cells/ml onto each filter membrane, which was made of Matrigel basement membrane matrix (1:8 in PBS) pre-coated clear Transwell-Col membranes with pores of 0.45μm. After incubation at 37°C in 5% CO_2 for about 5-6 days, the epithelial cells would form a confluent monolayer. The method to measurement of intracellular pH in primary prostate epithelial cells was described in chapter 2 section 2.5.1.

3.3.7 *In vitro* Escherichia coli 055:B5 LPS stimulation

The stimulation experiment was performed in cultured epithelial cells. LPS from *E.coli* 055:B5 (Sigma) was used. Primary prostate epithelial cells were stimulated with 1 μg/ml LPS for 24h. RT-PCR was performed to detect the expression of CFTR, CAII, and pro-inflammatory cytokines in LPS stimulated or control cells.

3.3.8 Antibacterial assay *in vitro*

The isolated cells were plated onto Transwell-Col membranes (0.45 cm^2) coated with Matrigel and cultured like before. For infection, a total of 1×10^5colony-forming units (CFU) of *E.coli DH5α* were added to the apical compartment of the epithelial cells. For blocking of CFTR or carbonic anhydrase, the *E coli* treated epithelial cells were preincubated with 10 μM $CFTR_{inh}$-172 (Sigma), a specific CFTR channel blocker (Muanprasat C, 2004) or anti-CFTR antibody (1:500, Alomone labs) or 50 μM Acetazolamide (Sigma), a carbonic anhydrase inhibitor for 24h before the addition of bacteria. Same concentration of DMSO or control IgG was added as control. After 18h, the apical medium was collected for CFU counting on a Luria broth agar plate after overnight incubation.

3.3.9 Bacterial prostatitis model

The adult 12-week-old male SD rats weighed between 250 and 350 g were used in the present study. A strain of *E.coli DH5α* was grown overnight in a Luria broth in a shaker at 37°C. The bacterial cells were pelleted, washed three times in sterile PBS and resuspended to 1×10^8 cells /ml. The rats were divided into two groups. Each group was anesthetized with ketamine (50 mg/kg) and xylazine (12 mg/kg) and subjected to

laparotomy to expose the ventral prostate. One group was injected 200ul of the *E.coli* suspension with a 1ml/100U insulin syringe and 30-G needle directly beneath the capsules of two sides of ventral lobes. The other group was injected the same amount of *E.coli* combined with 10μM $CFTR_{inh}$-172. We excluded two rats from the study which died of sepsis. The animals were killed 48h after surgery and the ventral prostates from each rat were weighted, sliced into pieces and sonicated for 30 min in 10 ml PBS. The sonicated tissue was cultured quantitatively using the pour plate technique; the dilutions of the homogenates were plated on a LB plate and incubated overnight at 37°C. The number of colonies was then counted. The bacterial counts were expressed as the log of CFU per gram of prostate.

3.3.10 Antibacterial assays in different concentration of bicarbonate and pH

E.coli DH5α was grown in a Luria broth at 37°C in a shaker to grow to log phase. Assay solutions were prepared as the Table 2 using NaCl to keep the same concentration of sodium in the solutions. The solutions were made without fixing the pH and allow the change of HCO_3^- to alter its pH. The osmolarity of each solution is the same. A concentration of 1×10^9 cells/ml of *E.coli* was incubated at 37°C in the absence or presence of different concentration of $NaHCO_3$ for 2 h and then OD_{600} was read. Another set of experiments was to examine the bactericidal activities of pH. We maintained the HCO_3^- concentration at 25 mM (physiological concentration), and a range of different pH values (7.35, 7.95, 8.14 and 8.24) which was corresponding with different concentration of bicarbonate was achieved by using HCL. *E.coli* was incubated for 2 h and OD_{600} was read.

3.3.11 Intracellular cAMP measurement

E.coli cells were exposed to different concentrations of HCO_3^- in LB broth for 2h and the cultures were harvested by centrifugation at 3,000 × *g* for 10 min. The pelleted cells were treated with 0.1M HCl provided with the cAMP enzyme immunoassay system (Assay Designs, Ann Arbor, MI). After incubating for 30 min and centrifugation at 3,000 × *g* and 4°C for 10 min, the cAMP concentrations in supernatants were determined by using the kit according to the manufacturer's instructions. The average intracellular cAMP concentration (determined in triplicate) was expressed in picomoles per milliliter (pmol/ml).

3.3.12 Human prostate sample collection

Seven human prostate samples were obtained by transurethral resection from the suspected benign hyperplasia patients. Four samples from the patients with prostatitis showed evidence of lymphocytes infiltrates that were primarily centered in the peri-acinar region and stroma around acini and ducts. Tissue samples were obtained immediately after surgery and fixed in 4% paraformaldehyde (PFA) for paraffin section. The Ethics Committee of Peking University Shenzhen Hospital granted approval for the study prior to sample collection.

3.3.13 Statistical analysis

Statistical analyses were performed by Prizm 4.0 software. Results were presented by mean ± S.E.M. Groups of data were compared by student's *t*-test. p value < 0.05 was considered statistically significant.

3.4 Results

3.4.1 CFTR expression in the epithelial cells of rat ventral prostate

In order to use a rat prostate model to investigate the role of CFTR in prostatitis, we first examined its expression in rat prostate since CFTR expression in the prostate has not been demonstrated in any species other than the human. Immunohistochemistry revealed that CFTR immunoreactivity was detected in the apical surface of the epithelial cells of the rat ventral prostate (Figure 3.1).

3.4.2 CFTR expression in cultured rat primary epithelial cells

Epithelial cells were separated from the stromal cells by taking advantage of the fact that stromal cells attach faster than epithelial cells. The purity of epithelial cells culture was assessed by light microscopy. From the Figure 3.2A we can see that the prostate epithelial cells in culture showed polyhedral shapes that apposed to each other, forming discrete colonies. The separately cultured prostate stromal cells exhibited an elongated spindle-shaped morphology that is typical of cultured fibroblast (Figure 3.2B). Secretory cells expressed cytokeratins 8 and 18, whereas basal cells expressed cytokeratins 5 and 14. The results of immunofluorescent staining showed that the cultured cells expressed the cytokeratin 5&8 which is specific for epithelial cells (Figure 3.3).

We further confirmed CFTR expression in a primary culture of rat prostate epithelial cells. RT-PCR results revealed a PCR product with expected size of rat CFTR (481 bp) (Figure 3.4A). Western blot also showed a band of 160 KD as expected of CFTR (Figure 3.4B). Immunofluorescent staining also localized CFTR protein to the plasma membrane of the culture epithelial cells (Figure 3.4C),

3.4.3 Involvement of CFTR in mediating prostatic bicarbonate secretion

To investigate the role of CFTR in prostatic HCO_3^- secretion, we measured the intracellular pH (pHi) in the established culture of prostate epithelial cells. Cellular alkalization was induced by removing HCO_3^-/CO_2 from the perfusate (Figure 3.5A), and the rate of pHi recovery, which reflects HCO_3^- extrusion, was measured. When extracellular Cl^- was removed from the apical perfusion solution, the rate of pHi recovery was greatly attenuated in comparison with that in the Cl^--containing solution (Figure 3.5B), indicating the operation of a Cl^--dependent HCO_3^- extrusion process, probably involving an anion exchanger. However, the rate of pHi recovery, in the absence of Cl^- or inactivation of the Cl^-/ HCO_3^- exchanger, could be increased by an adenylyl cyclase activator, forskolin, indicating a cAMP-dependent HCO_3^- extrusion pathway (Figure 3.5C). The forskolin-induced pHi recovery could be blocked by NPPB (100 μM) (Figure 3.5D), a blocker known to inhibit CFTR, suggesting that CFTR may be responsible for the HCO_3^- secretion in the cultured prostate epithelial cells. These results indicate a direct role of CFTR in mediating prostate HCO_3^- secretion and an indirect role, possibly working in parallel with a Cl^-/ HCO_3^- exchanger for HCO_3^- extrution.

3.4.4 Rat prostate epithelial cells respond to *E coli*-LPS with up-regulated cytokines, CFTR and CA II expression

To mimic bacteria-induced inflammation in prostatitis, *Ecoli*-LPS, an endotoxin present in the outer membrane of the bacteria was used. We challenged the cultured prostatic epithelial cells with 1ug/ml *E.coli*-LPS for 24h and performed RT-PCR to

examine the expression of pro-inflammatory cytokine IL-6 (414bp), IL-1β (313bp) and TNF-α (292bp), with GAPDH (340bp) as the internal marker. The primers and annealing temperature used in the RT-PCR are shown in Table 3.1. We observed that IL-6, IL-1β and TNF-α mRNA expression were upregulated by *E.coli*-LPS (Figure 3.6A). We also examined the effect of *E.coli*-LPS on CFTR and CAII expression in cultured prostate epithelial cells. As shown in Figure 3.6C, E, CFTR and CAII mRNA and protein expression were significantly up-regulated upon stimulation of *E.coli*-LPS, as demonstrated by semi-quantitative RT-PCR and western blot analysis, respectively. These results suggest that CFTR and its mediated HCO_3^- secretion may be up regulated by inflammatory cytokines upon bacterial infection/inflammation, resulting in the alkaline shift in pH observed in prostatitis.

3.4.5 Bactericidal capacity of prostatic epithelial cells *in vitro* and involvement of CFTR

What is the physiological significance of the upregulation of CFTR and therefore enhanced CFTR-mediated prostatic HCO_3^- secretion during prostatitis? Since HCO_3^- has been implicated in bacterial killing, the enhanced CFTR-mediated HCO_3^- secretion in prostatitis may serve as a host defense mechanism. To test this, we inoculated 1×10^4 colony-forming units (CFU) of the gram-negative bacteria *E.coli*, which are responsible for up to 80% of the bacterial prostatitis in humans (Mitsumori K, 1999), to the primary culture of rat prostate epithelial cells and found no bacterial colony growth in the collected medium, indicating bactericidal capacity of the epithelial cells. When 1×10^5 CFU *E.coli* were added to the cells in the absence or presence of CFTR inhibitor, $CFTR_{inh}$-172 (10 μM) or CFTR antibody, we observed significantly larger number of

bacterial colonies in the medium collected from the $CFTR_{inh}$-172 and CFTR antibody treatment groups as compared to the non-treated control group (Figure 3.7A, B). To test whether this bactericidal activity was due to HCO_3^-, the cells were pretreated with carbonic anhydrase inhibitor, acetazolamide (50 μM), and it was found that the bactericidal capacity of the culture was greatly attenuated (Figure 3.7C). As controls, direct addition of CFTR inhibitor /antibody or acetazolamide to the bacterial culture (1×10^5 CFU) at the concentrations used did not affect the growth of *E.coli* (Figure 3.7D), excluding direct effect of the inhibitors/antibody on the bacteria.

3.4.6 Involvement of CFTR in bacterial killing *in vivo*

To further confirm the involvement of CFTR-mediated HCO_3^- secretion in bacterial killing in a physiological context, we established an *in vivo* prostatic bacterial infection model. Following bacterial inoculation (2×10^7 CFU) to the prostate, all samples collected from the bacterial prostatitis groups showed acute inflammation with severe infiltration of polymorphonuclear cells (PMNs) into bacteria-containing space. Injecting *E.coli* combined with 10μM $CFTR_{inh}$-172 resulted in a significantly higher number of bacteria isolated from the prostates, as compared to the control, 6.422 ± 0.168 $\log_{10}$ CFU/g vs. 5.224 ± 0.102 $\log_{10}$ CFU/g, respectively (Figure 3.8A). We further examined the expression of CFTR, CAII, IL-1β and TNF-α and they were all up regulated in bacteria-infected prostates (Figure 3.8B, C). These results suggest that the CFTR-mediated HCO_3^- secretion may be upregulated upon bacterial infection and involved in bacterial killing *in vivo*.

3.4.7 Bicarbonate itself but not alkaline pH is mainly responsible for bacterial killing

Since HCO_3^- is weak base and the bactericidal effect we observed *in vitro* and *in vivo* could be due to its buffering effect on the pH rather than HCO_3^- itself. To distinguish the two, we tested the bactericidal capacity of solutions with different concentrations of HCO_3^- (Table 3.2).Our results showed that the bacterial count of *E.coli* was significantly reduced by 80mM HCO_3^- with a significantly lower absorbance ratio (0.540 ± 0.012) as compared to HCO_3^- concentration at 0 mM (0.677 ± 0.015), 25 mM (0.723 ± 0.018) and 50 mM (0.623 ± 0.013) (Figure 3.9A). To exclude possible involvement of pH in the bacterial killing, we made up solutions with different pH (7.35-8.24) while keeping a constant HCO_3^- concentration at 25mM. The results showed that there was no significant difference in the bacterial killing capacity between groups with different pH values, at 7.35 (0.743 ± 0.033), 7.95 (0.700 ± 0.032), 8.14 (0.670 ± 0.031) and 8.24 (0.647±0.015) (Figure 3.9B). These results suggested that the antibacterial activities observed with 80 mM or 50 mM HCO_3^- were mainly due to HCO_3^- itself but not alkaline pH.

3.4.8 Bicarbonate suppresses the expression of initiation factors IF1, IF2 and IF3 in *E.coli*

What might be the molecular mechanism underlying the bacterial killing effect of HCO_3^-? Previous study in our lab demonstrated that when *E.coli* was exposed to different concentrations of HCO_3^-, their intracellular cAMP levels were elevated in a HCO_3^- concentration-dependent manner. Since elevated cAMP levels in bacteria are known to suppress protein synthesis (Bhattacharya, 1977; Kaul R, 1990), therefore, the

effect of HCO_3^- on suppressing the genes of bacterial initiation factors which are known to particitate in the process of protein biosynthesis in *E.coli* was examined. As shown in Figure 3.10, RT-PCR analysis of *E.coli* cultured in the absence or different concentrations of $NaHCO_3$ showed that the expression of IF1, IF2 and IF3 genes was significantly inhibited by HCO_3^- at the concentration of 80mM as compared to HCO_3^- at 0mM. However, alkaline pH with a constant HCO_3^- of 25 mM did not suppress these genes expression, excluding significant involvement of pH in bacterial killing.

3.4.9 The expression of CFTR and CAII is up-regulated in human prostatitis

While both *in vitro* and *in vivo* experiments on rat prostate epithelial cells strongly indicate that the CFTR-mediated HCO_3^- secretion is enhanced in prostatitis, which has bactericidal capacity, it remains to be confirmed that this host defense mechanism is also present in human prostate. We thus examined CFTR and CAII expression in human prostate hyperplasia samples with inflammation. Immunohistochemical results showed CFTR immunoractive signal at the apical border of the human prostatic epithelium (Figure 3.11A). Compared to the tissue without inflammation, the expression of CFTR in the prostate glands evident of lymphocytes infiltration (Figure 3.11B) was much stronger, indicating that the expression of CFTR is up-regulated in human prostatitis. The expression of CAII was detected in the cytoplasm of human prostate epithelial cells (Figure 3.11C), which was also up-regulated in the inflamed area of the clinical prostate hyperplasia samples (Figure 3.11D). The upregulation of both CFTR and CAII in the inflamed human prostate tissues indicate that the CFTR-mediated HCO_3^- secretion may also be enhanced upon inflammation, which may be responsible for the high pH observed in human prostatitis.

A)

B)

Figure 3.1 Expression of CFTR in rat prostate. (A) Immunohistochemical staining of CFTR in SD rat prostate. CFTR was expressed at the apical surface of rat ventral prostate epithelium. (B) Negative control in the absence of primary antibody. Scale bar: 50μm.

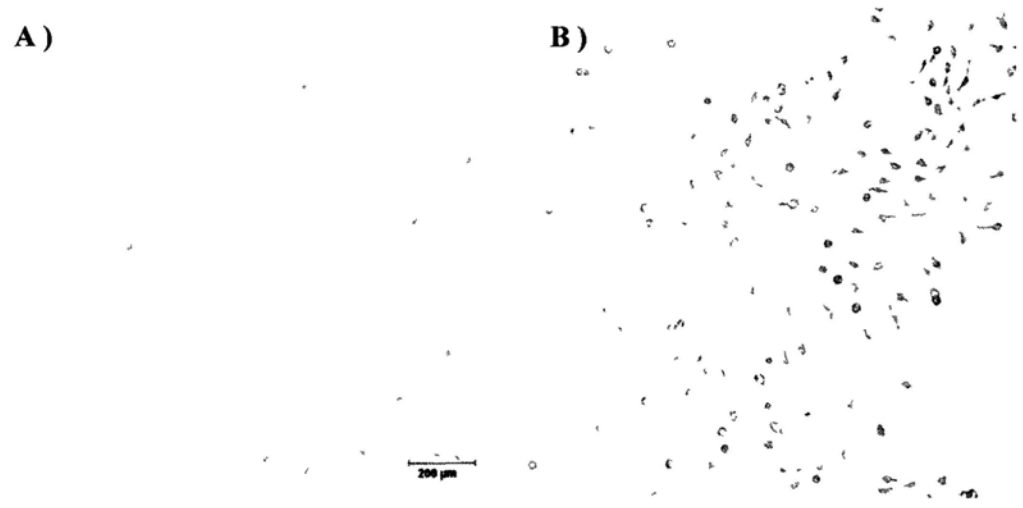

Figure 3.2 Phase contrast morphology of cultured cells *in vitro*. (A) The morphology of cultured rat prostatic epithelial cell. (B) The morphology of cultured stromal cells. Magnification 40×. Scale bar: 200 μm.

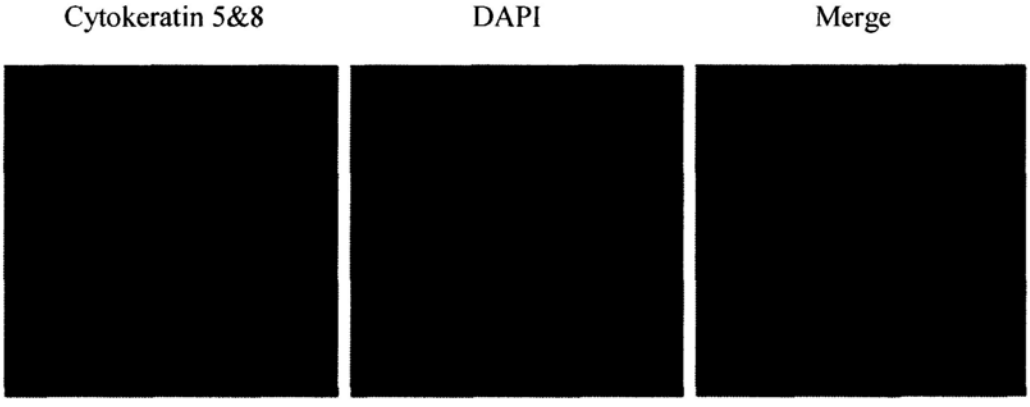

Figure 3.3 Immunofluorescence staining for the expression of cytokeratin 5&8 in cultured rat prostate epithelial cells. The cultured prostate epithelial cells were stained with cytokeratin 5&8 (left, green). Cell nuclei were counterstained with DAPI (middle, blue). Merged image was shown in the right panel. Magnification 200×, Scale bar: 20 μm.

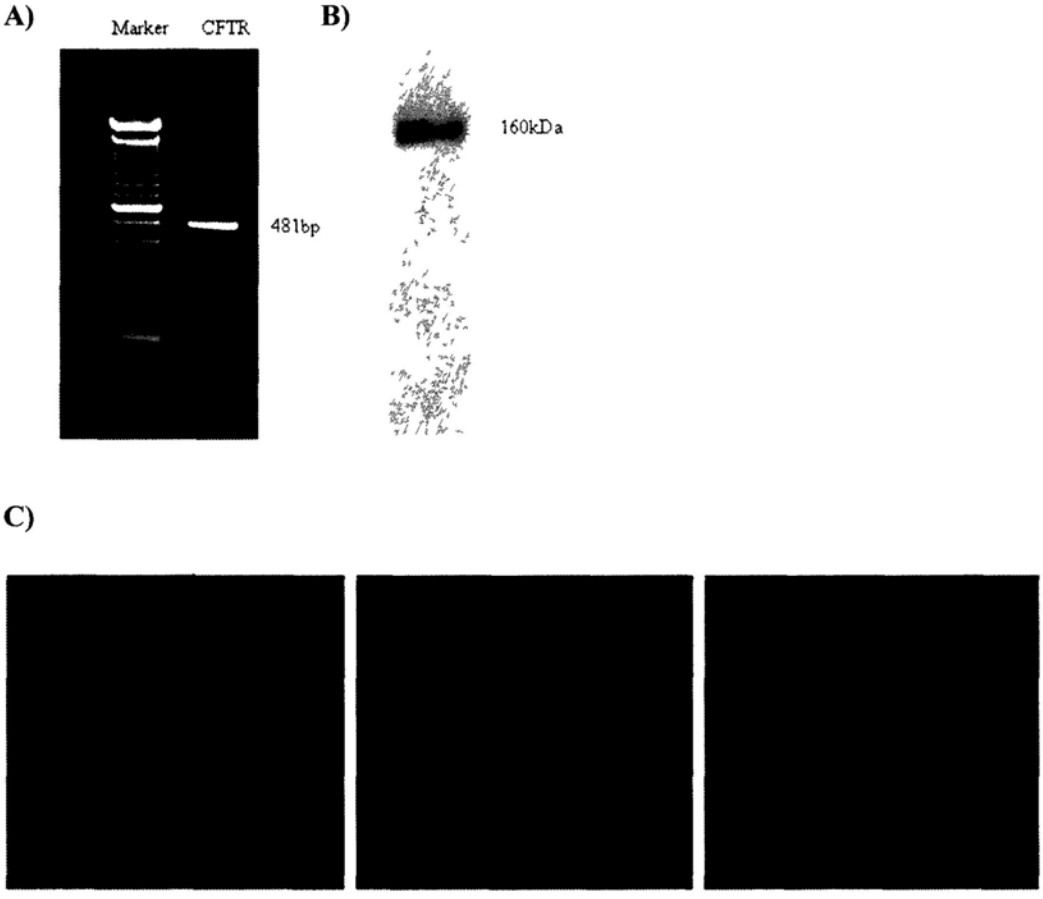

Figure 3.4 Expression of CFTR in cultured rat prostate epithelial cells. (A) CFTR transcript was detected by RT-PCR in cultured rat prostate epithelial cells with predicted amplification products at 481bp. (B) CFTR protein was detected in rat prostate epithelial cells by Western blotting using polyclonal CFTR antibody (1:500) which recognizes a band at MW 160 kDa. (C) Immunofluorescence staining for the expression of CFTR (left, green) in cultured cells .Cell nuclei was counterstained with DAPI (middle, blue). Merged images are shown in the right panel. Magnification 200×.

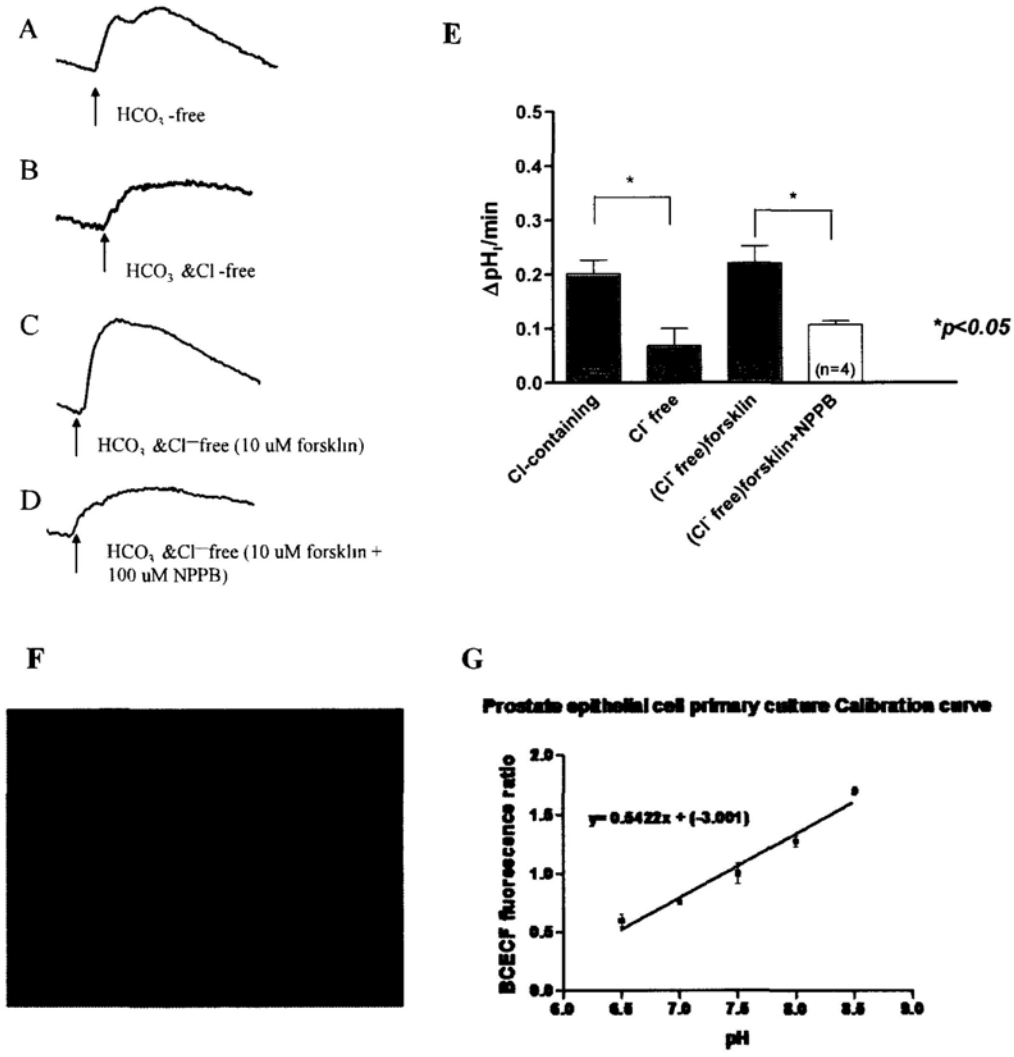

Figure 3.5 Involvement of CFTR in mediating cAMP-stimulated bicarbonate secretion by rat prostate epithelial cells. (A) The pHi recovered quickly after cellular alkalinization induced by removing bicarbonate/CO_2 from perfusate in the presence of Cl^-. (B) The rate of pHi recovery was markedly attenuated when extracellular Cl^- was removed from the perfusate. (C) In the absence of Cl^-, forskolin (forsk., 10 μM) stimulated pHi recovery. (D) The forskolin-induced pHi recovery could be blocked by NPPB (100μM). The scales in A-D are the same. (E) Summary of pHi recovery rates under different conditions after cellular alkalinization induced by removing bicarbonate/CO_2 from perfusate. (*$P < 0.05$) (F) The image of cells loaded with ECBCF. (G) Calibration of florescence ratio into intracellular pH value.

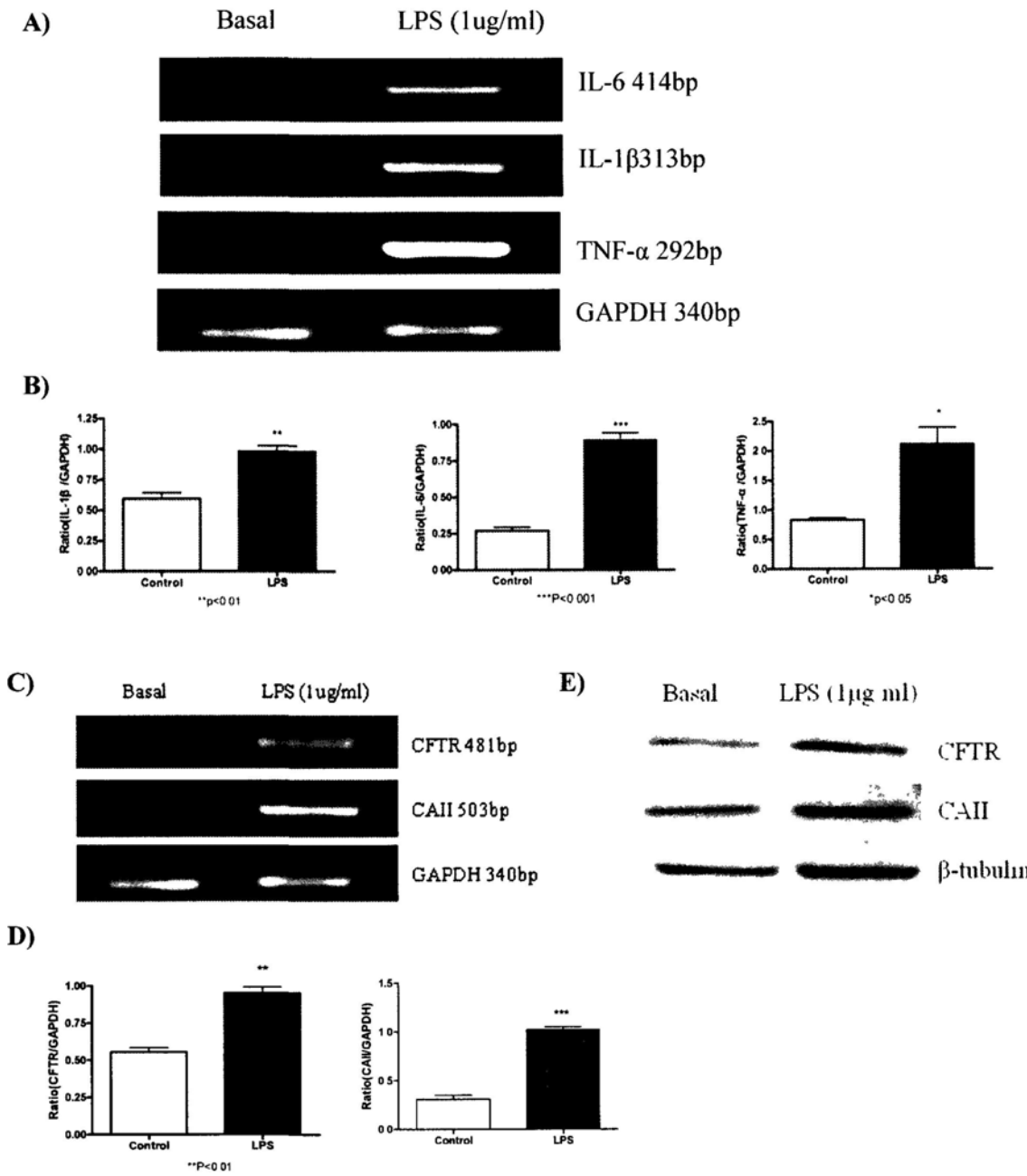

Figure 3.6 LPS-induced upregulation of cytokines, CFTR and CAII expression in rat prostate epithelial cells. Primary rat prostate epithelial cells were treated with 1μg/ml LPS for 24h. (A, C) The expression levels of IL-6, IL-1β, TNF-α, CFTR and CAII were evaluated by RT-PCR. GAPDH was used as control. (B, D) Quantification of the ratio of transcript to GAPDH. (E) LPS upregulates the protein expression of CFTR and CAII as detected by western blot, with β-tubulin used as the internal control.

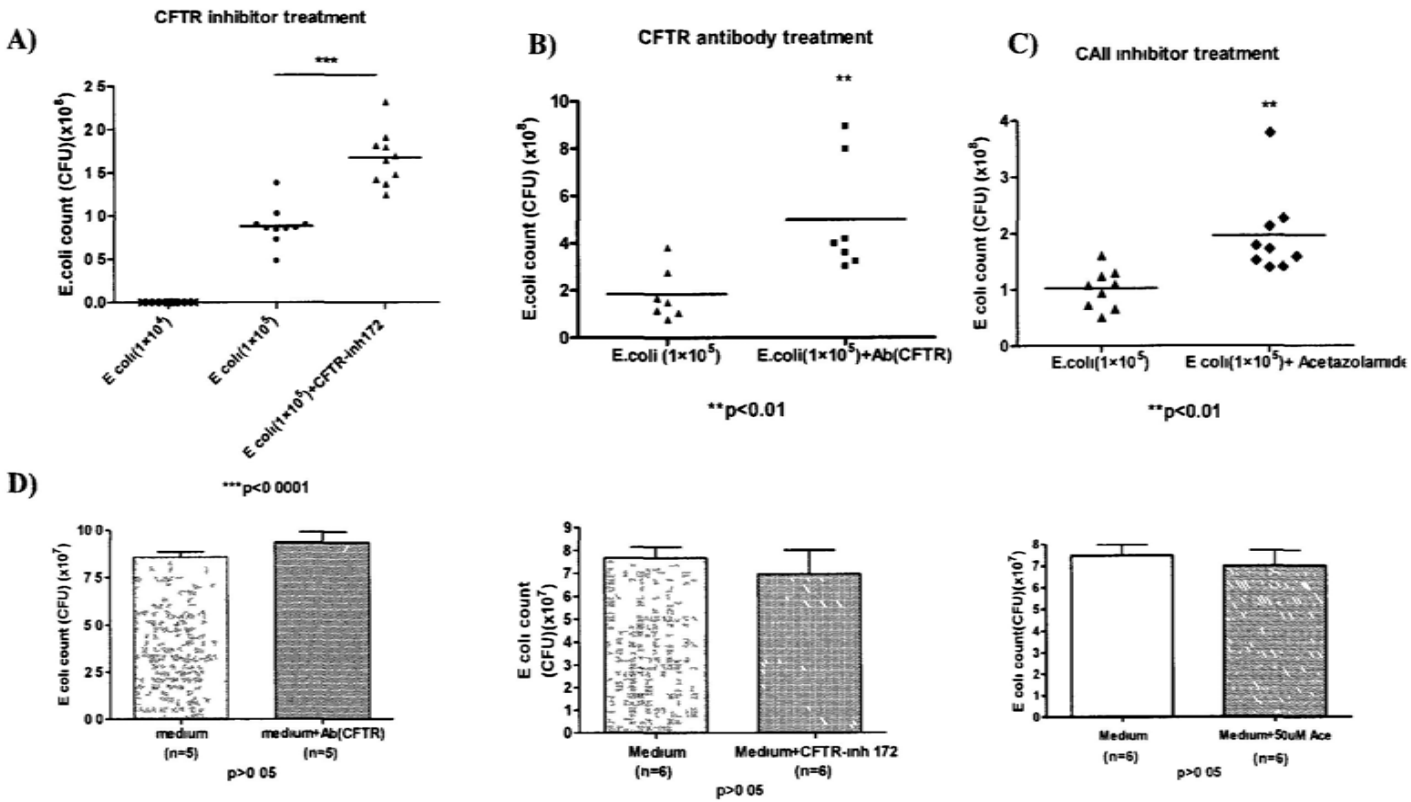

Figure 3.7 Involvement of CFTR and CAII in bacterial killing *in vitro*. CFTR inhibitor (A), CFTR antibody (B) or acetazolamide (C) were added with 1×10^5 CFU of *E.coli* to block CFTR or CAII activity and their effect on bacterial activity 18 hours after inocubation was shown. When 1×10^4 CFU of *E coli* was inoculated to the apical compartment of the rat prostate epithelial cells for 18h, there was no bacterial activity detected in the culture medium (A). Direct addition of CFTR-inh-172 or CFTR antibody or acetazolamide into the bacterial culture (1×10^5 CFU) did not affect the growth of *E.coli* (*D*). (**P<0.01, ***P<0.001)

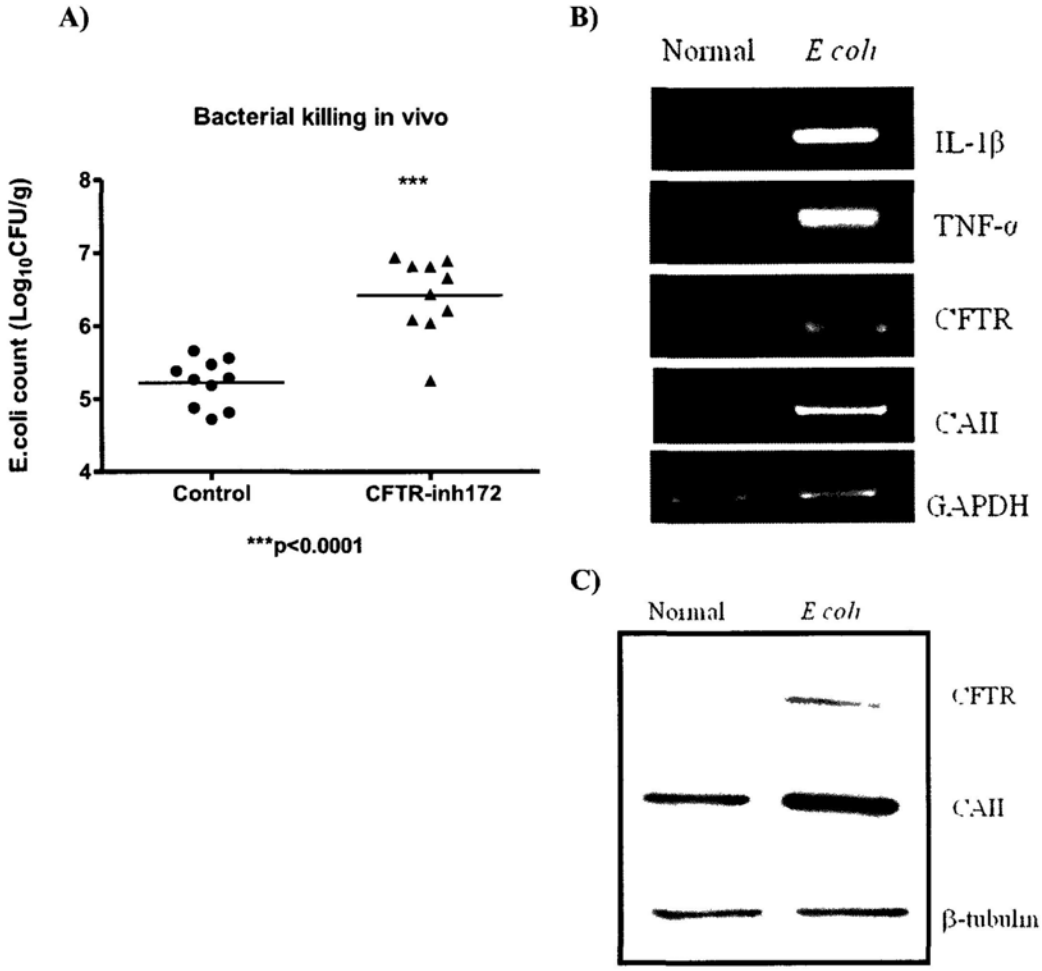

Figure 3.8 Bacterial killing effect of CFTR *in vivo* and upregulation of cytokines, CFTR and CAII in *E coli*-infected rat prostate. (A) Comparison of *E coli* bacterial activities recovered from rat prostatitis models without or with CFTR-inh 172 (10 μM). *E.coli* bacterial prostatitis in SD rats was established as described in Materials and Methods. Each point indicates the bacterial CFU per gram of prostate tissue weight (***P<0.001). (B) *E.coli* up-regulated the expression of cytokine genes, CFTR and CAII in rat prostate as determined by RT-PCR. (C) Expression of CFTR and CAII protein was significantly up-regulated in *E.coli* -infected rat prostate as determined by western blot.

Table 3.1 Primers and RT-PCR conditions

Primer name		Sequence(5'→ 3')	Length (bp)	Annealing temperature(°C)
GAPDH	Forward	GACCACAGTCCATGCCATCACTGC	340	55
	Reverse	GCTGTTGAAGTCGCAGGAGACAAC		
CFTR	Forward	AACTGAGACCTTACGCAG	481	55
	Reverse	AGAAGCTCTGGTCCTCTG		
CAII	Forward	ATGACCCTTCCCTACAGC	503	56
	Reverse	GGTCACACATTCCAGCAG		
IL-1β	Forward	CAACAAAAATGCCTCGTGC	313	58
	Reverse	TGCTGATGTACCAGTTGGG		
IL-6	Forward	AAATCTGCTCTGGTCTTCTGG	414	55
	Reverse	TTAGATACCCATCGACAGG		
TNF-α	Forward	TACTGAACTTCGGGGTGATCG	292	58
	Reverse	CCT TGTCCCTTGAAGAGAACC		
E.coli 16S	Forward	CTCCTACGGGAGGCAGCAG	162	55
	Reverse	GWATTACCGCGGCKGCTG		
E.coli IF1	Forward	ATGGCCAAAGAAGACAATATTG	216	55
	Reverse	AGCGACTACGGAAGACAATG		
E.coli IF2	Forward	TTTCCGCTTCAATCACTTTAC	165	55
	Reverse	CCTTGCTGAAACTGTCTACTG		
E.coli IF3	Forward	AAAGGCGGAAAACGAGTTC	541	55
	Reverse	CCTTACTGTTTCTTCTTAGGAGCG		

Table 3.2 Solutions for different concentration of HCO_3^-

HCO_3^- conc.(mM)	NaCl(mM)	$NaHCO_3$(mM)	KH_2PO_4(mM)	Na_2HPO_4(mM)	KCl(mM)	PH value
0	137	0	1.47	7.81	2.68	7.35
25	112	25				7.95
50	87	50				8.14
80	57	80				8.24

A)

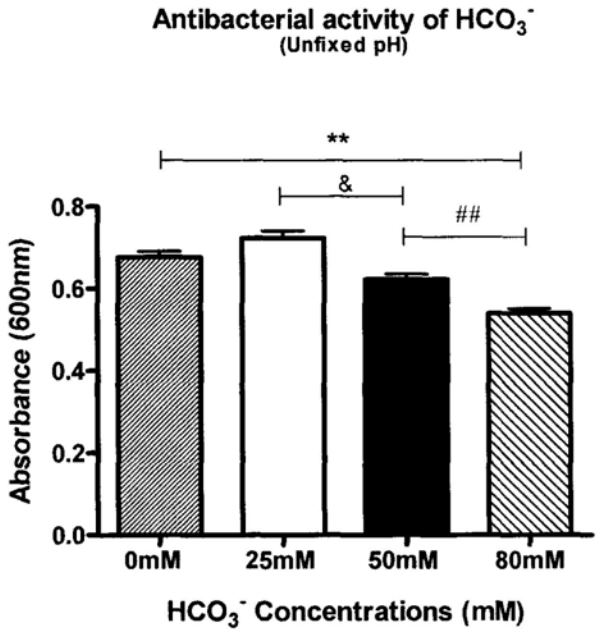

B)

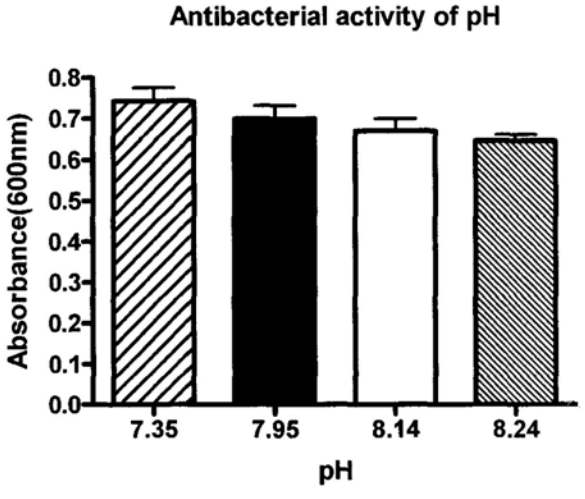

Figure 3.9 HCO_3^- but not pH exhibited bactericidal capacity *in vitro*. (A) *E. coli* activities remained after incubation with different concentrations of HCO_3^-. The activity of *E.coli* was inhibited by 80 mM HCO_3^- and 50 mM HCO_3^-, but not 25mM HCO_3^-. (B) Insignificant effect on bacterial activities of varied pH (at constant 25 mM HCO_3^-) at 7.35, 7.95, 8.14 and 8.24. (**P<0.01vs 0 mM HCO_3^- , $^{\#\#}$P<0.01vs 50 mM HCO_3^-, $^{\&}$P<0.05 vs 25 mM HCO_3^-)

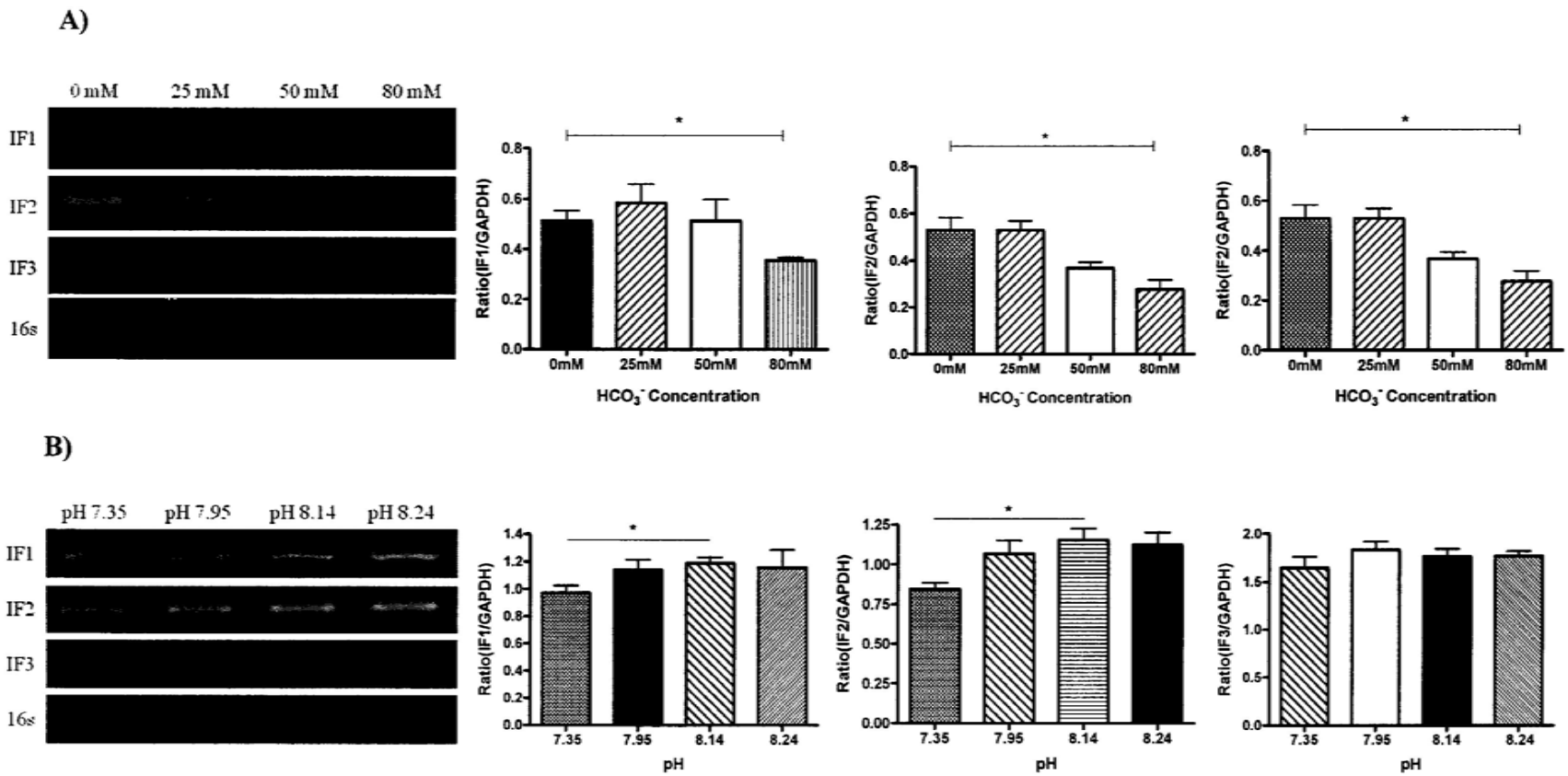

Figure 3.10 Effect of HCO_3^- and pH on expression of *E. coli* initiation factors IF1, IF2 and IF3. (A) The mRNA expression of initiation factors was significantly inhibited by 80 mM HCO_3^-. (B) Alkaline pH with a constant HCO_3^- of 25 mM did not suppress IF1, IF2 and IF3 gene expression. (*P<0.05)

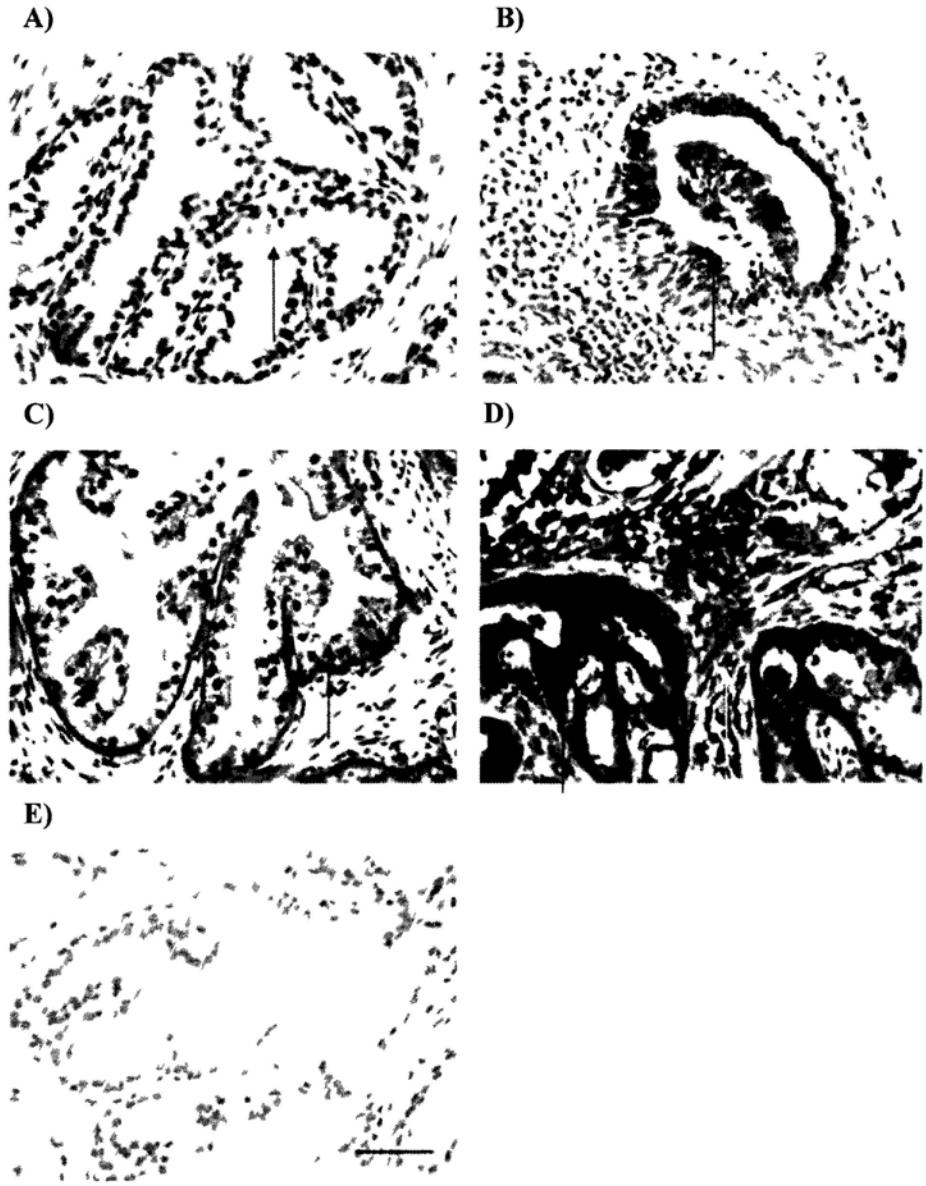

Figure 3.11 Expression of CFTR and CAII in human hyperplasia prostate with inflammation. CFTR (A, B) and CAII (C, D) was detected in human hyperplasia tissue .There was lymphocytes infiltration (Yellow arrow, B, D) in the inflamed area of the clinical prostate hyperplasia samples. Note that the expression of CFTR and CAII was stronger in the area with lymphocytes infiltration (Red arrow, B, D) than those without infiltration (Red arrow, A, C) (E) Negative control. Scale bar 50μm.

3.5 Discussion

Almost all cases of prostatitis, whether it is bacterial or non-bacterial, exhibit a characteristic alkaline shift in pH (Fair WR, 1978, Pfau A, 1978; Blacklock NJ, 1974; Weidner W, 1992; White MA, 1975); however, the question as to how this change in pH is brought about in prostatitis has not been addressed to any significant extent. The present study has investigated the possible mechanism underlying this pH change and demonstrated for the first time the involvement of CFTR in mediating prostatic HCO_3^- secretion, which may be enhanced upon bacterial infection or inflammation. Apart from demonstrating CFTR expression in rat prostatic epithelium, which is consistent with that previously found in human prostate (Walker J, 1995; S.Hihnala,2006; Qiao D,2008), we have also elucidated the functional roles of CFTR in the prostate in health and disease. By measuring the rate of pHi recovery from cellular alkalization, in the presence or absence of extracellular Cl^- in conjunction with the use of the cAMP agonist and CFTR inhibitor, we have demonstrated that prostatic epithelium can extrude HCO_3^- under unstimulated condition through a Cl^-/ HCO_3^- exchanger since removal of extracellular Cl^- greatly attenuated the pHi recovery rate. Under this condition, when the anion exchanger is inactivated, prostatic epithelium can be stimulated to secrete HCO_3^- through a cAMP-dependent pathway which can be blocked by CFTR inhibitor. Therefore, similar to what we previously found in the uterus (Wang XF, 2003) and oviduct (Chen MH, 2010), CFTR in the prostate appears to be involved in HCO_3^- secretion either directly or indirectly as a recycling pathway for Cl^- to facilitate the operation of the anion exchanger, although the identity of the exchanger remains to be elucidated. Of note, the expression of SLC26A3 in the human prostate has been reported (Hoglund P, 1996) and we have also detected SLC26A6 in rat prostate (Xie C

unpublished data), both of which are known to be able to transport HCO_3^- across the apical membrane of many epithelia (Shcheynikov N, 2006) and work in concert with CFTR. The CFTR-mediated prostatic HCO_3^- secretion may be important for sperm motility upon ejaculation since prostate secretion is known to contribute to the semen volume and HCO_3^- is the key factor triggering sperm motility (Tajima Y, 1987; Zhou CX, 2005). The physiological role of the CFTR-mediated HCO_3^- secretion under normal condition warrants further studies.

One important observation made in this study is the upregulation of CFTR and CAII, along with several important inflammatory cytokines, upon *E. coli*-LPS challenge *in vitro* or *E. coli* infection *in vivo*. This suggests that a physiological consequence to bacterial infection or LPS challenge in the prostate would be the enhancement of the CFTR-mediated HCO_3^- secretion, which may be responsible for the increase in pH observed in prostatitis. Cytokines, such as IL-1β and TNF-α, have been reported to upregulate CFTR expression (Cafferate EG, 2000, Ajunoma, LC, 2008; He Q, 2010). IL-1β could activate the NF-κB protein, enabling it to enter the nucleus and bind to the κB-like response element at position -1103 to -1093 in the CFTR 5'-regulatiory element with a subsequent increase in CFTR promoter activity, resulting in increased CFTR mRNA (Brouillard F, 2001). The observed upregulation of CFTR and CAII upon bacterial infection or LPS challenge could be due to the elevated levels of cytokines induced by the pathogens. Since both bacterial and non-bacterial prostatitis have elevated levels of cytokines, including IL-1β and TNF-α (Alexander RB, 1998; Jang TL, 2003), these cytokines may enhance HCO_3^- production and HCO_3^- transport by upregulating CAII and CFTR, respectively. This may explain the characteristic alkaline

shift in pH in almost all categories of prostatitis. Of clinical interest, it has long been observed in prostatitis the more severe the inflammation (e.g. the larger number of infiltrated PMNs), the greater the alkaline shift in pH found (White MA, 1975). Interestingly, the present study also found enhanced CFTR and CAII expression in human hyperplasia tissues where inflammation was more prominent. Taken together, the present study has provided a molecular mechanism underlying prostatic HCO_3^- secretion and its upregulation in bacterial infection or upon inflammation, which may explain the long observed pH increase associated with prostatitis.

More importantly, the present study has also demonstrated the physiological significance of the CFTR-mediated prostatic HCO_3^- secretion in the host defense against bacterial infection. While the characteristic increase in pH in prostatitis has been considered of diagnostic value (Thin RN, 1991), its physiological role has not been explored. In this study, both *in vitro* and *in vivo* experiments have demonstrated that prostatic epithelial cells have bactericidal activities, which are largely dependent on CFTR-mediated HCO_3^- secretion since inhibitor of either CFTR or CAII greatly attenuates bacterial killing by both the primary prostatic epithelial culture and rat prostate. Since CFTR is involved in prostatic HCO_3^- secretion, the CFTR-dependent bacterial killing capacity of the prostate could be due to a direct effect of HCO_3^- or indirect effect through altered pH. We have demonstrated that the HCO_3^-, rather than alkaline pH, is mainly responsible for bacterial killing since varying pH at a constant HCO_3^- concentration does not produce significant bactericidal effect, whereas, significant bacterial killing can be observed at a HCO_3^- concentration greater than 50 mM. One immediate question that follows is whether the prostate can secrete such high

concentrations of HCO_3^-. The answer is yes since the mean pH often observed in prostatitis is 8-8.3 (Meares EM, 1990; Wagenlehner FM, 2005), which, according to Henderon-Hasselbalch equation, is equivalent to over 90 mM HCO_3^-. This high concentration of HCO_3^-, as demonstrated in the present study, is able to significantly reduce bacterial activity. The previous experiment by Tang XX in our lab demonstrated that HCO_3^- does so by elevating bacterial cAMP levels, presumably through its well-established sensor soluble adenylyl cyclase (Chen Y, 2000), thereby suppressing the bacterial initiation factors genes, which are known to participate in the process of protein biosynthesis in *E.*coli (Gualerzi. C. O, 1990; Grill S, 2001). IF1 could stimulate IF2 and IF3 activities and act as a protein factor for the stabilization of the initiation complex that is essential for cell viability (Cummings, H.S., 1994). The observed suppressing effect of HCO_3^- on these initiation factors is consistent with its bactericidal activity.

The bactericidal effect of HCO_3^- could be explained by its presently demonstrated ability to induce an increase in cAMP in the bacteria since activation of cAMP has been reported to suppresse protein synthesis in bacteria (Kaul R, 1990). Of note, the expression of sAC, a distinctive form of adenylyl cyclase, in bacteria is well documented (Beeler JA, 2004; Jeroen Roelofs, 2002) and its role as a HCO_3^- sensor has been reported to induce cAMP increase in a number of cell types including lung, sperm (Xie F, 2006; Sayner SL, 2006). Taken together, HCO_3^- may exert its bactericidal effect by acting on sAC to induce increase in cAMP production, which in turn suppresses protein synthesis and thus reduces the viability of bacteria. While most previous studies have implicated HCO_3^- in bacterial killing either by altering pH (Corral L.G, 1988) or increase the susceptibility of bacteria to antimicrobial peptides (Dorschner RA, 2006). In the present

study, we have demonstrated a direct bacterial killing effect of HCO_3^- through cAMP dependent pathway. Together with the demonstrated CFTR and CAII upregulation, therefore enhanced prostatic HCO_3^- secretion, upon bacterial infection, the present finding suggests a host defense mechanism against bacterial infection in the prostate. The long observed alkaline shift in pH in prostatitis turns out to be physiologically important. Of note, it has been reported that the pH in bacterial prostatitis is significantly higher than the nonbacterial prostatitis (Chandiok S, 1992). In fact, this could be the reason why a surprisingly low prevalence of bacterial prostatitis, only 5-10%, is found among all cases of prostatitis (Schaeffer AJ, 1981). We suspect that considerable number of cases of bacterial infection would be gone unnoticed because of the enhanced CFTR-mediated HCO_3^- secretion upon bacterial infection. Consistent with this notion, the present study found that when low CFU of *E coli* was inoculated to the prostatic cell culture, no bacterial activity was found after 18 hours incubation, indicating the bactericidal capacity of the prostatic epithelial cells. However, this bactericidal capacity is greatly attenuated by treatment with CFTR inhibitor or antibody. Taken together, the present finding has revealed a previously undefined role of CFTR and its mediated prostatic HCO_3^- secretion in the host defense against bacterial infection. The present findings may have implications beyond prostatitis since CFTR is expressed in a wide variety of tissues where bacterial infections are readily contracted. For example, patients with cystic fibrosis, a genetic disease caused by CFTR mutations, frequently present with chronic lung infection but the exact cause remains obscure. In light of the present finding, this may now be explained by possible defect in the secretion of bacterial killing HCO_3^- due to CFTR mutations.

Although the present findings provide an explanation to the characteristic increase in pH in both bacterial and non-bacterial prostatitis, we have only elucidated its importance in bacterial prostatitis. It remains unclear whether the elevated HCO_3^- content or alkaline pH would be of any physiological significance in non-bacterial prostatitis, the most common and least understood form of prostatitis. Of note, it has been reported that cAMP is a key intracellular second messenger, which at increased levels has been shown to have anti-inflammatory and tissue-protective effects (Erdogan S, 2008). An increase in cAMP level during inflammation has been shown to inhibit the proinflammatory and tissue-destructive properties of leukocytes (Houslay M.D, 2003). It is therefore tempting to speculate that the enhanced CFTR-mediated prostatic HCO_3^- secretion is not only important for bacterial killing in bacterial prostatitis, but may also play a key role in non-bacterial prostatitis by increasing the cAMP level of immune cells to suppress their inflammatory responses. Interestingly, extracellular pH has also been suggested to play a role in modulating inflammation. For example, neutrophils have been reported to be less active at a pH of 7.4 than at a lower pH (Trevani AS, 1999). Therefore, both elevated HCO_3^- content or alkaline pH (as compared to a normal pH of 6.3 in the prostate observed in non-bacterial prostatitis may be important for suppressing inflammation. Further work is required to investigate these possibilities.

In summary, the present study has elucidated the molecular mechanism underlying the long observed but unexplained characteristic alkaline shift in pH in prostatitis and revealed a previously undefined role of CFTR in host defense against bacterial infection in the prostate. The present findings also point to the possible role of the CFTR-mediated HCO_3^- secretion in anti-inflammatory process. Further work along this line

will not only confirm the diagnostic value of the characteristic pH increase in prostatitis but may also provide new strategies for the treatment of prostatitis.

Chapter 4

CFTR as a tumor suppressor in prostate cancer development

4.1 Summary

Apart from its well-established ion channel function, CFTR has been proposed to either directly or indirectly impact various cellular functions including cell proliferation, apoptosis and differentiation. On the other hand, while the relationship between the CFTR gene and cancer risk has been investigated, the conclusion is still controversial. Moreover, the biological significance of CFTR in tumorigenicity is completely unknown. Therefore, functional characterization of CFTR with respect to its abilities to mediate a gain of oncogenic activity or loss of tumor suppressor function is urgently needed.

In this part of study, we found that CFTR was down-regulated in aged rat prostate, and human prostate cancer cell lines and carcinoma specimen. Our gain and loss of function studies showed that knockdown of CFTR profoundly enhanced cell proliferation, cell adhesion, invasion and migration, while inhibited apoptosis in prostate cancer cell lines, overexpression of CFTR dramatically suppressed tumorigenic phenotype of cancer cells. More importantly, we demonstrated that forced overexpression of CFTR in prostate cancer cells and ultrasound-mediated gene transfer of CFTR inhibited xenograft tumor growth *in vivo*.

Mechanistically, multiple mechanisms were identified to contribute to CFTR-mediated tumor suppressive effects. Firstly, CFTR chloride channel function was implicated in the regulation of apoptosis in prostate cancer cells. Secondly, CFTR up-

regulated the transcription level of miR-34a and miR-193b, both of which have been indicated as tumor suppressors in multiple cancers. Thirdly, 11 cancer-related genes were found to be up- or down-regulated by CFTR using PCR-array. All together, we propose that *CFTR* acts as a tumor suppressor, mutations or down-regulation of which may play an important role in prostate cancer through multiple underlying mechanisms.

4.2 Introduction

Prostate cancer is the most frequently diagnosed malignancy and the second leading cause of cancer deaths in men of USA and UK (Jemal A, 2007). One of the most troubling aspects of prostate cancer is that, after androgen ablation therapy, androgen-dependent prostate cancer inevitably progresses to an androgen independent state, for which no effective treatment has been developed (Santos AF, 2004). Although several molecular pathways have been proposed to explain the pathogenesis of this disease, to date the mechanisms for the development and progression of prostate cancer remain largely unknown.

Recently, ion channels have been implicated in cancer development including prostate cancer (Mariot P, 2002; Vanden Abeele F, 2003; Prevarskaya N, 2007). By providing the fluxes of essential signaling ions, perturbing intracellular ion concentrations, regulating cell volume and maintaining cellular pH, plasma membrane ion channels play important role in influencing cell fate decision (Prevarskaya N, 2007; Lang F, 2005). Prostate cancer cells are also known to express a variety of plasma membrane ion channels which are known to be critically involved in proliferation, differentiation, and apoptosis (Prevarskaya N, 2007). However, the role of anion

channels in prostate cancer development and progression has not been studied to any significant extent.

The cystic fibrosis transmembrane conductance regulator (CFTR) is a cAMP-regulated anion channel capable of conducting both Cl^- and HCO_3^-, which is expressed in epithelial cells of a wide variety of tissues including the prostate. Mutations in CFTR gene cause cystic fibrosis (CF), a common autosomal recessive disease with a wide range of severity and manifestation (Rowe SM, 2005; Riordan JR, 2008). In addition to its well-established ion channel function, CFTR has been proposed to play a key role in the maintenance of epithelial cells homeostasis that either directly or indirectly impact various cellular functions, including cell proliferation (Gallagher AM , 2001), apoptosis (Barrière H, 2001) and differentiation (Skowron-zwarg M, 2007). Disruption of these processes may result in abnormal tissue growth or even cancer.

Interestingly, improved life expectancy among patients with CF has unmasked a significant increase in the incidence of malignancies. For example, a 30 year follow-up study showed that the risk of malignancies amongst CF patients clearly increased with age and peaked after the third decade of life (Sheldon CD, 1993). It has even been suggested that defective CFTR should be added to the growing list of genes conferring an increased susceptibility to cancer. Despite all these observations and predictions, the physiological significance of CFTR and possible underlying mechanisms in tumorigenicity are completely unknown.

In chapter 3, we demonstrated the role of CFTR as a well-known anion channel in the host defense of the prostate. Here the functional role of CFTR in prostate cancer was investigated. Our preliminary results showed that CFTR expression in rat prostate

decreased remarkably during aging and it negatively regulated cell growth in prostatic epithelial cells. These results promoted us to speculate on its possible involvement in the pathogenesis of diseases associated with the aging prostate such as prostate hyperplasia or prostate cancer. We hypothesized that CFTR may play an important role in prostate cancer development. To test this hypothesis, we first examined the expression of CFTR in human prostate adenocarcinoma lesions as well as human prostatic cell lines. Then we examined the biological functions of CFTR in prostate cancer development by gain and loss of function studies in prostate cancer cell lines. To confirm the observation *in vitro*, we performed the tumorigenicity *in vivo* model to assess the role of CFTR in prostate cancer development. In addition, the mechanisms underlying the tumor suppressor effect of CFTR were further elucidated.

4.3 Materials and Methods

4.3.1 Testosterone treatment in castrated rat

The adult 12-week-old male SD rats weighed between 250 and 350 g were used in the present study. In brief, the male rats were castrated under anesthesia and kept under stable condition for one week. From the seventh day, testosterone diluted by sesame oil was subcutaneously injected into the back of rats at 10 mg/kg body weight for 10 days and the rats of control group were injected with sesame oil only. The rats were killed by CO_2 and the ventral lobes of prostate obtained from each rat were weighted. The tissue was then frozen in liquid nitrogen and subjected to the gene expression study.

4.3.2 Testosterone treatment in prostate epithelial cells *in vitro*

Rat prostate epithelial cells were cultured in 35mm culture dishes as described in chapter 3 section 3.3.2. Stock solutions of testosterone were prepared freshly in 100% ethanol and, added to the medium at a final concentration of 1 μM with a final ethanol concentration not exceeding 0.02% (v/v). Control cell cultures were treated with medium containing 0.02% ethanol. In these experiments culture media were changed daily.

4.3.3 Prostate cancer cell line culture

The PC-3, DU-145, LNCaP cell lines were obtained from the American type culture collection (ATCC, Rockville, Maryland, USA). The prostate cell lines are briefly outlined below:

The PC-3 cell line is derived from a bone metastasis of a grade IV prostatic adenocarcinoma from a 62 year old male. PC-3 cells are adherent and epithelial like in morphology. The cell line is androgen insensitive and is highly tumorigenic.

The DU-145 cell line is derived from a brain lesion of a patient with metastatic prostate carcinoma and a history of lymphocytic leukaemia. DU-145 is an adherent cell line with an epithelial morphology. The cell line is tumorigenic in nude mice where it forms tumors consistent with the primary prostate cancer originally described. The DU-145 cell line is androgen insensitive.

The LNCap cell line is an androgen sensitive cell line. It is originated from a prostate carcinoma and is derived from the left supraclavicular lymph node metastatic site. It is an epithelial cell line that is adherent in nature.

PC-3 and Du-145 cell line were grown in Dulbecco's modified Eagle's medium (DMEM)/F12 supplemented with 50 unit/ml penicillin-streptomycin and 10% v/v fetal bovine serum (FBS). LNCap cell line was grown in RPIM-1640 medium supplemented with 50 unit/ml penicillin-streptomycin and 10% v/v FBS. The cells were incubated in a humidified incubator at 37°C, in 5% CO_2.

4.3.4 *In vitro* transfection

4.3.4.1 Knockdown of CFTR using ribozyme transgenes

The hammerhead ribozyme was first discovered as a self-cleaving domain in the RNA genome of different plant viroids and virusoids (Forster and Symons, 1987). Soon thereafter, it was demonstrated that the hammerhead motif could be incorporated into short synthetic oligonucleotides and transformed into a true, multiple turnover catalyst, suitable for cleaving in trans a variety of RNA targets (Uhlenbeck, 1987; Haseloff and Gerlach, 1988). All hammerhead motifs share a typical secondary structure consisting of three helical stems (I, II and III) that enclose a junction characterized by several invariant nucleotides (i.e., the 'catalytic core'). In most trans-acting hammerhead ribozymes, helix II is formed intramolecularly by the catalyst, whereas helices I and III are formed by hybridization of the ribozyme with complementary sequences on the substrate. The best triplets in terms of cleavage rates were found to be AUC, GUC and UUC (Figure 4.1).

For the CFTR knockdown system, hammerhead ribozymes were designed based on the secondary structure of CFTR (Figure 4.2) using the Zuker RNA mFold program (Zuker, 2003), targeting at a specific GUC or AUC site. Three separate designs were

used. The ribozymes were generated by touch-down PCR with the primers as in Table 4.2. The ribozymes were then cloned into the pEF6/V5-His vector (Invitrogen™) (Figure 4.3A). Plasmids DNA were prepared using Mini Plus or Midi Pus Plasmid DNA Extraction Kit (Viogene). For knock down experiments, 1 μg DNA was transfected into cells by Easyjet Plus electroporator (EquiBio, Kent, United Kingdom).

4.3.4.2 Overexpression of CFTR *in vitro*

For overexpression experiments, pEGFP-C3 vector system (BD Biosciences, Clontech) was used (Figure 4.3B). The GeneBank Accession was # U57607.The pEGFPC3 plasmid expressing wild-type CFTR was kindly provided by Professor Tzyh-Chang Hwang (University of Missouri-Columbia). For pEGFP-CFTR vector, the CFTR was cloned into Ava I sites (Figure 4.3C). To transform the constructs into bacteria for large scale DNA production, we transform DH5α *E.coli* and plate transformants on LB-kanamycin plates. The cells were transfected with 2 μg DNA and 7μl Lipofectamine 2000 reagent (Invitrogen). In order to obtain the maximum transfection efficiency, cells were seeded onto culture dish with DNA: liposome complex pre-loaded in medium.

4.3.4.3 Establishment of Stable clones

For pEF6/V5-His clones, the prostate cells PC-3 and DU145 were selected in full medium containing 5μg/ml Blasticidin S for 2-3 weeks and then later were routinely cultured in a maintenance medium containing 0.5μg/ml Blasticidin S. Cell lysates were collected for RT-PCR or western blot to check for the expression of CFTR.

For pEGFP-C3 clones in prostate cancer cells, the transfected cells were selected in full medium containing G418 (Calbiochem, Schwalbach, Germany) at 800 μg/ml for LNCap cells and 500 μg/ml for PC-3 cells. Fresh medium containing G418 was changed every three days. After 2-3 weeks of selection, G418 resistant cells growing in single colony were isolated. Cells raised from a single colony were then transferred to a 12-well plate for expansion. Confluent cell in 12-well plate was transferred to 6-well plates and allowed to grow until confluence. Cell lysates from every single clone were collected for western blotting to check for the expression of the transfected gene. The expression of gene cloned in the pEGFP-C3 vector was confirmed by RT-PCR or western blotting using anti-CFTR antibody. Stable cell lines were then maintained in 500μg/ml G418 for LNCap cells and 300 μg/ml for PC-3 cells for subsequent study.

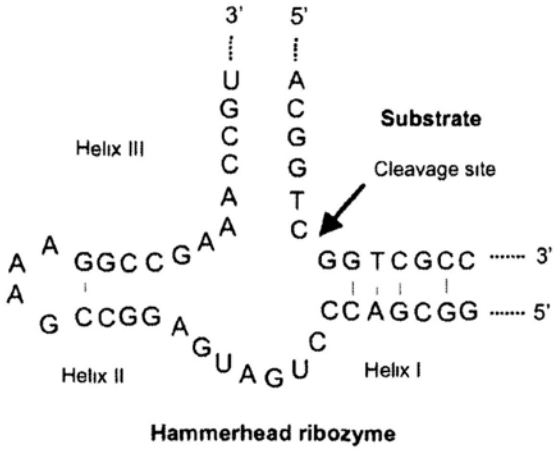

Figure 4.1 Secondary structure of the hammerhead ribozyme with bound substrate

Figure 4.2 The simulated secondary structure of CFTR

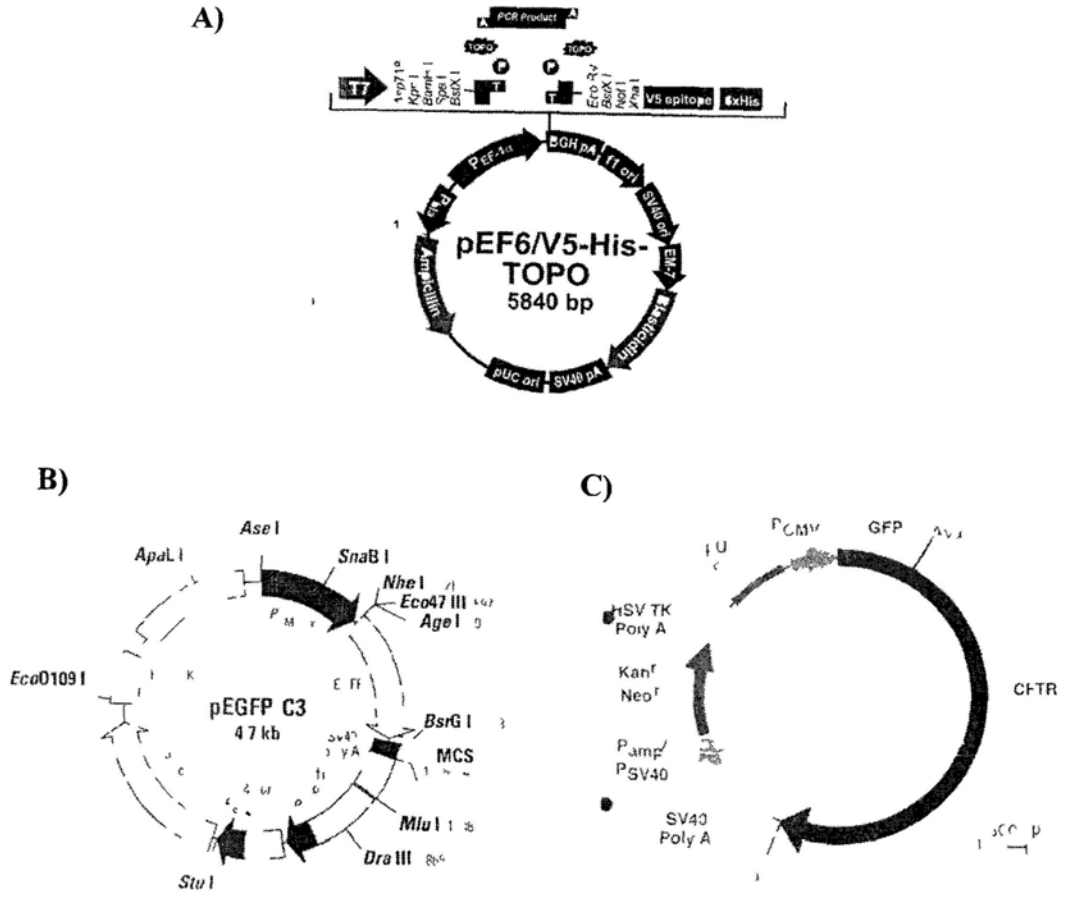

Figure 4.3 Cloning vector map (A) pEH6/V5-His expression vector (B) pEGFP-C3 expression vector and (C) pEGFP-CFTR expression vector

4.3.5 Western blot

Western blot was performed as described in chapter 2 section 2.3.3. Antibodies used were listed in chapter 2 Appendix A.

4.3.6 MTS proliferation assay

The growth rate of cells was measured using the CellTiter 96 MTS Aqueous One solution cell Proliferation assay (Promega) at the indicated time points. This assay is based on the bio-reduction of 3-(4,5-dimethylthiazol-2-yl)-5- (3-carboxymetho xyphenyl)-2-(4-sulfop henyl)-2H-tetrazolium by metabolically active cells to form a product, in the presence of phenazine methosulfate, that is soluble in tissue culture medium and can be measured by spectrophotometry. The quantity of the formazan product is directly proportional to the number of living cells in culture. In brief, 3,000 cells in 200µl of normal medium were seeded into each well of a 96-well plate. Following the appropriate incubation period, the medium was removed and 100ul of full medium and 20 µl of MTS reagents was added and the plate was incubated for 2 hours at 37°C. Intensity at 490 nm was measured. For MTS proliferation assay, each time point was set up with at least three wells and each experiment was duplicated.

Cell growth was presented as percentage increase and calculated by comparing the absorbance obtained for each incubation period using the following equation:

Percentage increase = (day 3 or 5 absorbance) – day 0 absorbance / day 0 absorbance

Within each experiment at least four duplicate wells were set up and the entire experiment protocol was repeated three times.

4.3.7 Induction of apoptosis by UV and H_2O_2

Prostate epithelial cells were plated on 35mm culture dishes for one week. The cells were exposed to a range of UV dose (0, 1, 5, 10 mJ/cm^2) using CL-1000 ultraviolet crosslinker (UVP). Twenty-four hours later, the cells were harvested. Cleaved caspase-3 antibody was used for in vitro caspase-3 activation assay.

Prostate cancer cells were seeded at a density of 1×10^5 cells in culture flask (for flow cytometry) or over-slips in culture dishes (for TUNEL assay) and treated with the H_2O_2 for 2h. Morphological changes were observed using a phase-contrast microscope. Estimation of the percentage of apoptotic cells by flow cytometry analysis was carried out as described as section 4.3.9.2. DNA fragmentation was evaluated by TUNEL using in situ cell death fluorescein kit (Roche Diagnostics).

4.3.8 TUNEL and Hoechst staining

Chromatin fragmentation was assessed by using a fluorescent TUNEL technique (terminal deoxy-transferase-mediated dUTP FITC nick-end labeling; In Situ Cell Death Detection Kit, Roche, Indianapolis, IN, USA). Briefly, cells were fixed with 4% paraformaldehyde, rinsed with phosphate-buffered saline (PBS), and incubated with terminal deoxy-terminal transferase and FITC-dUTP. Cells were then counterstained with DAPI and incorporated fluorescein and DAPI staining visualized by fluorescence microscopy.

4.3.9 Flow Cytometry

4.3.9.1 *Cell cycle analysis*

For cell cycle analysis, cells were seeded in culture flask and grown for 24 hours. The cells were washed twice with ice-cold PBS and then harvested. The cells were then resuspended in 1 ml 1xPBS. Ethanol fixation was then performed by adding 3 ml of cold absolute ethanol to the cell suspension gently. The cells were fixed at 4°C for 1 hour. After fixation, the cells were washed twice with 1xPBS and stained with 1 ml of Propidium Iodide (PI) (20 μg/ml) staining solution with RNase A (10μg/ml) at 37°C for 20 min. Flow cytometry was then performed by using BD FACSCalibur System (BD Biosciences).

4.3.9.2 *Apoptotic flow cytometry*

Annexin-V conjugated with fluoresceine isothiocyanate (Annexin V-FITC) and PI staining kit (BD Biosciences) was used to detect living and apoptotic cells using flow cytometry. The cells were seeded in culture flask and grown for 24 hours. The cells were then cultured in 0.8 mM H_2O_2 for 2 hours and then harvested and washed twice with 1xPBS. The cells were then resuspended in 1ml 1x binding buffer and stained with FITC Annexin V (BD Biosciences) and PI according to manufacturing protocol. Living cells were negative for Annexin VFITC and PI. Early apoptotic cells were detected after binding with Annexin V-FITC. Flow cytometry was then performed using BD the FACSCalibur System (BD Biosciences). All experiments were performed at least in triplicates.

4.3.10 Measurement of intracellular pH in PC-3 cells

The method of intracelluar pH measurement in PC-3 cells was performed as described in chapter 2 section 2.5.1. In pH measurement, the rate of pH recovery was

expressed as ΔpH/min, which was obtained from the ratio of two wavelengths (490/440) in the initial 100-200 sec of pH change.

4.3.11 *In vitro* tumor cell Matrigel adhesion assay

The ability of tumor cells to adhere to an artificial Matrigel basement membrane was examined using an *in vitro* Matrigel adhesion assay. The 96-well plate had been pre-coated with Matrigel (5μg/well, BD Matrigel™ Basement Membrane Matrix) and air dried in an oven to form an artificial basement membrane. This membrane was then rehydrated in 100μl of serum free medium for 40 minutes before cell seeding. After rehydration, 4×10^4 cells were seeded in 200μl of normal medium and incubated for 40 minutes. Following incubation, non adherent or loosely attached cells were washed off using 150μl PBS. Adherent cells were then fixed in 4% formaldehyde (v/v) for 5 minutes before being stained in 0.5% crystal violet solution (w/v) in distilled water. The remaining adhered cells were then visualized under the microscope and random fields counted. At least 4 random fields per well were counted and a minimum of 4 duplicate wells were set up per sample, the experimental procedure was repeated three independent times.

4.3.12 *In vitro* tumor cell motility assay

Cellular motility was assessed using a cytodex-2 bead motility assay. Cells (1×10^6) for each cell type were incubated with growth medium containing 100μl of cytodex-2 beads(Pharmacia, Piscataway, New Jersey) for 4 hours to allow the cells to adhere to the beads. The beads were washed twice in 5ml of normal growth medium to remove

non-adherent or dead cells. After the second wash the beads were resuspended in 1ml of growth medium. Two hundred microlitres of this solution was then added to a 24 well plate containing a further 800µl of normal medium and incubated overnight. Following incubation, any cells that had migrated from the cytodex-2 beads and adhered to the base of the well were fixed in 4% formaldehyde (v/v) for 5 minutes, stained with 0.5% crystal violet (w/v) and counted, following removal of cytodex-2 beads through several extensive washes with PBS. At least 4 random fields were counted per well and 4 duplicate wells were set up per sample. The entire experimental procedure was repeated three independent times.

4.3.13 *In vitro* tumor cell migration (wound healing) assay

A wounding/migration assay was also used to assess the migratory properties of the prostate cancer cells. Cells were grown in a 24 well plate to reach confluence and the monolayer of cells was scraped with a fine gauge needle. After wounding the cells were given 15 minutes to recover. The 24 well plates were placed on a heated plate (Lecia GmbH, Bristol, UK) to maintain a constant temperature of 37°C. The closure of the wound via the migration of cells into the wound was tracked and recorded using a CCD camera attached to a Lecia DM IRB microscope (Lecia GmbH, Bristol, UK) and a time-lapsed video system (Panasonic, Japan) over a 90 minute period. The tape was played back and images saved at 0, 15, 30, 45, 60, 75 and 90 minute time points. Cell migration was measured using Optimus 6 motion analysis software. The distance that the wound fronts had migrated into the wound at each time point could then be determined by subtracting the distance between the two fronts at any given time point from that at the

initial 0 minute experimental start point. The experimental procedure was repeated for three independent times.

4.3.14 *In vitro* tumor cell Matrigel invasion assay

The invasive capacity of the cells used in this study was determined using an *in vitro* Matrigel invasion assay. This assay measures the cells ability to degrade and invade through an artificial basement membrane and migrate through 8μm pores. The major components of matrigel includes laminin, collagen type IV, proteoglycans, matrix degrading enzymes and several growth factors. At room temperature, Matrigel polymerizes to produce biologically active matrix materials resembling the basement membrane which provides a suitable ECM environment for studies of cancer cell invasion in vitro.

The working Matrigel solution was made up in serum free medium to a concentration of 50μg per 100μl, added to the inserts and allowed to set in a drying oven. Once dried, these inserts were placed into sterile 24 well plates to rehydrate for approximately 40 minutes. Once rehydrated, the serum free medium was removed and 1ml of normal medium was added to the well containing the insert in order to sustain any cells that may have invaded through the insert. A total of twenty thousand cells were added to the transwell inserts over the top of the artificial basement membrane. The plate was then incubated for 72 hours at 37°C, 5% CO_2 and 95% humidity. After 72 hours, the inserts were removed from the plate and the inside of the insert was cleaned thoroughly with tissue paper. Any cells which had invaded through the membrane and passed to the underside of the insert were fixed in 4% formaldehyde (v/v) in PBS for 5

minutes before being stained in 0.5% crystal violet solution (w/v) in distilled water. These cells could then be visualised under the microscope and random fields counted. At least 4 random fields per insert were counted and duplicate inserts were set up for each test sample. The experimental procedure was repeated for a minimum of three times.

4.3.15 Soft agar anchored independent assay

Cells (2×10^4) were mixed with 0.3% soft agar in DMEM/F12 medium supplemented with 10% FBS at around 37°C to 40°C, and immediately seeded on a layer of 0.7% agarose layer in 6-well plates. After 14-21 days incubation at 37°C and 5% CO_2 for 2–3 weeks, colonies were stained with 0.01% crystal violet and colony formation was evaluated by counting the number/frequency of colonies containing more than 20 cells. Assays were performed in triplicates.

4.3.16 Xenograft experiment in nude mice

Tumorigenicity of CFTR knockdown cells were investigated by tumor xenograft experiments. The athymic female nude mice of 4-6 weeks old were provided by the Laboratory Animal Service Center (LASEC), the Chinese University of Hong Kong and maintained in filter-topped units. All experimental procedures were under ethical approval by Animal Research Ethics Committee of the university. Approximately 100 μl suspension of CFTR knockdown or overexpressed cells and the same amount of vector control cells (about 2×10^6 in 2.0 mg/ml Matrigel) was injected subcutaneously. 5 mice were injected with saline as a sham control. The mice were monitored by measuring

tumor growth and body weight. The mice with tumor size larger than 1cm in any dimension were terminated. Tumor formation in nude mice was monitored over about 4 week period. Tumor weight to body weight ratios was measured.

4.3.17 Ultrasound-mediated gene transfer of CFTR gene-loaded microbubbles into the tumor

Nude mice were used in the experiment. Under anaesthesia, about 2×10^6 prostate cancer cells PC-3 were subcutaneously injected into the animals. The tumors were allowed to grow to less than 0.5 cm in any dimension before following CFTR gene transfer mediated by ultrasound-microbubble technique. The plasmid peGFPC3 and peGFP-CFTR for injection were prepared using the EndoFree plasmid kit (Qiagen Inc., Valencia, CA) according to the manufacturer's instructions. To achieve CFTR transgene expression in tumor, the ultrasound-microbubble-mediated system was applied. Briefly, after mixing peGFPC3 or peGFP-CFTR with sulphur hexafluoride microbubbles (Bracco Imaging B.V., Switzerland) at a ratio of 1:1 (v/v), the mixed solution containing 200 μg of plasmid in 200 μl was injected into the vein of tail. Immediately after injection, the ultrasound transducer was directly applied to the tumor site and a continuous-wave output was applied for a total 5 minutes. The same procedure would be repeated once a week for about 2-3 weeks. At the end of the experiment, the animals were sacrificed and the tumor tissues were collected for further analysis.

4.3.18 RT-PCR

RT-PCR was performed as described in chapter 2 section 2.3.2. Primers used were listed in Table 4.2.

4.3.19 Real-time PCR

Total RNA was extracted using Trizol and 400 ng total RNA was further transcribed to cDNA with 1X PCR buffer, 0.5 mM dNTP, 0.5 μM random hexamers (Applied Biosystems), 5 mM $MgCl_2$, 0.02 μM DTT and 3 units M-MLV reverse transcriptase (Life Technologies, Cergy Pontoise). Dilutions of the cDNA were used for real-time quantitative PCR (5′ fluorogenic nuclease assay) using Perkin-Elmer's ABI Prism 7700 Sequence Detector System. Reaction mixtures are 1X Taqman Universal PCR Master Mix, 50 nM Forward primer, 50 nM Reverse primer, 200 nM RNA probe (VIC^{TM}). A S18 rRNA probe and primers were used as an endogenous control gene (S18 control kit, Perkin-Elmer). PCR conditions were: 2 min 50°C, 10 min 95°C and 40 cycles of 15 sec 95°C, 1 min 60°C. The PCR assays were performed in separate tubes and relative quantitation of the mRNAs was performed using the standard curve method according to the manufacturer's instructions (PE Applied Biosystems, User Bulletin 2: ABI PRISM 7700 Sequence Detection System). Primers for the qPCR used in the present study were not provided by ABI Company.

4.3.20 TaqMan real-time PCR for Micro RNA

RNA was isolated from the cells using the TRIZOL reagent. The expression of mature microRNAs was assayed using TagMan MicroRNA Assays (Applied Biosystems, Foster City, CA, USA) specific for has-miR-34a and has-miR-193b and RUN48. Real-

time PCR was performed using the TaqMan Gene Expression Master Mix (Applied Biosystems) and the ABI 7500 Fast real-time PCR machine. RUN48 was used as an endogenous control. All TaqMan PCRs were performed in triplicates.

4.3.21 Human Cancer PathwayFinder PCR array

RNA from stable transfectant was extracted using TRIzol reagent (Invitrogen). RNA was dissolved in DNase/RNase free ddH2O. RNA concentrations were measured by Nanovue Spectrophotometer (GE Healthcare).

RNA was converted into PCR template with RT^2 First Strand Kit and then combined the template with RT^2 SYBR Green qPCR Master Mix. Add equal aliquots of the mixture to each well of Human Cancer PathwayFinder PCR array plate (SABiosciences, QIAGEN) containing the predispensed gene-specific primer sets, and perform PCR.

4.3.22 Statistical analysis

Statistical analyses were performed by Prizm 5.0 software. Results were expressed as means ± S.E.M, and Student's unpaired *t*-test was used for 2 groups of statistical analysis. P value <0.05 was considered statistically significant.

4.4 Results

4.4.1 Age-dependent CFTR and CAII expression in rat ventral prostate

Many changes, both morphological and biochemical would take place during aging or prostate development process. We examined rat prostates of different ages from 10 days to 210 days. RT-PCR and real-time PCR were used to detect the mRNA expression

of CFTR and carbonic anhydrase II (CAII) in rat ventral prostate of different ages. In chapter 3, we reported the expression of CFTR was upregulated along with CAII in the inflammation of prostate, so here in addition to CFTR, we also examined the expression of CAII during aging. Figure 4.4 showed that the mRNA and protein expression of both CFTR and CAII was decreased remarkably with increase in the age. Immunohistochemical studies showed that CFTR was localized in the apical plasma membrane of rat prostate epithelial cells while CAII was localized in the cytoplasm of epithelial cells (Figure 4.5). The expression of both CFTR and CAII was dramatically decreased in prostate tissues of older rats. The findings provide us a hint to study the possible involvement of CFTR in age-related processes, i.e. the loss of CFTR physiological function could cause some diseases which are associated with advancing age such as BPH and prostate cancer (Sampson N, 2007).

Circulating androgens, particularly testosterone, are known to play important roles in prostate growth. During aging, the testosterone levels were decreased. To mimic the process of aging, we manipulated testosterone level by castration to study how androgen regulates prostate growth and gene expression of CFTR and CAII. In the present study, the castration-induced regression and testosterone stimulated re-growth of the rat ventral prostate and corresponding CFTR and CAII expression were studied. Two weeks after castration, the total prostate weight was markedly decreased. Within 7 days after subcutaneous (s.c.) injection with 10mg/kg testosterone, the total weight of prostate was normalized (Figure 4.6A). The mean ratio of wet weight of the ventral prostate to body weight was listed in Figure 4.6B. It showed that following castration, there was a significant decrease in the expression of CFTR and CAII at mRNA level as assessed by

RT-PCR; however the subsequent administration of testosterone restored the expression of CFTR and CAII to a normal level (Figure 4.6C). We then investigated whether addition of testosterone to the culture medium could also up-regulate the expression of CFTR and CAII *in vitro*. The results showed that the transcription level of CFTR and CAII was up-regulated remarkably after adding 2 μM testosterone to the medium (Figure 4.6D) for 24h in the cultured prostate epithelial cells. These data indicated that the expression of CFTR and CAII could be up-regulated by androgen *in vivo* and *in vitro*.

4.4.2 Inhibition of CFTR promotes cell growth and suppressed apoptosis in rat primary prostate epithelial cells

In an attempt to explore the physiological significance of CFTR in prostate epithelial cell behavior, we first used rat primary culture of prostate epithelial cells to investigate whether CFTR is involved in cell growth, determined by MTS cell proliferation assay. The results showed that when treated with 10 μM CFTRinh-172, the survival rate of prostate epithelial cells was significantly higher than that of control cells on day 3 and day 4 (Figure 4.7). Proliferating Cell Nuclear Antigen, commonly known as PCNA is a marker of cell proliferation in early G1 phase and S phase of the cell cycle and a nuclear protein involved in DNA synthesis and repair. Immunofluorescence detection of PCNA was evaluated in prostate primary epithelial cells with and without CFTRinh-172. The results showed that there were a significantly higher number of cells expressing PCNA after CFTRinh-172 treatment (Figure 4.8). These results indicated that blocking CFTR promoted cell proliferation in vitro in prostate primary epithelial cells

Then, we induced cell apoptosis by UV radiation and compared the expression level of activated caspase-3 in cells with or without CFTRinh-172. UV radiation has multiple cellular targets that trigger different signaling cascades leading to apoptosis. We determined the UV dose to be 1 mJ/cm^2 to stimulate the cell apoptosis response. Caspase-3 has been identified as a key mediator of apoptosis in mammalian cells. It was reported that UV radiation could trigger activation of caspase-3 (Zhan Q, 2002), which was verified in rat prostate epithelial cells by western blot (Figure 4.9). Interestingly, pretreating cells with CFTRinh-172 could block UV-induced activation of caspase-3 in rat prostate epithelial cells.

4.4.3 Reduced CFTR expression in human prostate cancer samples

The reduced expression of CFTR in aged prostate and the inhibitory role of CFTR in cell growth prompted us to speculate that CFTR might be involved in the development of age related diseases such as prostatitis and prostate cancer. Thus, we set up to determine the expression of CFTR in human prostate cancer samples. Due to the fact that clinical samples used for RNA and protein extraction were a result of homogenisation of biopsied tissues, it is difficult to distinguish the source (normal epithelial, cancer) of the CFTR mRNA transcript and protein level, so we conducted immunohistochemical staining in normal and malignant prostate tissues which could clearly indicate the localization of CFTR protein in human prostate tissue. The results showed that CFTR was strongly expressed in the normal prostate tissue and its localization was mainly confined to the ductal epithelium. In tumor tissue, however, CFTR protein levels were dramatically reduced or absent in the prostate cancer cells,

particularly in specimens with higher Gleason scores (Figure 4.10) indicating its role in the development and progression of prostate cancer.

4.4.4 The expression of CFTR in prostate cell lines

The expression of CFTR was examined in six prostate cell lines using conventional RT-PCR. PC-3, DU-145, LNCaP were cancer cell lines, whereas PZHPV-7, PNT-1A and PNT2-C2 were immortalized prostatic epithelial cell lines. CFTR presented at relatively low levels in prostate tumor cells, compared with normal prostate epithelial cells. This would indicate that in solid human tumors, CFTR exists at lower levels (Figure 4.11).

4.4.5 Functional studies of CFTR using prostate cancer cell lines

4.4.5.1 Generation of CFTR stable knock-down and overexpression cells

Functional genomic studies rely on gain-of function or loss-of –function models. To prepare for the functional studies of CFTR, knockdown and overexpression clones of CFTR were made.

As shown by RT-PCR, western blot and immunofluorescent staining, PC-3 and DU145 cells transfected with the CFTR ribozyme transgene exhibited markedly reduced level of CFTR expression compared with wild-type or vector control cells (Figure 4.12). In addition, RT-PCR, real-time PCR and western blot confirmed the significantly increased expression level of CFTR in LNCap and PC-3 CFTR over-expressed cell lines using peGFPC3 vector system (Figure 4.13).

4.4.5.2 The effect of CFTR on tumorigenic phenotype of prostate cancer cells

4.4.5.2.1 CFTR suppresses cell growth in prostate cancer cells *in vitro*

To assess whether knockdown or overexpression of CFTR would influence the cell growth in prostate cancer cells. Our results showed that CFTR knockdown significantly increased the growth of PC-3 and DU145 cells *in vitro*. The cell growth rate of PC-$3^{CFTRrib2}$ and $DU145^{CFTRrib2}$ after a 3 or 5 day incubation period is much faster than wild-type and vector control transfected cells (Figure 4.14A, B). Meantime, CFTR over-expression significantly decreased the growth of LNCap and PC-3 cells *in vitro* from day 3 and 5 onwards (Figure 4.14C, D). Taken together, these results indicated that CFTR could inhibit cell growth in prostate cancer cells *in vitro*.

4.4.5.2.2 Effect of CFTR on cell cycle progression and apoptosis

To investigate the underlying mechanisms of how CFTR influences cell growth, we studied cell cycle progression and apoptosis in CFTR over-expressed cells and CFTR knockdown cells using flow cytometry.

Overexpression of CFTR causes G2/M arrest in LNCap cells

Decrease in proliferation could be resulted from cell cycle arrest. To further elucidate the results from cell growth, the cell cycle profiles of CFTR overexpressed cells were analyzed by flow cytometry (Figure 4.15 A, B, E). The results showed that $LNCap^{peGFP\text{-}CFTR}$ cells showed a significant G2 arrest (23.5 ± 0.3% G2) when compared to $LNCap^{peGFPC3}$ control (18.0 ± 0.4 % G2) ($p<0.0001$). Meanwhile, the population of S phrase of $LNCap^{peGFP\text{-}CFTR}$ cells was 17.5 ± 0.6 % which was significantly lower than that in $LNCap^{peGFPC3}$ cells (27.6 ± 1.6 % S) ($p<0.01$). These results demonstrated that a

greater percentage of CFTR-overexpressing LNCap cells accumulated in G2/M, but with reduced number in S phase compared to the control; however there were no significant changes in the G1/S progression or the G2/M phases of PC-3^{CFTRrib2} cells when compared to its vector controls (Figure 4.15C, D, F).

CFTR promotes both basal and hydrogen peroxide (H_2O_2)-induced apoptosis

To investigate whether the inhibitory effect of CFTR on the growth of prostate cancer cells involves apoptosis, we determined the proportion of apoptotic cells in CFTR knock-down and overexpressed cells on basal and H_2O_2-induced condition, respectively. The propidium iodine (PI) staining and Annexin-V binding were used in cell apoptotic flow cytometry. Staining cells simultaneously with FITC-Annexin V (green fluorescence) and the non-vital dye propidium iodide (red fluorescence) allows the discrimination of intact cells (FITC-PI-), early apoptotic (FITC+PI-) and late apoptotic or necrotic cells (FITC+PI+).

Results showed that the percentage of apoptotic cells of PC-3^{CFTRrib2} cells was less than its vector control PC-3$^{pEF/His}$ cells in normal condition (Figure 4.16A), but there was no statistic significance which was due to the relatively large standard deviation. If the cells were treated with 0.8mM H_2O_2 for 2 hrs, PC-3 CFTR knockdown group showed lower percentage of apoptotic cells than that of control group, with 9.9% in PC-3^{CFTRrib2} group compared to 4.2 % in control group (Figure 4.16B). The data are summarized in Figure 13C .These data indicate that knockdown of CFTR has potent anti-apoptotic effect in PC-3 cells. In the CFTR over-expression cell line system, CFTR induced a significant increase in apoptotic cells. As shown in Figure 4.17A and 4.18A, in normal condition, the percentage of apoptotic cells of PC-3$^{peGFP\text{-}CFTR}$ and LNCap$^{peGFP\text{-}CFTR}$ group

was 32.7 ± 0.4 % and 6.6 ± 0.5 % which is much higher than PC-3^{peGFPC3} group (13.9 ± 0.3 %) and LNCap^{peGFPC3} group (0.1 ± 0.01 %) Moreover, PC-3 and LNCap CFTR over-expression group showed higher percentage of apoptotic cells compared with their control after 0.8 mM H_2O_2-treatment, respectively. i.e, 48.6 ± 0.2 % Vs. 21.7 ± 1.2 %in PC-3 (Figure 4.17B) and 3.9 ± 0.1 % Vs. 1.1 ± 0.1 % in LNCap cells (Figure 4.18Б). The data are summarized in Figure 4.17C and 4.18C. Taken together, these observations indicate that knockdown of CFTR protects cells against apoptosis while overexpression of CFTR promotes apoptosis in basal and hydrogen peroxide (H_2O_2)-induced condition.

The TUNEL method is another common method to identify apoptotic cells in situ. Cleavage of genomic DNA during apoptosis may yield double stranded as well as single strand breaks ("nicks"), which can be identified by labeling free 3'-OH terminal. In TUNEL analysis, fluorescently conjugated dUTPs are added to the 3′-OH groups of the DNA fragments, making the apoptotic cells visible by fluorescent microscopy. Results showed that in basal condition, there was almost no TUNEL positive cells in CFTR knockdown cells and their control cells, however after treated with 0.8 mM H_2O_2, PC-3 and DU145 CFTR knockdown cells had a lower percentage of TUNEL positive cells, with 18.5% and 15.6% apoptotic cells compared to 82.5 % and 62 % apoptotic cells in control group, respectively (Figure 4.19). These data further indicate that knockdown CFTR has potent anti-apoptotic effect in both PC-3 and DU145 cell lines.

4.4.5.2.3 CFTR impairs the adhesion ability of prostate cancer cells

Cell adhesion is essential in all aspects of cell growth, cell migration and cell differentiation. The relationship between tumor cell adhesion to the extracellular matrix

(ECM) and metastasis formation is very intimate. In order to survive in the adverse extracellular-matrix microenvironment, the tumor cells would activate anti-apoptotic mechanisms. The enhanced cell-matrix interaction is critical in approaching tumor cells to migrate in epithelial-mesenchymal transition (EMT). To investigate the effect of CFTR on the ability of prostate cancer cells to adhere to the extracellular matrix, we used the in vitro cell-matrix adhesion assay. Knockdown of CFTR exhibited a significant promotion effect on cell-matrix adhesion of the cells. The number of adhesion cells for PC-$3^{CFTRrib2}$ and $DU145^{CFTRrib2}$ was 197.0 ± 7.5 and 227.2 ± 19.2 respectively, compared with wild type and vector control cells which was 114.2 ± 13.8 for $PC\text{-}3^{WT}$, 81.2 ± 8.2 for $PC\text{-}3^{pEF/His}$, 125.8 ± 12.3 for $DU145^{WT}$ and 131.4 ± 15.0 for $DU145^{pEF/His}$ (Figure 4.20 A, B).

As CFTR appeared to promote apoptotic effect, we would like to investigate the cell-matrix interactions in CFTR over-expressing cells. It showed that LNCap CFTR over-expression group had much lower number of attached cells, with 6.6 ± 1.2 in $LNCap^{peGFP\text{-}CFTR}$ group compared to 21.2 ± 3.4 in peGFPC3 control group (Figure 4.20C). Moreover, the number of attached cells in$PC\text{-}3^{peGFP\text{-}CFTR}$ group was 45.6 ± 7.0, which is much lower than $PC\text{-}3^{peGFPC3}$ (96.2 ± 8.8) (Figure 4.20D). The results demonstrated that CFTR significantly impaired the adhesion ability of prostate cancer cells, possibly through inhibition of cell-matrix interaction.

4.4.5.2.4 CFTR impairs the motility of prostate cancer cells

During invasion and metastasis, cancer cells move within tissues by their motility. Coupled with proteolysis, cell motility provides a basis of tumor cell invasion and

endothelial cell formation of capillary generation during angiogenesis. Cell migration involves multiple processes that are regulated by various signalling molecules (Ridley AJ, 2003) .We also examined the effect of CFTR on cellular motility using the cytocarrier based cell motility assay and in vitro migration/wounding assay. In CFTR knockdown cells, cell motility was significantly increased in PC-$3^{CFTRrib2}$ and $DU145^{CFTRrib2}$ cells (Figure 4.21A, B). The number of migrating PC-$3^{CFTRrib2}$ cells was 468.0 ± 44.8 compared with 274.2 ± 37.9 for PC-3^{WT} cells and 277.2 ± 53.6 for PC-$3^{pEF/His}$ cells ($p<0.05$). The number of migrating $DU145^{CFTRrib2}$ was 260.0 ± 14.7 compared with 150.3 ± 15.8 for $DU145^{WT}$ and 146.0 ± 10.1 for $DU145^{pEF/His}$ ($p<0.01$). Furthermore, the number of migrating cells of $LNCap^{peGFP\text{-}CFTR}$ cells and PC-$3^{peGFP\text{-}CFTR}$ cells was 17.7 ± 1.8 and 49.7 ± 6.9. It was significantly lower than control vector $LNCap^{peGFPC3}$ cells (44.7 ± 4.3) and PC-$3^{peGFPC3}$ cells (137.0 ± 16.8), $p<0.01$ (Figure 4.21C, D).

In the wounding assay, we also found that the motility was increased significantly in PC-3 with CFTR knockdown. CFTR knockdown cells showed a significantly increased cellular migration compared with control. There was a significantly increase in migrated distance for PC-$3^{CFTRrib2}$ cells 60 minutes after wounding (Figure 4.22). The average distance migrated over 90 minutes for PC-$3^{CFTRrib2}$ cells was 29.5 ± 5.4μm versus both PC-3^{WT} (12.0 ± 4.4μm) and PC-$3^{pEF/His}$ (18.7 ± 1.1μm), $p<0.05$. These data demonstrated that knockdown of CFTR could increase the motility of prostate cancer cells.

4.4.5.2.5 CFTR inhibits prostate cancer cell invasion *in vitro*

To examine possible role of CFTR in suppressing cancer invasion, an *in vitro* matrigel invasion assay was performed. The results revealed that there were significant changes in the invasion potential of the CFTR knockdown or over-expressed cells. Invasion was increased significantly after knockdown of CFTR and the number of invading cells for PC-3^{CFTRrib2} was 213.0 ± 20.8 compared to 117.7 ± 8.8 for PC-3$^{pEF/His}$ ($p<0.05$) (Figure 4.23). In contrast, forced expression of CFTR in the prostate cancer cell line resulted in a dramatic reduction in the degree of invasion. The number of invading cells for LNCap$^{peGFP\text{-}CFTR}$ and PC-3$^{peGFP\text{-}CFTR}$ was 6.7 ± 1.8 and 77.3 ± 9.2 compared to 47.3 ± 6.2 for LNCap^{peGFPC3} cells ($p<0.01$) and 188.3 ± 11.9 ($p<0.01$) for PC-3^{peGFPC3} cells (Figure 4.24), respectively. The data suggested that the presence of CFTR suppresses or limits the invasive nature of prostate cancer cells.

4.4.5.2.6 Knockdown of CFTR enhances anchorage independent growth

Anchorage-independent growth is a hallmark of transformed cells which lose their contact inhibition, while most normal epithelial cells are anchorage dependent. The process of anchorage-independent growth of cancer cells in vitro is considered a key feature of tumor phenotype, particularly with respect to metastatic potential (Gupta GP, 2006). A soft agar anchorage-independent growth assay was used to study the effect of CFTR in tumor transformation in vitro. Cells were seeded in soft agar to mimic anchorage-independent growth conditions. Results showed that knockdown CFTR in PC-3 cells could increase the number of colonies formed in soft agar when compared to its corresponding control, with an average 80 colonies/well in PC-3 ^{CFTRrib2} cells while 5 colonies/well in PC-3$^{pEF/His}$ group (Figure 4.25). These data have shown that CFTR

impaired the ability of anchorage independent growth and knockdown of CFTR may contribute to increase tumor transforming properties.

4.4.5.2.7 Tumor-suppressive effect of CFTR *in vivo*

CFTR inhibits tumor growth in vivo

To further evaluate the tumorigenic effect of CFTR knockdown *in vivo*, PC-$3^{CFTRrib2}$ cells and vector control cells were subcutaneously (s.c.) inoculated into athymic nude mice. Four mice were included in each group. The growth rate of tumors was monitored and tumor sizes were measured 4 weeks after inoculation. As shown in Figure 4.26A, the tumor-to-body ratios of tumors after injecting PC-$3^{CFTRrib2}$ cells were 0.88 ± 0.08 % compared with 0.50 ± 0.13 % for that of PC-$3^{pEF/His}$ ($p<0.05$). The CFTR knockdown group demonstrated higher tumor-to-body ratio, suggesting that knockdown CFTR in prostate cancer cells promoted the tumor growth *in vivo*.

The effect of CFTR in tumorigenicity was further investigated using CFTR overexpression cells. PC-$3^{peGFPC3\text{-}CFTR}$ and vector control cells were subcutaneously (s.c) inoculated into athymic nude mice. The tumor-to-body ratios of tumors after injecting PC-$3^{peGFPC3\text{-}CFTR}$ cells were 0.63 ± 0.09 % compared with 1.40 ± 0.33 % for that of PC-$3^{peGFPC3}$ ($p<0.05$) (Figure 4.26B). The CFTR overexpression group demonstrated significantly slower tumor growth than the vector control group. In contrast, using immunohistological staining of CFTR and a proliferation marker PCNA in paraffin-fixed tumor sections, we found a strong staining for CFTR and a significantly lower proliferation rate in PC-$3^{peGFPC3\text{-}CFTR}$ mice compared to those of PC-$3^{peGFPC3}$ mice.

Ultrasound-mediated gene transfer of CFTR attenuated the tumor growth in vivo

Next, we investigated whether forced overexpression of CFTR in prostate tumor *in vivo* would result in reduced tumor formation, we directly transfer CFTR containing plasmids to the tumor of athymic nude mice mediated by ultrasound-microbubble technique. The results of the pilot experiments suggested that CFTR can be effectively transfected into the tumor in vivo by this technology. As shown in Figure 4.27, the size of tumor treated with peGFP-CFTR DNA was remarkably smaller than that of tumor treated with control DNA. The results indicated that gene transfer of CFTR could attenuate the tumor growth in *vivo*.

4.4.6 Possible mechanisms underlying tumor suppressive effects of CFTR

The current functional results indicate CFTR as a tumor suppressor gene in prostate cancer; however the possible mechanisms by which these processes occur are still unclear. In the following study, we aimed to elucidate the underlying mechanisms of CFTR in the regulation of tumorgenic phenotype in prostate cancer cell lines.

4.4.6.1 CFTR as an ion channel to modulate apoptotic activity

Cl^- channel has been suggested to potentiate cell apoptosis by mediating intracellular acidification (Lagadic-Gossmann D, 2004; Kumar S, 2007). To further identify the potential influence of CFTR as a Cl^- channel, we first determined the channel function of CFTR in pH_i regulation in prostate cancer cell lines. We treated the PC-3 cells with CFTRinh-172 and evaluated the change of pH_i by BCECF loading. The PC-3 calibration curve was shown in Figure 4.28A. As shown in Figure 4.28B, C, the pH_i was increased when the cells were treated with CFTRinh-172 for 24 h. The pH_i of cells after adding CFTRinh-172 was 7.72 ± 0.13 which was higher than that in basal

condition (7.56 ± 0.12). Although there was no statistic significance between these two groups, the slight change of pH_i indicates CFTR function is required for maintaining adequate intracellular acidification in prostate cancer cell lines, which has been implicated in mediating apoptosis in various cellular systems.

On the other hand, Cl^- channels have also been suggested to correlate closely with the onset of apoptosis, through interaction with Bcl-2 family of proteins, both *in vitro* and *in vivo* (Poulsen, K. A., 2010; Elble, R. C. 2001). To investigate whether CFTR is involved in mediating the changes in ion fluxes such as Cl^- that ultimately lead to apoptosis, we observed the effect of extracellular Cl^- on apoptotic responses in the presence or absence of CFTR. Western blot analysis of anti-apoptotic protein Bcl-2 was used to identify the changes in apoptotic activities. It seemed that in normal condition, the expression level of Bcl-2 in PC-$3^{pEF/His}$ and PC-$3^{CFTRrib2}$ cells was almost the same (Figure 4.29A). However, when the PC-$3^{pEF/His}$ cells were treated with 0.8mM H_2O_2, chloride depletion in the media strikingly enhanced apoptotic response as demonstrated by a marked decrease of Bcl-2. On the contrary, chloride depletion did not have significant effect on H_2O_2-induced apoptosis in PC-$3^{CFTRrib2}$ cells (Figure 4.29B). These results showed that the changes in apoptotic activities in response to changes in extracellular Cl^- were abolished when CFTR is inhibited or down-regulated. The observed enhanced apoptosis and down-regulation of Bcl-2 in the CFTR-expressing cells on H_2O_2 treatment promoted us to speculate that the chloride-transporting function of CFTR might contribute to its proapoptotic effect, similar to that of other reported chloride channels.

4.4.6.2 CFTR regulates the transcription level of miRNA-34a and miRNA-193b in prostate cells

Recently miRNAs have been implicated in the regulation of various biological processes which are deregulated in cancer cells such as proliferation, apoptosis and differentiation (Kloosterman WP, 2006; Hermeking H, 2010). Specifically, both miR34a and miR193b have been characterized as tumor suppressor in various human cancers. In this part of the studies, we determined the expression of miR34a and miR193b in both normal and malignant prostate epithelial cells. We first compared the expression of miR-34a and miR-193b after blocking the function of CFTR in the cultured rat prostate epithelial cells. Our results showed that when the cells were pretreated with 10 μM CFTRinh-172 for 24 h, the expression of miR-34a was significantly reduced (Figure 4.30A). Next we compared the transcription level of miR-34a and miR-193b in CFTR knock-down or overexpression cells. As showed in Figure 4.30B, a significantly higher amount of miR-34a was observed in LNCaP cells expressing wild-type p53 compared with p53-null PC3 cells and p53-mutated DU145 cells. The expression of miR-34a and miR-193b was greatly reduced in PC-3^{CFTRrib2} cells and remarkably increased in LNCap$^{peGFP\text{-}CFTR}$ cells compared with their respective vector controls (Figure 4.30C, D). These results indicate that CFTR regulates both miRNA-34a and miRNA-193b expression in prostate cancer cell lines.

4.4.6.3 Overexpression of CFTR Tumor suppressive signaling in CFTR overexpressed cells

Apart from its well-established ion channel function, CFTR has been implicated in modulating various cellular functions through multiple downstream pathways. In an effort to further elucidate the underlying molecular pathways through which CFTR regulates tumorigenic phenotype both *in vitro* and *in vivo*, we undertook Human Cancer PathwayFinder PCR array (SABiosciences, QIAGEN) to screen for the candidate genes that have been indicated in cancer development. Totally, 84 cancer pathway-related gene transcripts were profiled and compared in CFTR overexpressing or vector control LNCap cells

As shown in Figure 4.31, we found there were 11 genes differentially expressed in CFTR overexpressing cells. Among the 11 genes, 9 genes were down-regulated while 2 genes were up-regulated after overexpression of CFTR (Table 4.1). Of particular interest, 8 out of the 9 genes that were down regulated by CFTR overexpression were related to cell invasion and metastasis in cancer, indicating that CFTR might play a critical role in the cancer progression.

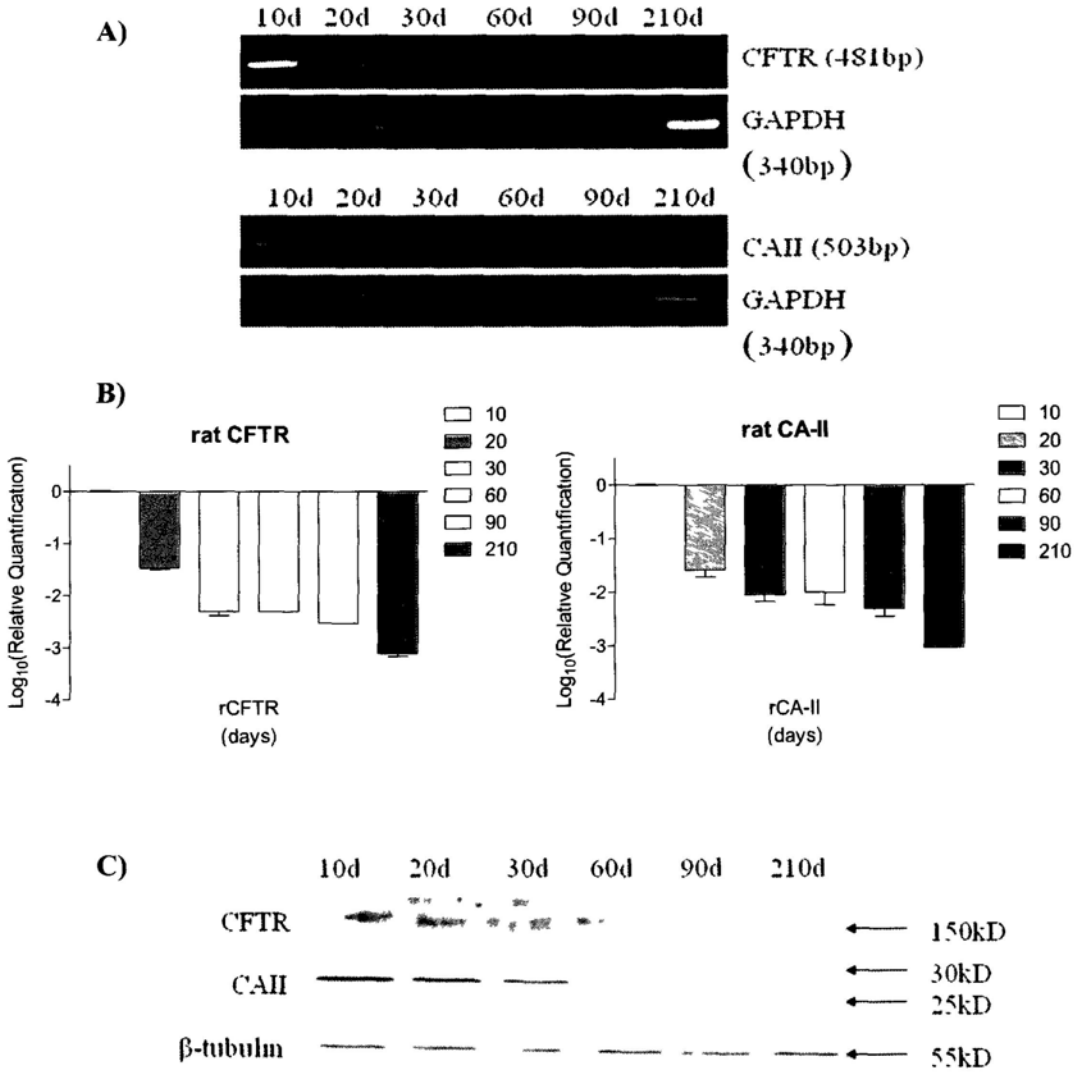

Figure 4.4 The expression of CFTR and carbonic anhydrase II (CAII) in rat ventral prostate with different ages. RT-PCR (A), real-time PCR (B), and western blot (C) showed the age-dependent expression of CFTR and CAII in rat prostate.

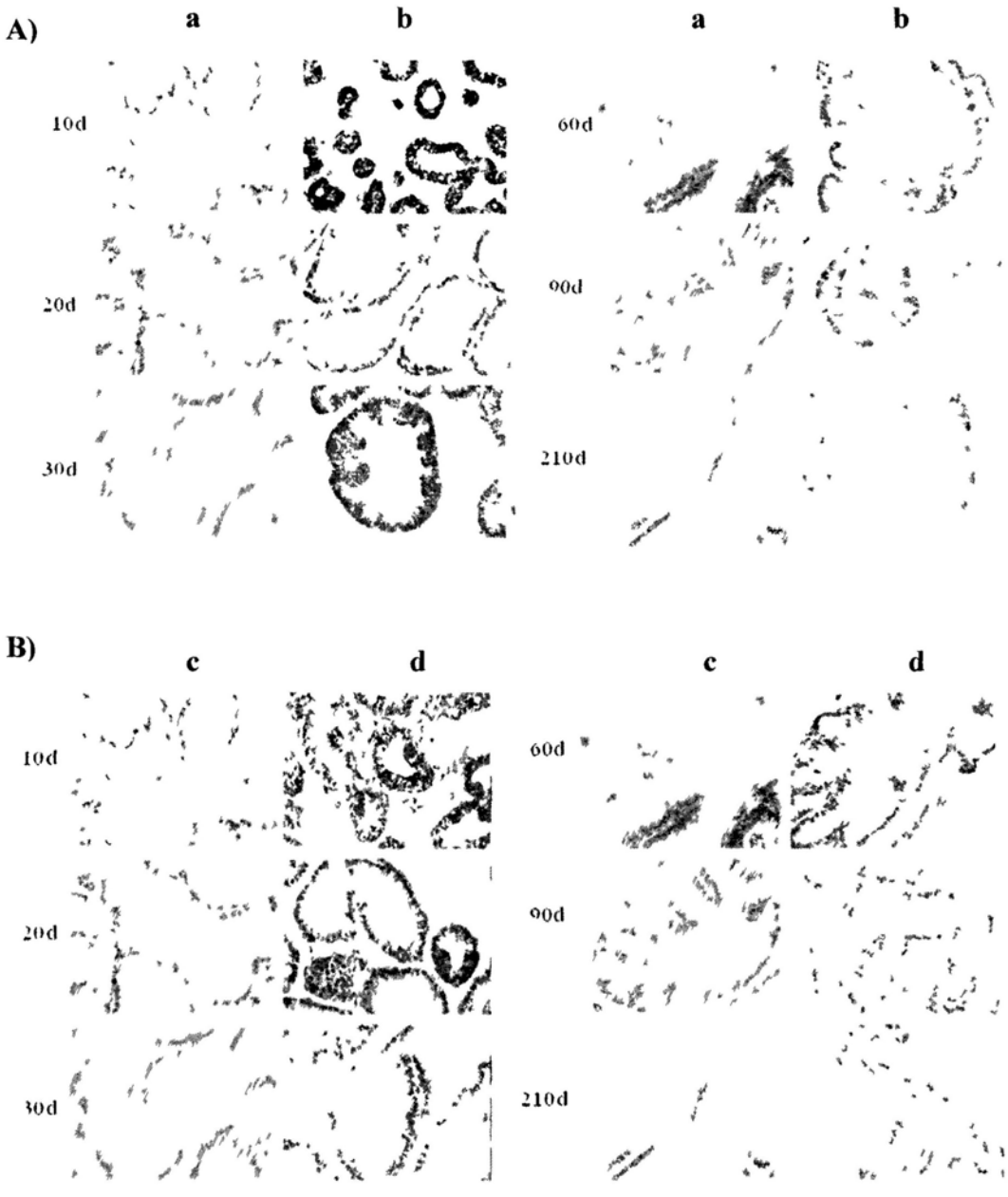

Figure 4.5 Immunolocalization of CFTR and CAII in rat ventral prostate with different ages. (A). Immunostaining for the CFTR (b) was detected in the apical surface of the epithelial cells of the rat ventral prostate. The negative control is showed in (a). (B). Immunostaining for the CAII (d) was detected in the apical surface of the epithelial cells of the rat ventral prostate. The negative control is showed in (c). Manification: ×400 Bar= 20μm

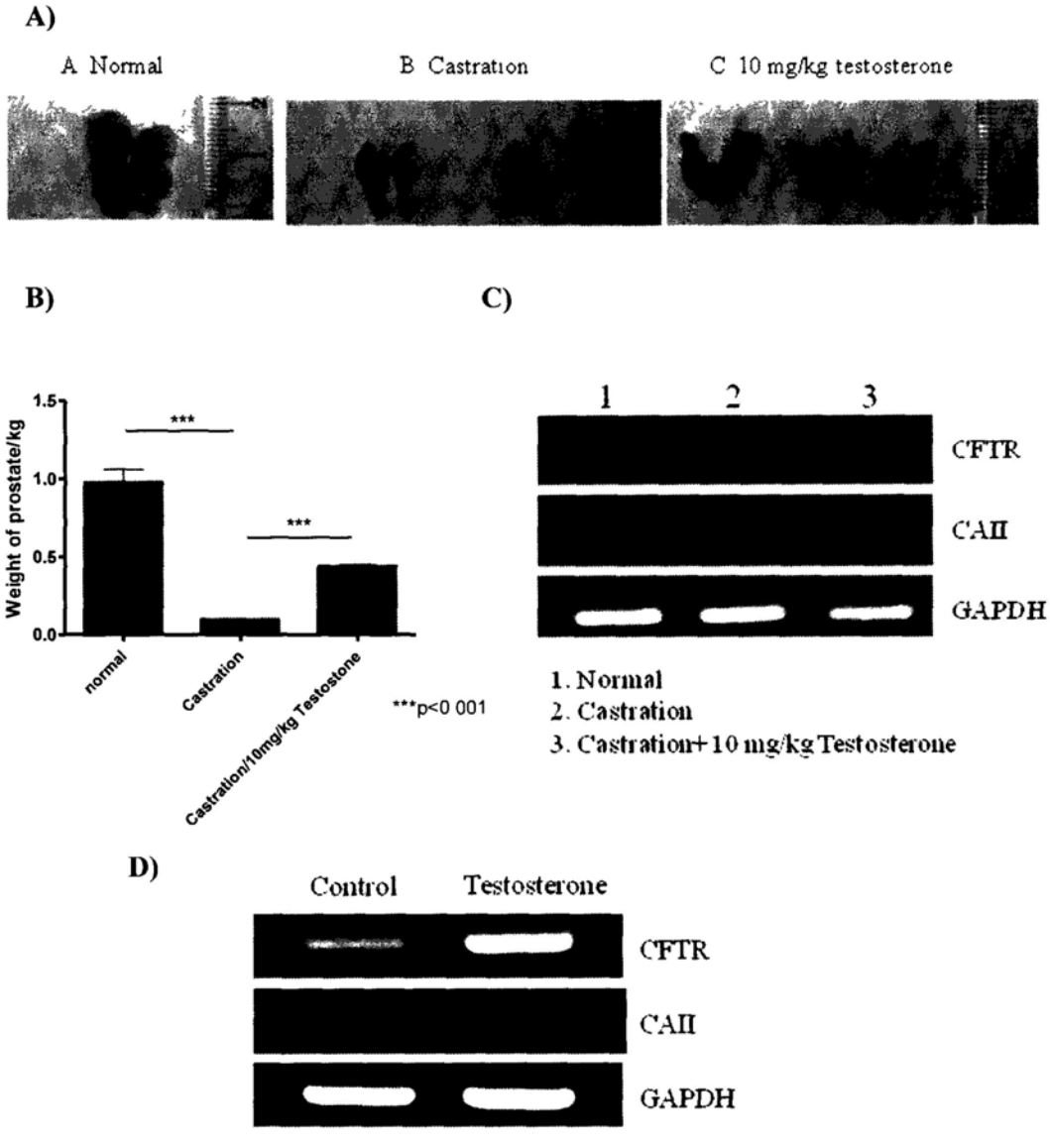

Figure 4.6 The effect of Testosterone on the expression of CFTR and CAII in prostate *in vivo* and *in vitro*. (A) The samples of rat ventral prostate in normal, castration and testosterone treated group. (B) Summarized data for the mean ratio of wet weight of the ventral prostate to body weight. (C) RT-PCR for the expression of CFTR and CAII in different groups in rats. (D) RT-PCR for the expression of CFTR and CAII in the cultured prostate epithelial cells after testosterone treatment.

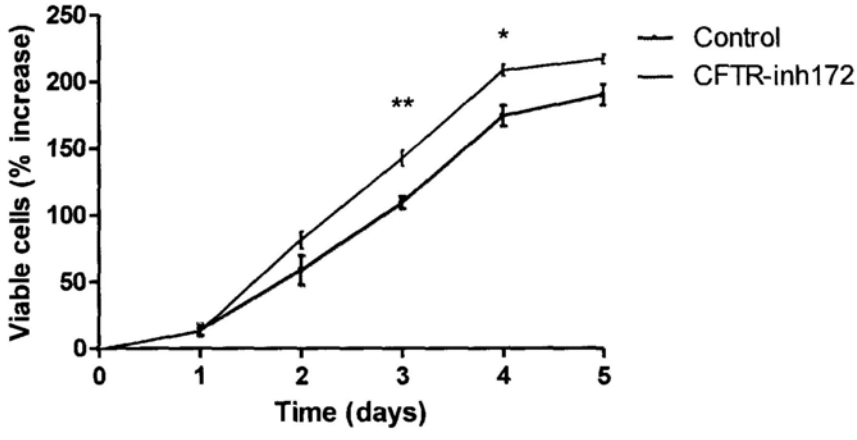

Figure 4.7 The effect of $CFTR_{inhibitor}$-172 on the proliferation of prostate primary epithelial cells measured by MTS cell proliferation assay. The growth rate of prostate epithelial cells was significantly higher than control cells on day 3 and day 4 after pretreated with $CFTR_{inhibitor}$-172. Data were presented by mean ± S.E.M. Significance were calculated by t-test *$p<0.05$ and **$p<0.01$.

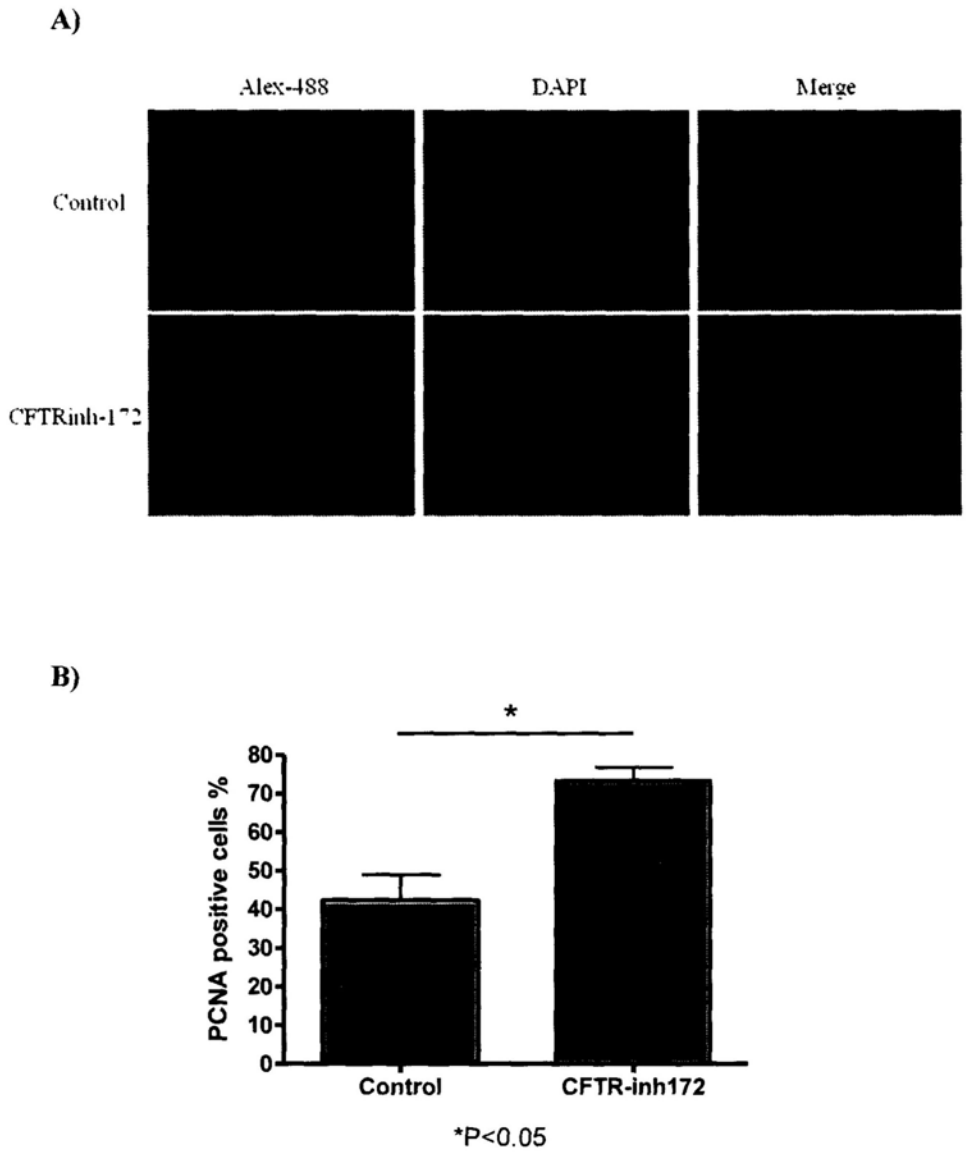

Figure 4.8 Immunofluorescence staining for proliferating cell nuclear antigen (PCNA) in prostate primary epithelial cells with and without $CFTR_{inhibitor}$-172. (A) Immunofluorescence detection of PCNA was evaluated in prostate primary epithelial cells with and without $CFTR_{inhibitor}$-172 (×400 Bar= 20μm). (B) A higher number of prostate primary epithelial cells treated with $CFTR_{inhibitor}$-172 were immunoreactive for PCNA. Data were presented by mean ± S.E.M. Significance were calculated by t-test *p<0.05.

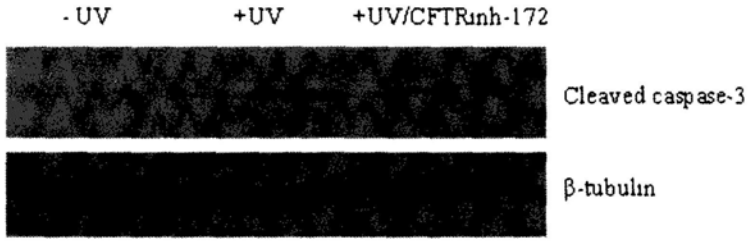

Figure 4.9 Expression of cleaved caspase-3 in prostate primary epithelial cells with and without $CFTR_{inhibitor}$-172 after UV radiation. UV radiation increased the expression of cleaved caspase-3 in prostate epithelial cells; however $CFTR_{inhibitor}$-172 could block the UV-induced activation of caspase-3.

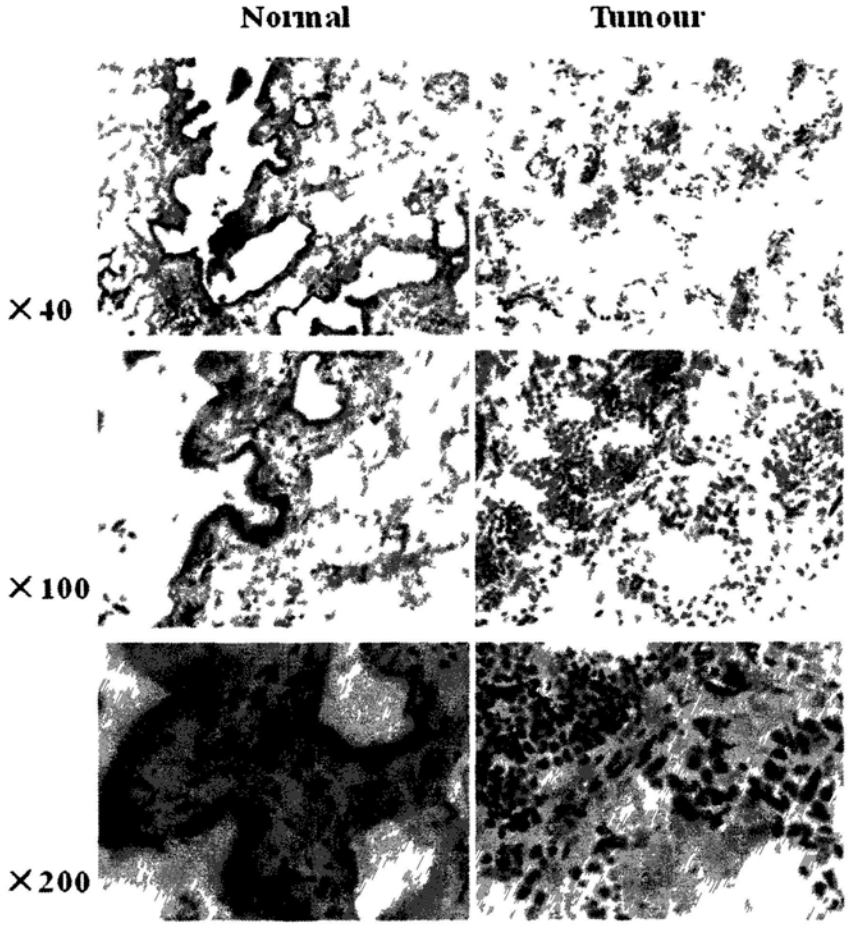

Figure 4.10 Immunohistochemical staining of human prostate specimens. Left, normal prostate tissue The CFTR protein was found to be stained in the normal prostate epithelial cells Right, prostate cancer tissue Staining of prostate cancer cells for CFTR was weakly positive in the prostate tumor specimens when compared with the intense epithelial staining of the normal prostate tissues

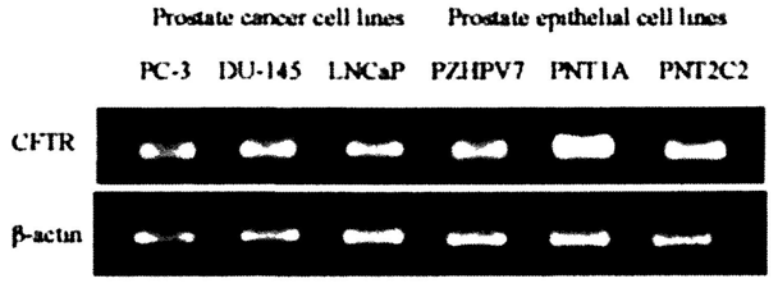

Figure 4.11 Conventional RT-PCR for the mRNA levels of CFTR in 6 prostate cell lines. Relatively lower CFTR expression was revealed in prostate cancer cell lines compared to prostate epithelial cell lines.

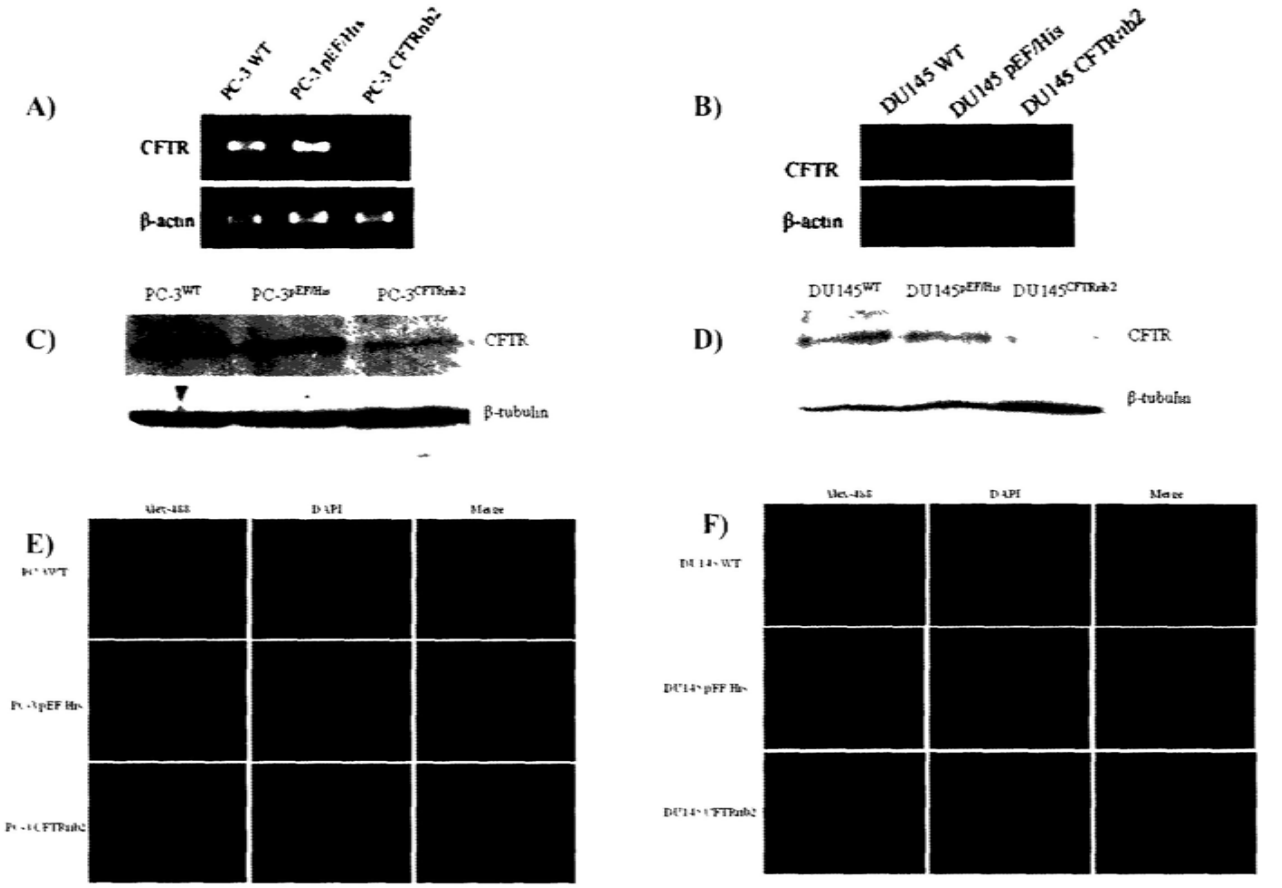

Figure 4.12 Knock down of CFTR in PC-3 and Du145 cells. Knock down of CFTR in PC-3 cells and DU145 cells were analyzed by RT-PCR (A, B), western blot (C, D) and immunofluorescence staining (E, F). For western blot, the whole cell lysate were probed with anti-CFTR (Alexis 804-214) antibody and β-tubulin was used as loading control. For immunofluorescence staining, PC-3 and DU145 cells were cultured in cover slips and stained with anti-CFTR (Alexis 804-214). Nuclei were counterstained with DAPI.

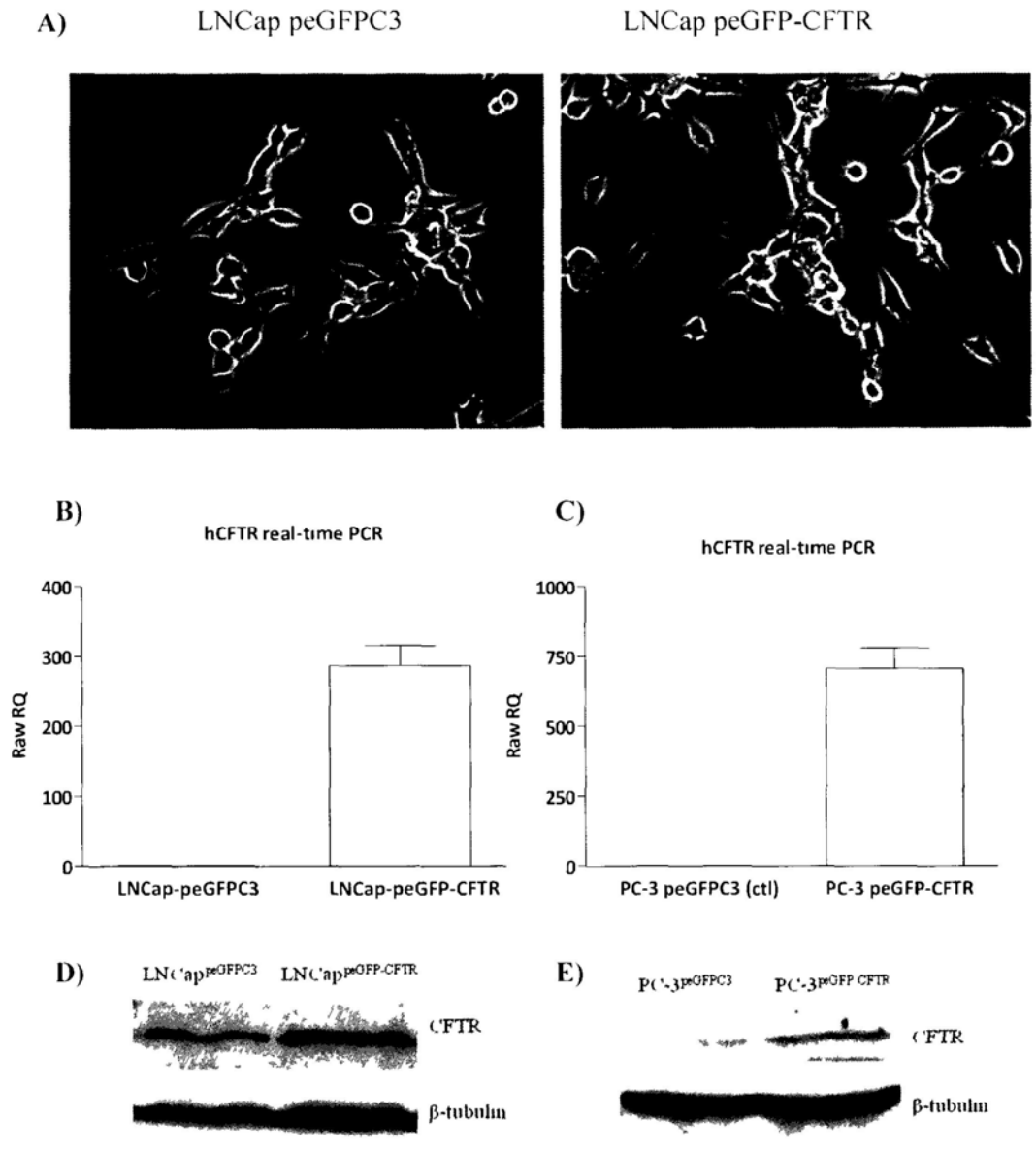

Figure 4.13 Overexpression CFTR in LNCap and PC-3 cells. Overexpression of CFTR in LNCap and PC-3 cells. (A) Phase contrast image of LNcap cells overexpressing CFTR compared to vector control. Note the CFTR expressing cells displayed an elongated morphology with extended processes. The expression of CFTR in LNCap was analyzed by real-time PCR (B, C) and western blot (D, E). For western blot, the whole cell lysate were probed with anti-CFTR (ACL-006) antibody. β- tubulin was used as loading control

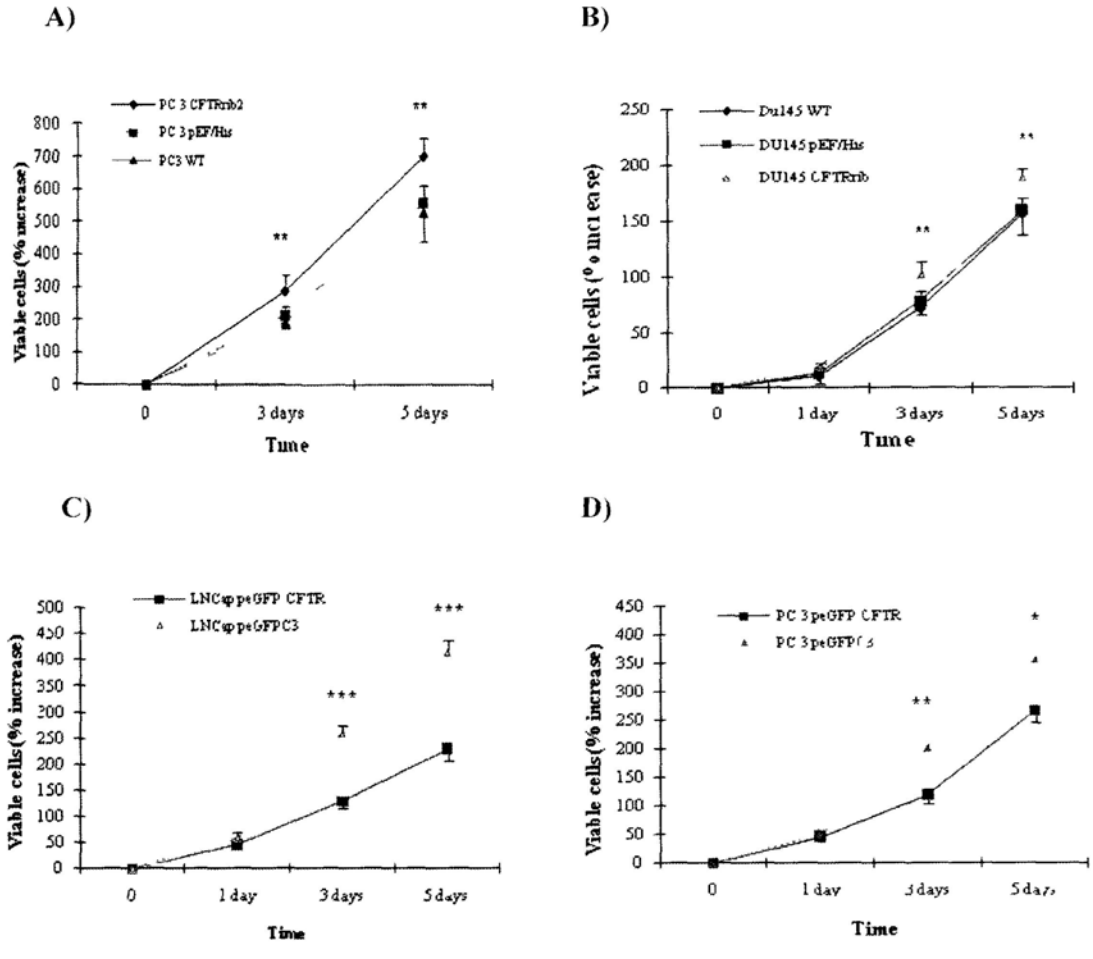

Figure 4.14 Proliferation studies of CFTR knock down and overexpression cells. (A, B) Knockdown of CFTR promotes the cell growth of PC-3 and Du145 cells (C, D) Overexpression of CFTR inhibits the cell growth of LNcap and PC-3 cells The growth rate was calculated as a percentage using the absorbance of day 1 as a baseline Error bars represent the S E M (n=6) Three independent experiments were done Significance were calculated by t-test *p<0 05, **p<0 01 and ***p<0 001 versus empty plasmid control cells

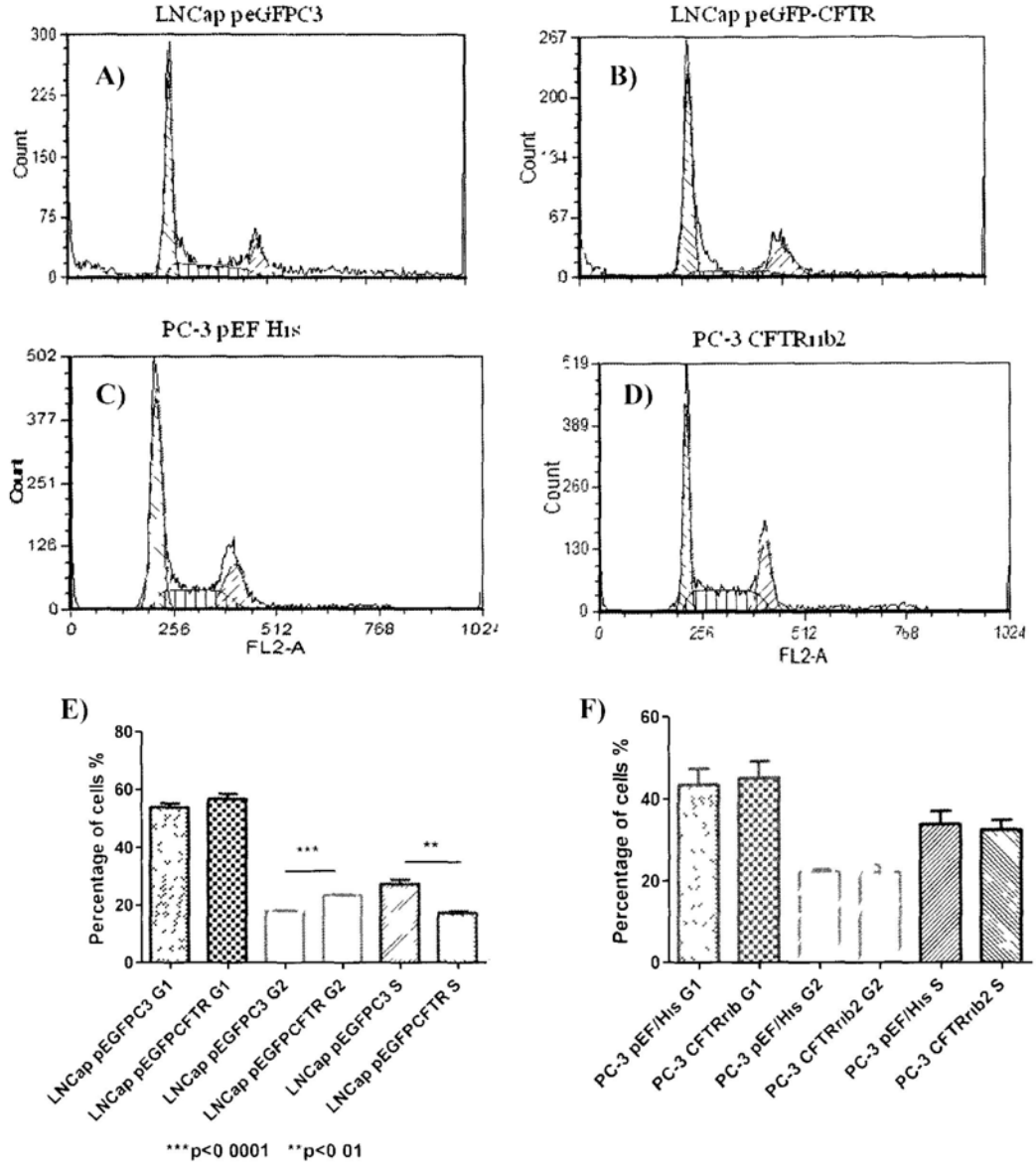

Figure 4.15 Cell cycle profiles of CFTR overexpression and knock-down cells. Cells were seeded in culture flask before FACs analysis. DNA profiles were shown in Figure A-D. The cell population in G2 phase of LNCap$^{peGFP\text{-}CFTR}$ cells significantly increased when compared to LNCap^{peGFPC3} control. Meanwhile, the population of S phase of LNCap$^{peGFP\text{-}CFTR}$ cells was significantly lower than that in LNCap^{peGFPC3} cells. No significant differences were observed in PC-3 CFTR knockdown cells. The data were summarized in Figure F. F. (Data were presented by mean ± S.E.M.. Significance were calculated by t-test **p<0 01; ***p<0.0001)

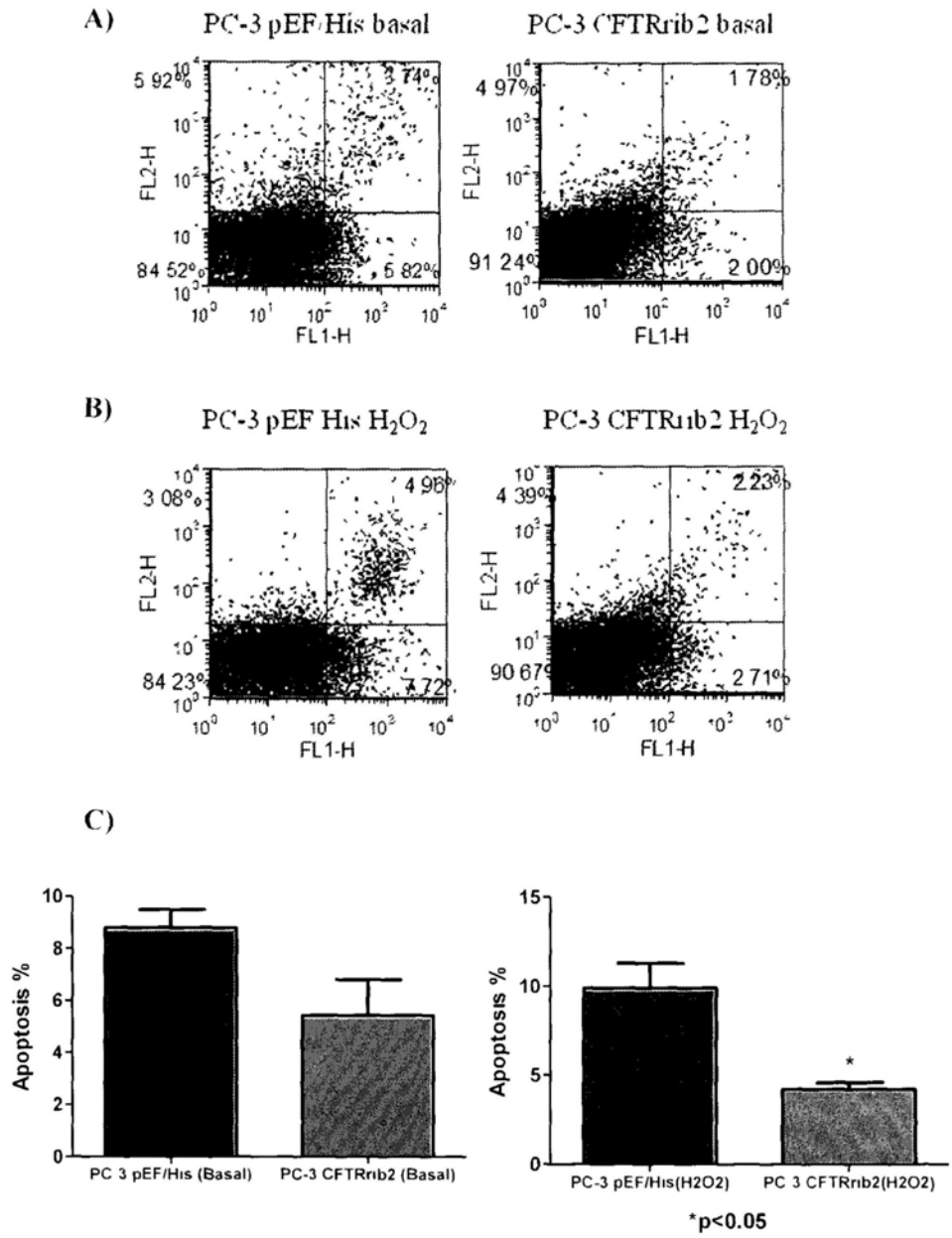

Figure 4.16 knock-down of CFTR inhibited both basal and H_2O_2 induced apoptosis in PC-3 cells using flow cytometry. Cells were seeded in culture flask before FACs analysis. Knock-down of CFTR inhibited the apoptosis in PC-3 cells on basal condition and H_2O_2-induced condition (A, B). Summarized data was shown in Figure C. (Data were presented by mean ± S.E.M.; Significance were calculated by t-test *p<0.05)

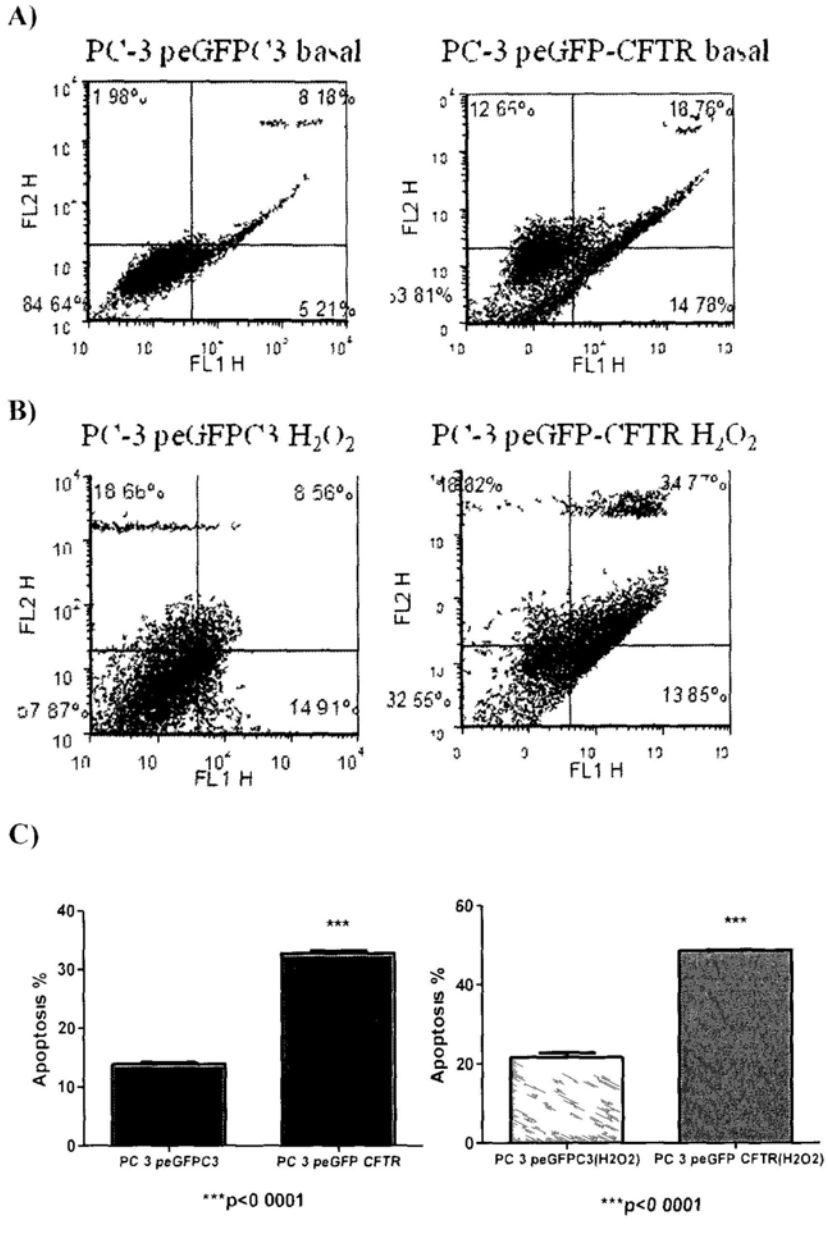

Figure 4.17 Overexpression of CFTR enhances apoptosis in PC-3 cells using flow cytometry. Cells were seeded in culture flask before FACs analysis Overexpression of CFTR significantly promoted the apoptosis in PC-3 cells on basal condition and H_2O_2-induced condition (A, B) Summarized data was shown in Figure C (Data were presented by mean ± S E M , Significance were calculated by t-test *p<0 05)

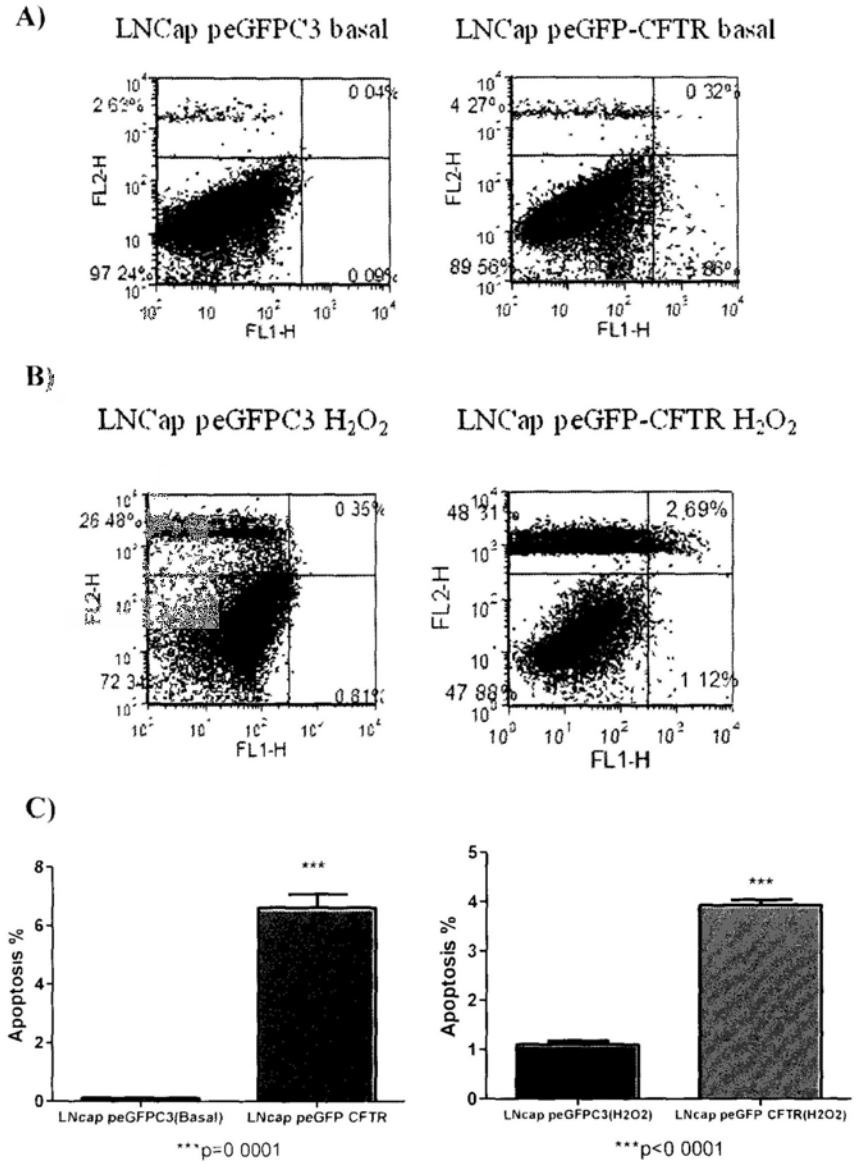

Figure 4.18 Overexpression of CFTR enhances apoptosis in LNCap cells using flow cytometry. Cells were seeded in culture flask before FACs analysis. (A) Overexpression of CFTR significantly promoted the apoptosis in LNCap cells on basal condition. (B) After treated by 0.8 mM H_2O_2, there were more apoptotic cells in CFTR-overexpression cells.Summarized data was shown in Figure C. (Data were presented by mean ± S.E.M.; Significance were calculated by t-test ***p<0.0001)

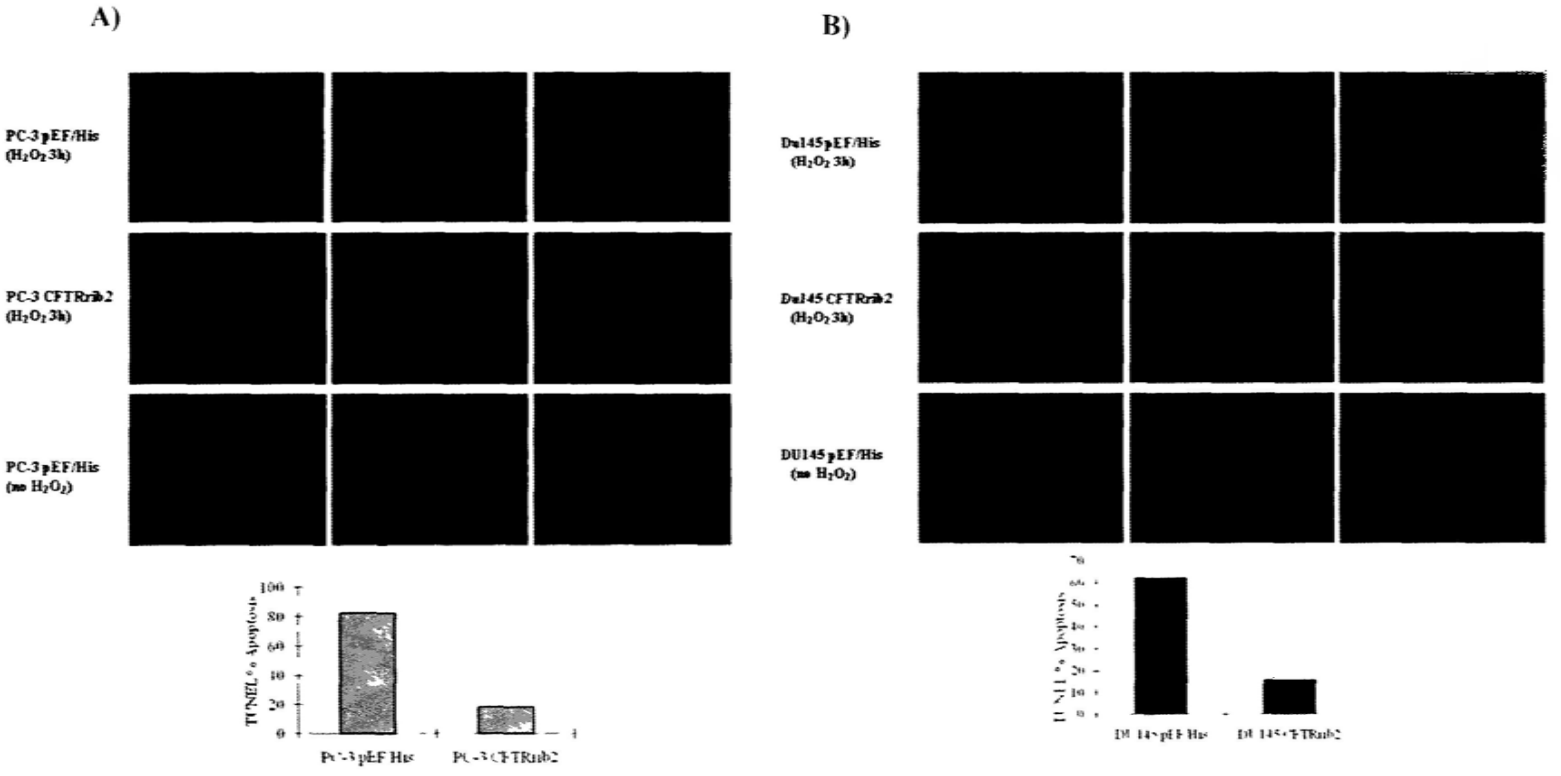

Figure 4.19 The anti-apoptotic function of knock-down CFTR in PC-3 cells after H_2O_2 treatment using TUNEL assay. Cells were seeded in cover slips before TUNEL analysis. There are lower percentage of TUNEL positive cells in PC-$3^{CFTRrib2}$ (A) and DU$145^{CFTRrib2}$ (B) cells compared with their vector control cells

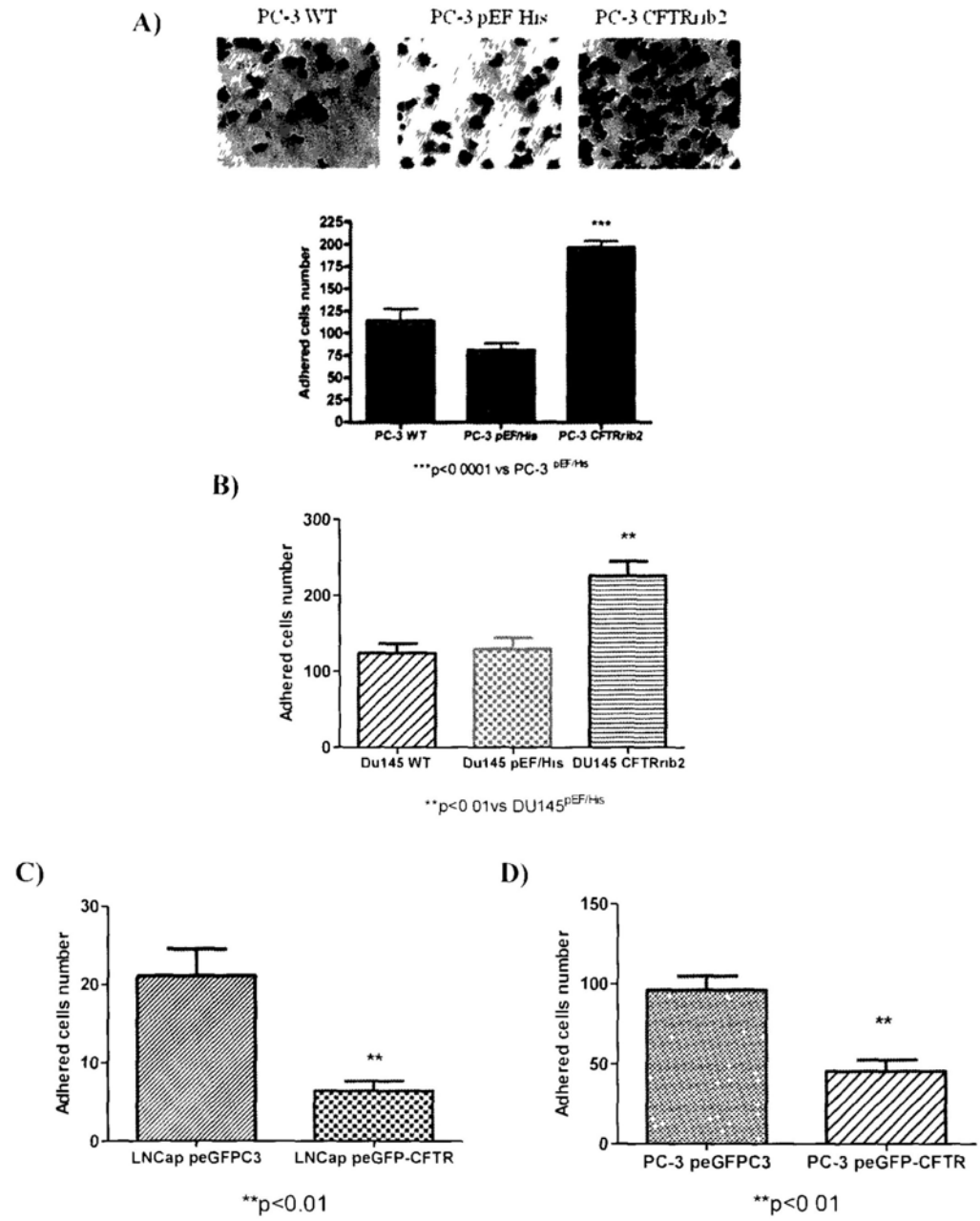

Figure 4.20 Adhesion assay of CFTR knock-down and overexpression cells. (A, B): Knockdown of CFTR increased adhesion of PC-3 and DU145 cells. (C, D): Overexpression of CFTR significantly decreased adhesion of LNCap and PC-3 cells using *in vitro* cell-matrix adhesion assay. Experiments were performed in 6 wells per cell line. Error bars represent the S.E.M. Significance were calculated by t-test **p<0.01; ***p<0.0001.

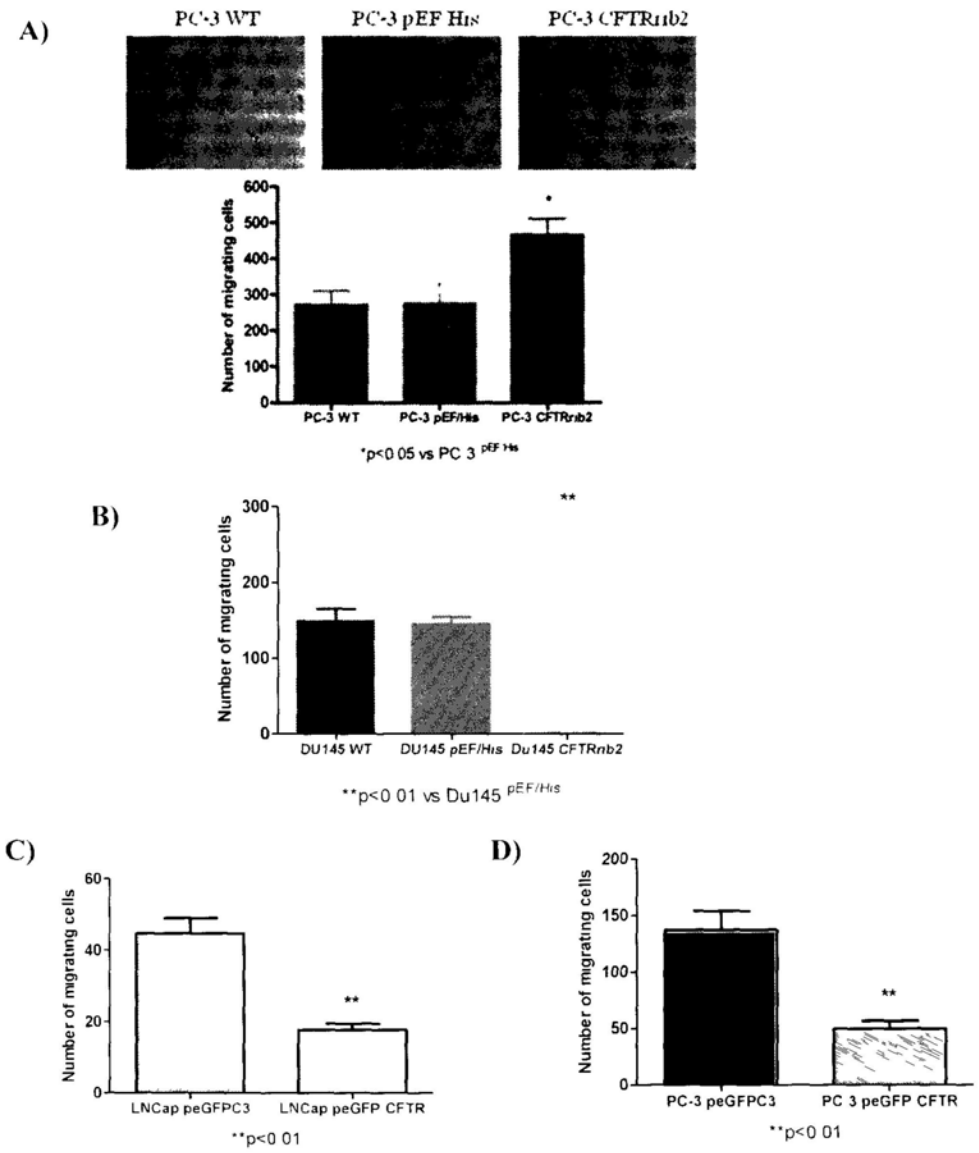

Figure 4.21 In vitro motility assay of CFTR knock-down and overexpression cells. The effect of CFTR on cell migration was determined using a cytodex-2 bead motility assay. (A, B): The motility of PC-$3^{CFTRrib2}$ and $DU145^{CFTRrib2}$ was markedly increased compared with plasmid control cells. (C, D): The motility of $LNCap^{peGFP\text{-}CFTR}$ and PC-$3^{peGFP\text{-}CFTR}$ was markedly decreased compared with plasmid control cells. Experiments were done in 6 wells per cell All experiments were repeated 4 times. Error bars represent the S.E M. Significance were calculated by t-test *p<0.05; **p<0.01.

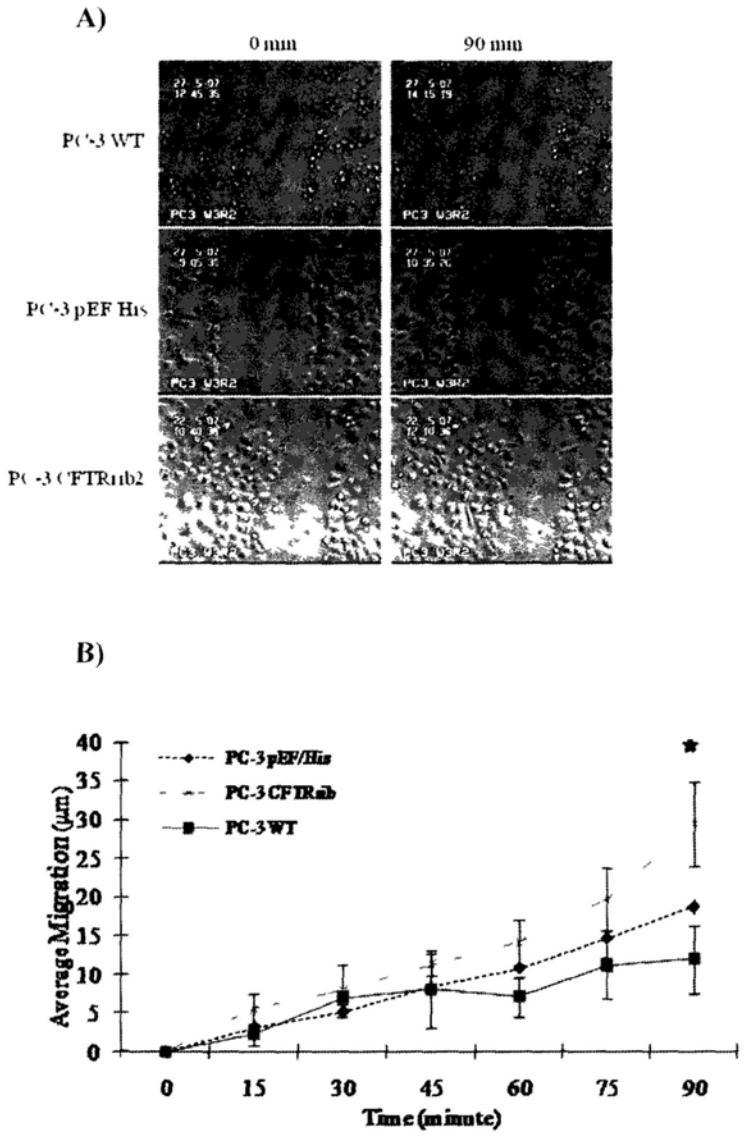

Figure 4.22 Migration assay of CFTR knock-down PC-3 cells. Knockdown of CFTR enhanced the migration of PC-3 cells using scratch wounding assay. Migration was recorded by Time Lapse Imaging and migrated distances were measured. Photomicrography of the front line of cells on 0 min and 90 min were shown in Figure A. All experiments were repeated 3 times. The movement ability was increased significantly in PC-$3^{CFTRnb2}$ cells compared with wild-type and empty plasmid control cells (B). Error bars represent the S.E.M. Significance was calculated by t-test, *$p<0.05$.

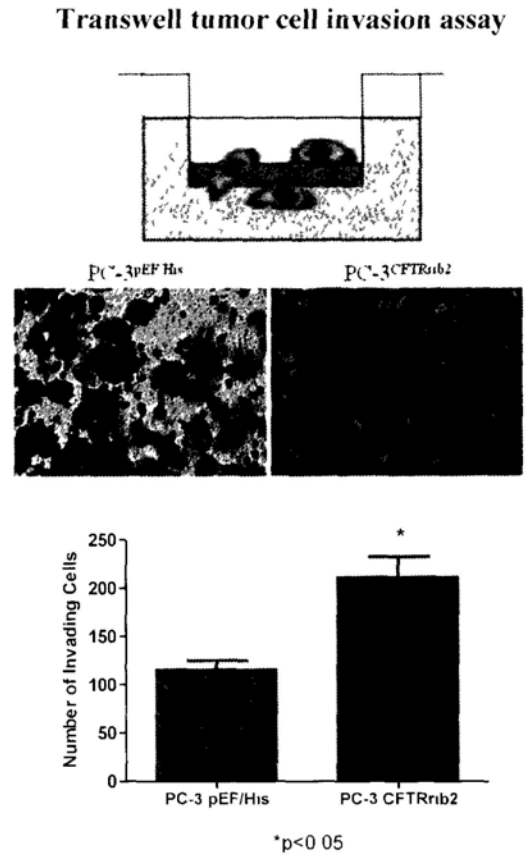

Figure 4.23 Invasion assay of CFTR knock-down PC-3 cells. The influence of CFTR knockdown on the invasiveness of PC-3 cells was determined by using the *in vitro* invasion assay. The invasiveness of PC-$3^{CFTRrib2}$ cells did not show any significant difference from that control vector transfected cells. (Data were presented by mean ± S.E.M.; Significance were calculated by t-test *$p<0.05$)

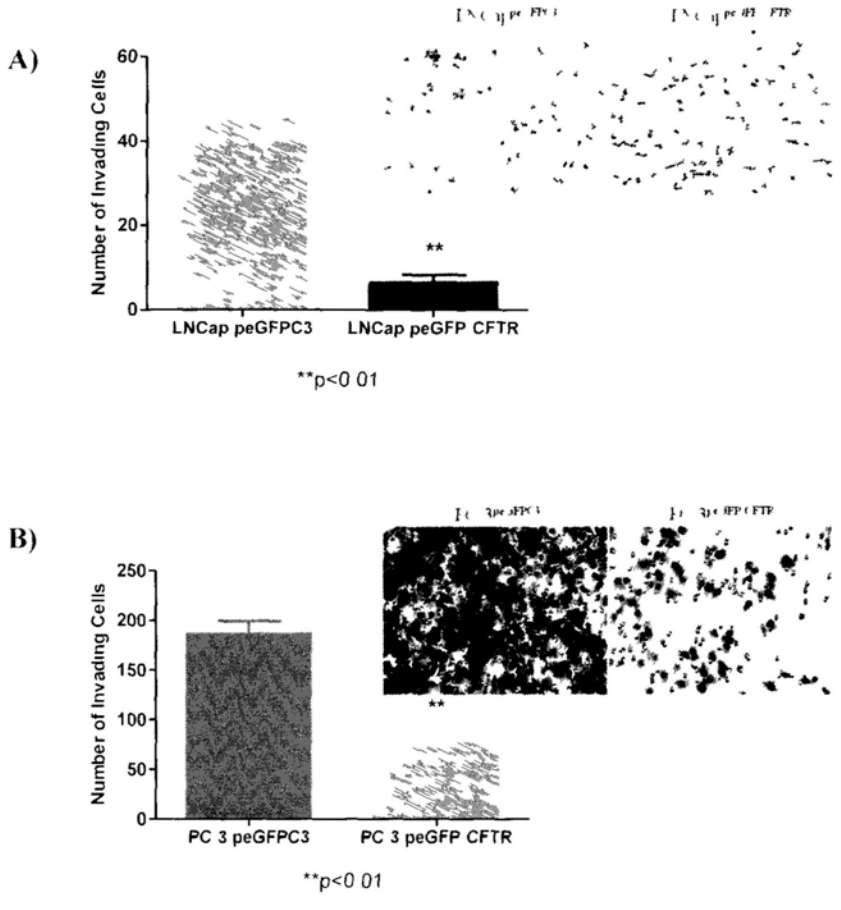

Figure 4.24 Invasion assay of CFTR overexpression LNCap and PC-3 cells. CFTR overexpression markedly reduced the invasiveness of LNCap and PC-3 as compared to vector control after 72h incubation (A, B) (Data were presented by mean ± S E M, Significance were calculated by t-test **p<0 01)

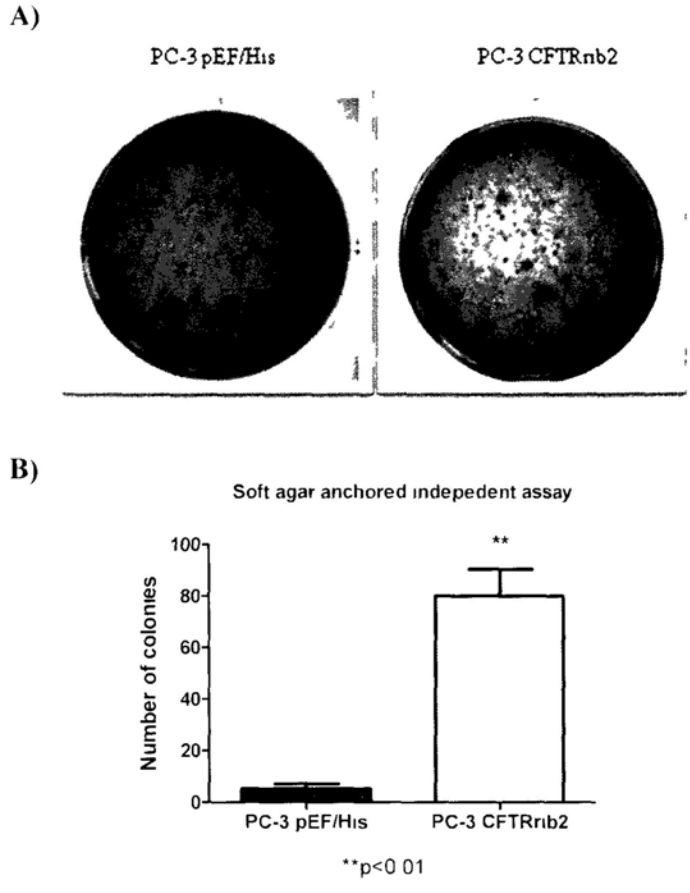

Figure 4.25 Colony formation assay of CFTR knock-down PC-3 cells. Cells were seeded in soft agar and the number of colonies was counted after 3 weeks. Representative images for formed colonies are shown in A. Knock-down of CFTR in PC-3 cells resulted in increase of colony formation when compared to PC-3$^{pEF\ His}$ control (B). (Data were presented by mean ± S.E.M.; Significance were calculated by t-test **p<0.01)

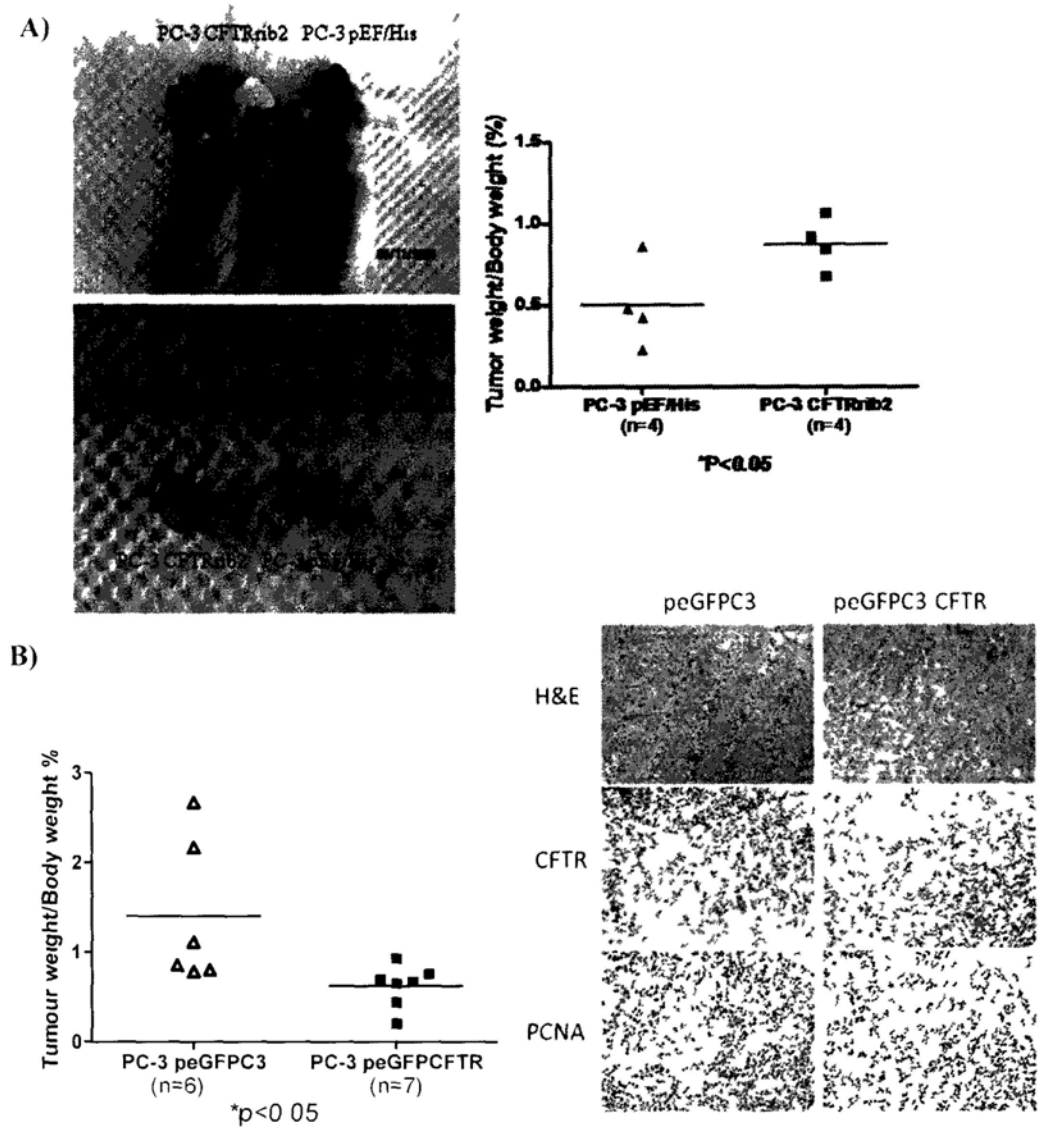

Figure 4.26 Tumorigenicity of CFTR *in vivo*. Cells were intrasubcutaneously injected into nude mice Tumor weight to body weight ratios was calculated (A) Knockdown of CFTR significantly increased the tumorigenicity of PC-3 cells when compared to PC-$3^{pEF\ His}$ control (B) Overexpression of CFTR significantly decreased the tumorigenicity of PC-3 cells when compared to PC-$3^{peGFPC3}$ control The results from immunohisological staining showed that the decreased PCNA-positive cells in paraffin-fixed tumor sections of PC-$3^{peGFP\ CFTR}$ compared to PC-$3^{peGFPC3}$ groups (Data were presented by mean ± S E M , Significance were calculated by t-test *p<0 05)

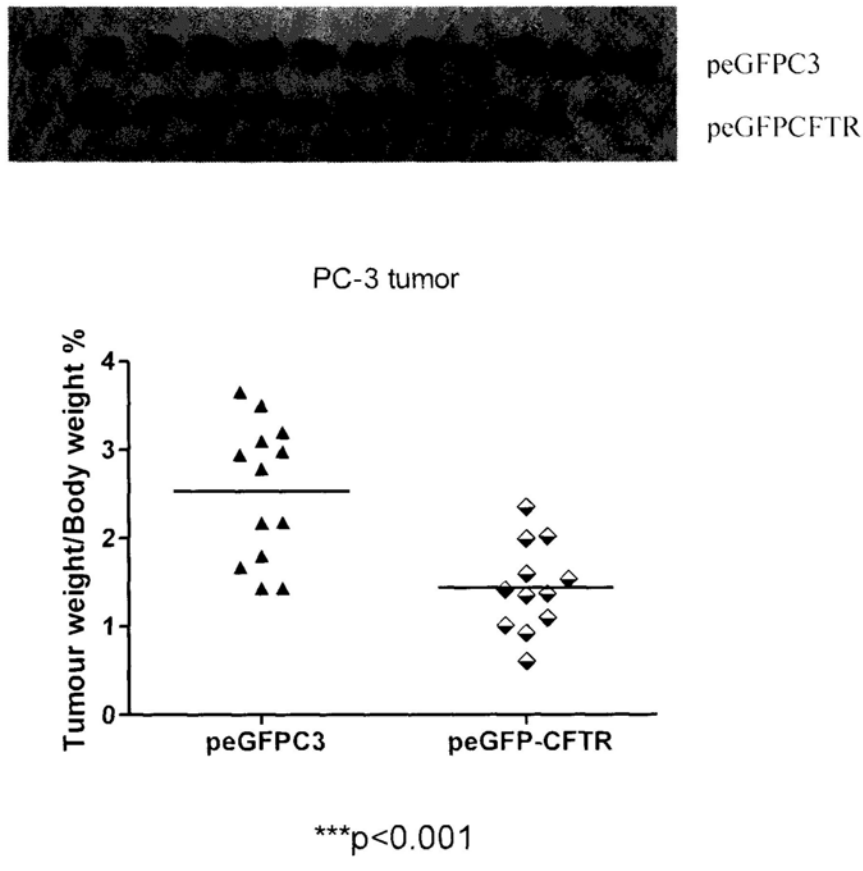

Figure 4.27 Ultrasound-mediated gene transfer of CFTR inhibited tumor growth. The size of tumor transfected with peGFP-CFTR plasmid was remarkably smaller than that tranfected with vector control. Data were presented by mean ± S.E.M.; Significance was calculated by t-test ***p<0.001.

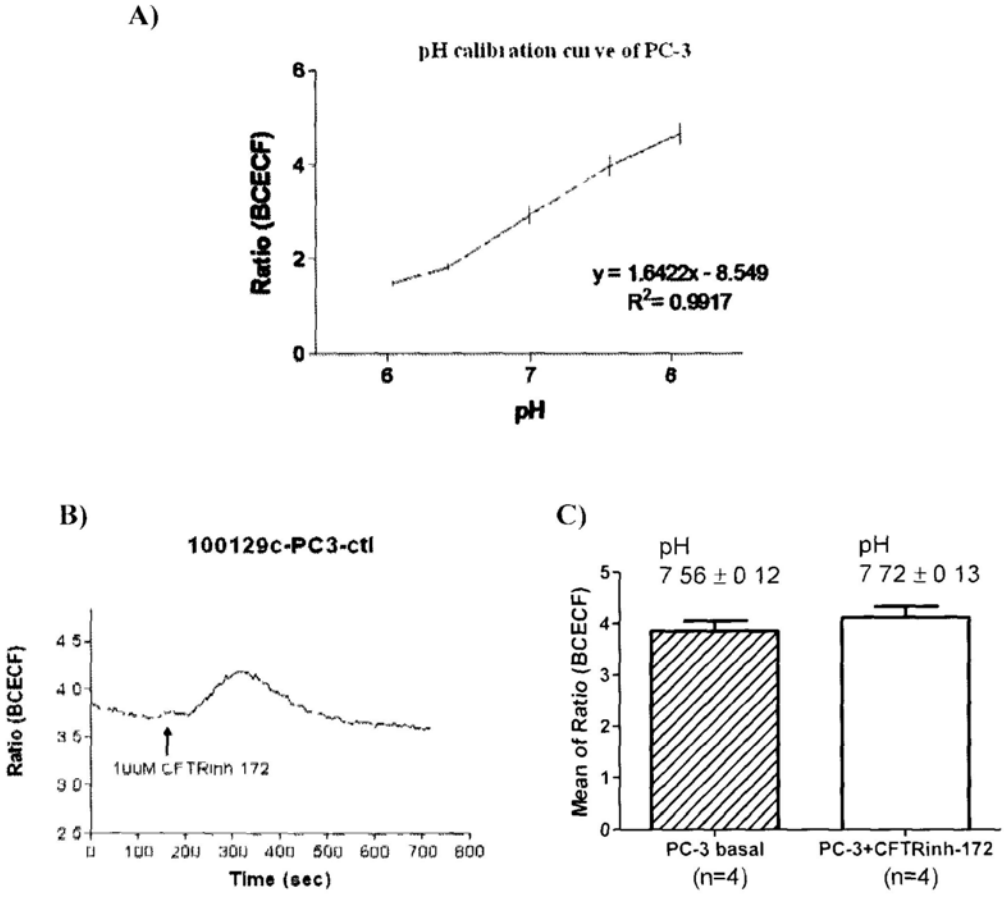

Figure 4.28 Effect of $CFTR_{inhibitor}$-172 on the intracellular pH in PC-3 cells. (A) The calibration curve with different pH of calibration solution converted to fluorescence changes. (B) Effect of $CFTR_{inhibitor}$-172 on the pHi in PC-3 cells. (C) The statistics of the calibrated pHi changes for basal control and $CFTR_{inhibitor}$-172 treatment. Blocking CFTR using $CFTR_{inhibitor}$-172 could increase the pHi of PC-3 cells. Data were presented by mean ± S.E.M.

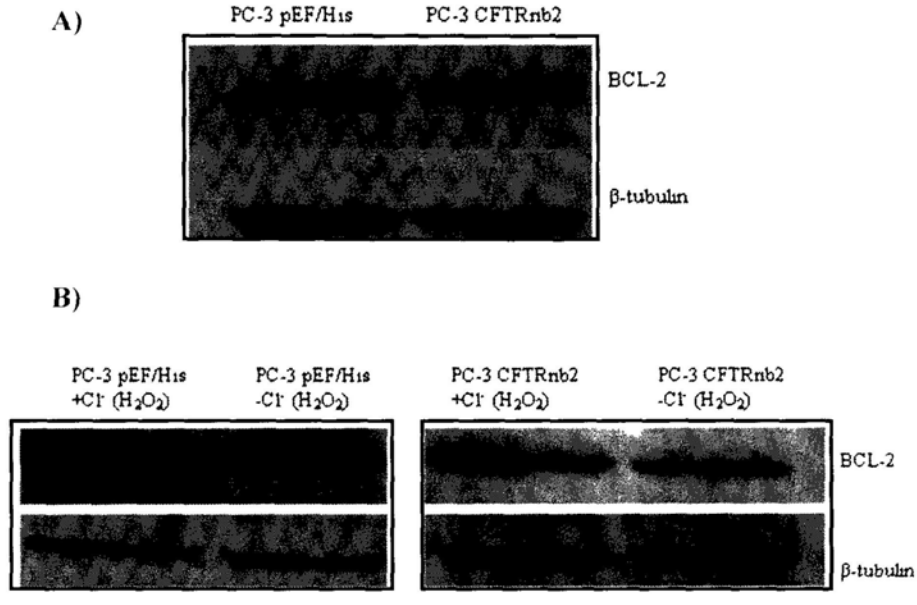

Figure 4.29 Western blot analysis of the effect of H_2O_2 and extracellular Cl^- on the expression of BCL-2 in the presence or absence of CFTR in PC-3 cells. (A) PC-$3^{pEF\ His}$ and PC-$3^{CFTRnb2}$ cells expressed the same protein level of Bcl-2 in chloride-containing solution. (B) After treated with H_2O_2, Bcl-2 expression was more significantly decreased in chloride-free solution compared to that in chloride-containing solution in vector control cells, whereas this difference was abrogated in CFTR knockdown cells.

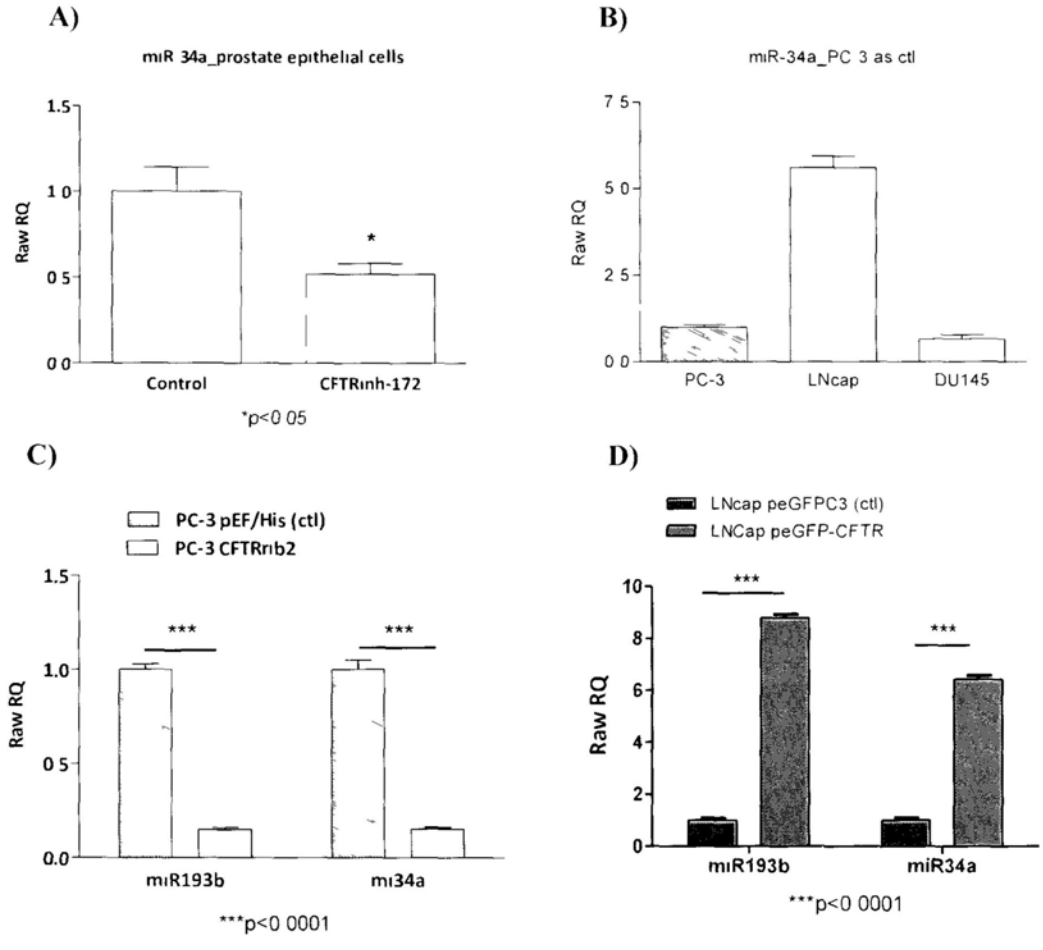

Figure 4.30 The expression of miR-34a and miR-193b in different prostate epithelial cells. (A) The expression of miR-34a was significantly reduced in cultured rat prostate epithelial cells after treating with 10 μM CFTRinh-172. (B) MiR34a was differentially expressed in PC-3, LNcap and DU145 cells depending on the p53 status. (C) The expression level of miR-34a and miR-193b transcript in PC-3^{CFTRrib2} was significantly lower than PC-3$^{pEF/His}$. (D) The expression level of miR-34a and miR-193b transcript in LNCap$^{peGFP-CFTR}$ cells was remarkably higher than LNCap^{peGFPC3} cells. Data were presented by mean ± S.E.M.; Significance was calculated by t-test, *p<0.05, ***p<0.001

GeneSymbol	Accession number	Regulation	Fold	P value	Description
CDKN1A	NM_000389	up	1.62	0.0003	cyclin-dependent kinase inhibitor 1A (p21)
FGFR2	NM_000141	down	3.00	0.0001	fibroblast growth factor receptor 2
HTATIP2	NM_006410	down	1.65	0.0178	HIV-1 Tat interactive protein 2, 30kDa
IL8	NM_000584	down	2.80	0.0035	Interleukin 8
ITGA1	NM_181501	down	2.11	0.0089	Integrin, alpha 1
MTSS1	NM_014751	down	2.78	0.0015	Metastasis suppressor 1
THBS1	NM_003246	down	2.95	0.0003	Thrombospondin 1
TNF	NM_000594	down	2.30	0.0012	Tumor necrosis factor (TNF superfamily, member 2)
TWIST1	NM_000474	down	11.22	0.0039	Twist homolog 1 (Drosophila)
EPDR1	NM_017549	down	1.90	0.0075	Ependymin related protein 1 (zebrafish)
VEGFA	NM_003376	up	1.61	0.0094	Vascular endothelial growth factor A

Table 4.1 Differential expressed genes in LNCap cells overexpressing CFTR using Human Cancer PathwayFinder PCR array. Genes are presented by symbols and descriptions Genes that were up-regulated are highlighted by Blue while down-regulated genes are highlighted by Pink Differences between groups are presented by fold-change Differentially expressed transcripts with $p<0.05$ and fold change >1.5 are reported

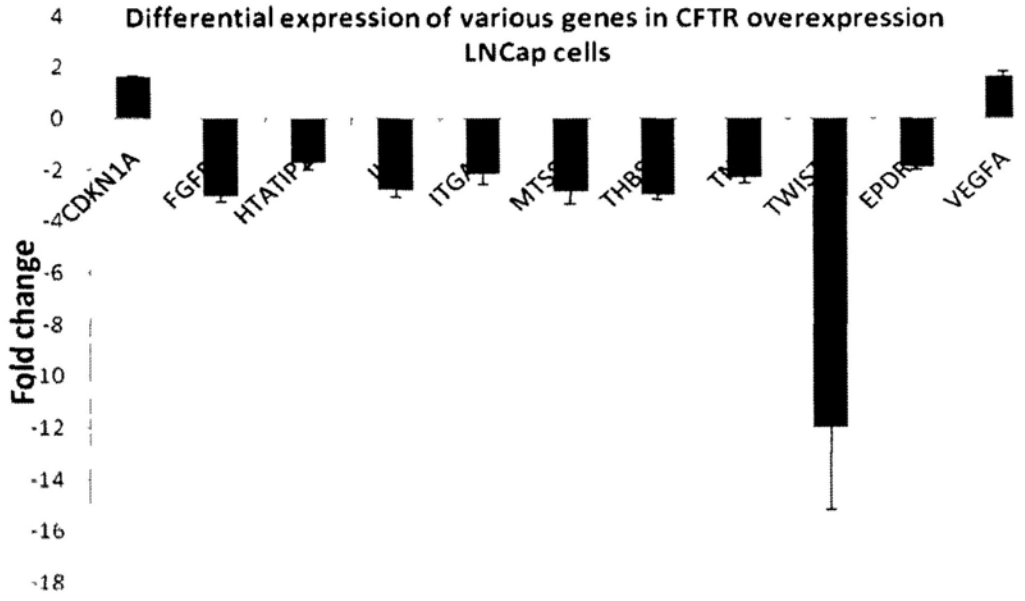

Figure 4.31 Real-time PCR for selected differentially expressed genes in CFTR overexpression LNcap cells. Gene expressions were compared by comparative ΔΔct method and data were presented by fold change. Differentially expressed transcripts with $p<0.05$ and fold change >1.5 were reported. Data were presented by mean ± S.E.M.

Table 4.2 Primers for RT-PCR

Primer name		Sequence(5'→ 3')
GAPDH	Forward	GAC CAC AGT CCA TGC CAT CAC TGC
	Reverse	GCT GTT GAA GTC GCA GGA GAC AAC
β-actin	Forward	ATG ATA TCG CCG CGC TCG
	Reverse	CGC TCG GTG AGG ATC TTC A
CFTR(rat)	Forward	AAC TGA GAC CTT ACG CAG
	Reverse	AGA AGC TCT GGT CCT CTG
CAII	Forward	ATG ACC CTT CCC TAC AGC
	Reverse	GGT CAC ACA TTC CAG CAG
CFTR(human)	Forward	AAA ACT TGG ATC CCT ATG AAC
	Reverse	GTG GGG AAA GAG CTT CAC
CFTR (ribozyme2)	Forward	CTG CAG AGA AGG CAT AAG CCT ATG CCT ACT GAT GAG TCC GTG AGG A
	Reverse	ACT AGT ACC CGG ATA ACA AGG AGG AAC GCT CTA TCG CGA TTT ATT TCG TCC TCA CGG ACT

4.5 Discussion

In addition to its well-established ion channel function, CFTR has been proposed to either directly or indirectly impact various cellular functions, including cell proliferation, apoptosis and differentiation. Disruption of these processes may result in abnormal tissue growth or even cancer. In fact, improved life expectancy among patients with CF has unmasked a significant increase in the incidence of malignancies. A large cohort study in North American and European patients with CF found that although the overall risk of cancer was similar to that of the general population, there was a marked increase in risk of malignancies affecting the gastrointestinal tract, pancreas and hepatobiliary system (Neglia JP, 1995; Maisonneuve P, 2003; Wilschanski M, 2007), Moreover, individuals who were CFTR mutation carriers were found to be at an increased risk for young onset of pancreatic cancer (McWilliams R, 2005). On the contrary, an inverse association between CF gene mutations and incidence of several cancers, such as melanoma (Warren N, 1991), breast cancer (Abraham EH, 1996), colon cancer (Padua RA, 1997), prostate cancer (Qiao D, 2008) and lung cancer (Li Y, 2010) has also been reported. The seemingly ambiguous results from these clinical correlation studies may be attributed to the differences in sample size, study design and various CFTR mutations included among individual studies. Thus, the issue of CFTR variations in the etiology of cancer is still highly controversial. On the other hand, hypermethylation of CFTR promoter has been reported in both cancer cell lines and primary tumor samples (Ding S, 2004; Bibikova M, 2006; Mishra DK, 2010), indicating DNA methylation mediated transcription silencing of CFTR may promote carcinogenesis. Taken together, functional characterization of CFTR with respect to its abilities to mediate a gain of oncogenic

activity or loss of tumor suppressor function is urgently needed to clarify the biological significance of CFTR in tumorigenicity.

In the present studies, we found age dependent downregulation of CFTR in rat prostate which may be due to the decreased testosterone levels during aging. Moreover, inhibition of its channel function in primary cultures of prostatic epithelial cells enhanced cell proliferation and resistance to UV induced apoptosis, indicating CFTR-mediated channel function is critical for maintaining normal cellular function in prostate epithelial cells, and therefore reduced expression of CFTR during aging should contributes to age-associated diseases, such as prostate cancer. This hypothesis was further supported by our finding that CFTR is downregualted in both prostate cancer cell lines and human prostate cancer specimen. Prostate cancer cell lines, which are commonly used as *in vitro* models, as well as for *in vivo* assessment of cancer progression, for both androgen-dependent (LNCap) and androgen-independent (PC-3 and DU145) prostate cancer cells, were genetically modified and used to study the role of CFTR in prostate cancer development and progression. In the present study, we employed methods to genetically alter the expression of CFTR in prostate cancer cells, namely the ribozyme transgenes approach and overexpression approach, respectively. The results demonstrated that CFTR could inhibit cell growth and promote apoptosis in prostate cancer cells. The enhanced cell survival rate by knockdown of CFTR was through both promoting proliferation and anti-apoptosis mechanism. Moreover, CFTR could impair the adhesion, motility and invasion ability of prostate cancer cells which indicates that CFTR may play a key role in the control of the aggressiveness of prostate cancer, via the mechanisms yet to be identified. These results prompted us to propose

that CFTR acts as a putative tumor suppressor in prostate cancer. This notion is further supported by our *in vivo* results, in which prostate cancer cells overexpressing CFTR grew much slower while CFTR knockdown cells grew remarkably faster than their corresponding control cells. Furthermore the ultrasound –mediated gene transfer of CFTR in prostate tumors attenuated the tumor growth *in vivo* which indicated that CFTR gene transfection has a therapeutical potential effect for treatment of prostate cancer.

Although the precise molecular mechanisms responsible for the function of CFTR in prostate carcinogenesis are unclear, our studies have indicated that several distinctive pathways may be responsible for the biological function of CFTR protein. Firstly, CFTR modulates apoptotic response through its ion channel function in prostate cancer cells. The process of apoptosis can be regulated by changes in extracellular and intracellular microenviornment, such as fluctuations in Cl^- concentrations and pH. Several Cl^- channels have been implicated in the regulation of apoptosis in a variety of cell types (Gottlieb RA, 1996; Hume, JR, 2010; Okada Y, 2006). Among the proposed mechanisms accounting for the proapoptotic effect of anion channels, cellular acidification have been demonstrated to trigger mitochondria apoptotic cascade involving Bcl-2 (Poulsen JH, 1994; Shen MR, 2002). We observed that the alteration in intracellular pH upon CFTR inhibition. We also investigated the effect of extracellular Cl^- on apoptotic responses in the presence and absence of CFTR. The H_2O_2-mediated apoptosis is associated with a decrease in antiapoptotic protein Bcl-2. This phenomenon can be abrogated when chloride was removed from the extracellular media, indicating the H_2O_2-mediated apoptosis depends on chloride transport by CFTR, similar to other reported Cl^- channels. Meantime, as an ion channel, CFTR has another potential role in

regulating apoptosis through HCO_3^- dependent pathway, which could activate sAC as secondary responses to the primary changes in the ion fluxes (Kumar S, 2009). sAC has been suggested to control mitochondria-dependent apoptosis through cAMP-PKA pathway. In our present study, we did not investigate CFTR mediated HCO_3^--dependent apoptotic activities, but its possible involvement warrants further studies.

Secondly, CFTR upregulates miR34a and miR193b, both of which are tumor suppressors. We report for the first time that CFTR could regulate miR-34a and miR-193b expression. Aberrant expression of miRNAs in cancer has been well documented and miRNA may function as oncogenes and tumor suppressors. p53 is a well known tumor suppressor that regulates various physiological process including cell growth, cell cycle arrest, DNA repair and apoptosis. miR-34 is a direct transcriptional target of p53 and miR-34 activation can promote growth arrest and cell apoptosis in response to cancer related stress and loss of miR-34 impairs p53-mediated cell death (He L, 2007). We found that the expression levels of miR-34a were remarkably decreased in androgen-independent PC-3 (null p53) and DU145 (mutated p53) cells compared to androgen-dependent LNCap (wild-type p53) cells which suggested that miR-34a expression is dependent on the p53 activity in prostate cancer cell lines. In our study, the expression of miR-34a was remarkably increased in $LNCap^{peGFP\text{-}CFTR}$ cells which suggested that CFTR regulates cell growth or apoptosis through a p53-dependent pathway in LNcap cells; however the fact that down-regulation of CFTR in PC-3 cells which contain nonfunctional p53 pathway also led to down-regulated expression of miR-34a suggests that CFTR can regulate miR34a expression through a p53-independent pathway. Besides miR-34a, we found that the expression of miR-193b was also

correlated with CFTR expression in prostate cancer cell lines. Knockdown of CFTR could significantly reduce the expression of miR-193b, while overexpression of CFTR up-regulated miR193b. MiR-193b has been reported to repress cell proliferation and regulate cyclin D1 in melanoma (Chen J, 2010). In addition, it was reported recently that miR-193b functioned as a suppressor in breast cancer by targeting urokinase-type plasminogen activator (uPA) expression and inhibition of miR-193b led to increased uPA expression (Li XF, 2009). uPA is a serine protease which is responsible for catalyzing the conversion of the inactive zymogen plasminogen into the active plasmin proteinases. The enhanced activity of uPA has been associated with regulating cancer cell motility, adhesion, invasion and metastasis by degrading the extracellular matrix proteins (Dass K, 2008; Chapman HA, 1997; Gohji K, 1997). The effect of CFTR on the transcription level of miR-193b in prostate cancer cells and the reported relationship between miR-193b and uPA suggest that CFTR may regulate the development of prostate cancer through uPA system. Although the exactly mechanism by which CFTR regulates the transcription level of miR-193b and miR-34a requires further studies, the presently demonstrated potent effects of CFTR as a tumor suppressor indicate its therapeutic potentials for suppressing cancer invasion/ metastasis.

Thirdly, CFTR regulates multiple cancer associated genes. We used Human Cancer PathwayFinder PCR array to elucidate the possible pathways involved in CFTR-mediated tumor-suppressive function. Gene expression profiling provides novel insights into cancer-related traits. The results showed that among 11 differentially expressed genes, TWIST1 showed the most significant change at transcriptional level after over-expression CFTR. TWIST1, which belongs to the family of basic helix-loop-helix

transcription factors, is suggested as an oncogene (Maestro R, 1999). It was reported that TWIST1 expression was found to be highly expressed in the majority of prostate cancers but only in a small percentage of benign prostate hyperplasia (Wai Kei Kwok, 2005). The increased TWIST1 protein was positively correlated with Gleason grading. Moreover, it was reported that high levels of TWIST were associated with increased invasion ability in prostate and breast cancer cells and was identified to be essential for the metastatic process (Yang J, 2004). Hypoxia is a microenviromental factor which plays an important role in tumor progression. It was reported that TWIST could be activated by hypoxia inducible factor-1 (HIF-1) (Yang MH, 2008) and epithelial hypoxia could attenuates CFTR protein and function (Zheng W, 2009). In our study, overexpression of CFTR remarkably down-regulated the transcription level of TWIST1 up to 11.2 fold indicting that CFTR, , may regulate tumor progression through TWIST1 signaling pathway. Besides TWIST1, a number of genes have been identified to participate in the CFTR signaling pathway in prostate cancer cells such as CDKN1A, FGFR2, HTATIP2, IL8, ITGA1, MTSS1, THBS1, TNF, EPDR1 and VEGFA. Together, we have identified differentially expressed genes in CFTR over-expressing cells which might participate in controlling prostate tumorigenesis, further supporting our hypothesis that CFTR functions as a suppressor of prostate tumor by multiple mechanisms.

Interestingly, in chapter 3, we reported the expression of CFTR was upregulated along with CAII in the inflammation of prostate. The efflux of intracellular HCO_3^- catalyzed by CAII was likely through prostate apical anion channel CFTR. In this part of study, we found that in addition to CFTR, the expression of CAII in rat prostate was also age dependent. Hypoxia and acidosis in the tumor microenviroment are critical in

driving tumor growth and metastasis. CAII is the key intracellular pH regulators which may control tumor growth. It was reported that CAII are significantly less expressed in non-small cell lung cancer (NSCLC) (Chiang WL, 2002) and colorectal tumors (Mori M, 1993) but overexpressed in nervous system tumors (Parkkila AK, 1995) and pancreatic tumors (Parkkila S, 1995). Therefore the clear-cut relationship between the expressions of CAII in normal and malignant cells and the possible interaction between CFTR and CAII in prostate cancer development need to be further investigated.

Taken together, the present study has for the first time, demonstrated a role of CFTR as a putative tumor suppressor in prostate cancer by both *in vitro* and *in vivo* functional studies. The newly identified tumor suppressive effects of CFTR may help to explain both the genetic and epigenic defects observed in multiple cancers. The potential usage of CFTR as a target for diagnosis, prognosis and treatment of prostate cancer warrants further investigation.

Chapter 5 General discussion

In this study, the biological functions of CFTR in prostatitis and prostate cancer were investigated. The results showed that CFTR is involved in prostate HCO_3^- secretion and that enhancement of CFTR-mediated HCO_3^- secretion in prostatitis has a direct role in host defense against bacterial infection. Furthermore, the present study also indicates that CFTR functions as a tumor suppressor in the development and progression of prostate cancer.

The functions of CFTR in prostate health (pH modulation/Host defense/ human reproduction)

CFTR is expressed in the prostate, however, the physiological role of CFTR in the prostate remains largely unknown. Normal human prostatic fluid has a pH value between 6.2-6.6 (Blacklock, 1974). Citrate acid, acid phosphatase and some alkaline substances or ions such as HCO_3^- in the prostate are responsible for maintaining the pH of prostatic fluid (Kavanagh JP, 1982; Hassan MI, 2010). Apart from its well known conductivity for Cl^-, CFTR has been shown to transport HCO_3^- across the membrane in response to cAMP in various systems (Collins FS, 1992). On the other hand, a variety of cAMP-evoking hormones and neurotransmitters such as adrenalin, prostaglandin E2 have been shown to activate CFTR (Scheckenbach KL, 2010). In our study, we have demonstrated that CFTR can regulate HCO_3^- secretion, which neutralizes prostate fluid and provides an optimal pH environment in the prostate in physiological condition. In addition, HCO_3^- is also important for the solubilization of macromolecules to prevent the aggregation of digestive enzymes and mucin (Quinton PM, 2008; Garcia MA, 2009). In

line with this notion, aberrant HCO_3^- secretion has been associated with the obstructive types of pancreatic diseases such as cystic fibrosis and chronic pancrititis (Cohn JA, 1998). The main function of the prostate is to store and secrete prostate fluid that constitutes part of the seminal fluid. Usually after ejaculation the semen should liquefy, allowing the sperm to acquire motility. Therefore we speculate that in normal condition the physiological amount of HCO_3^- secreted by CFTR in prostate may participate in the process of liquefaction. Taken together, we speculate that in physiological condition, CFTR is responsive to cAMP activating hormones and factors, which subsequently mediates prostate HCO_3^- secretion and contributes to maintaining the homeostasis and function of the prostate.

In chapter 3 we have demonstrated during bacterial infection, the increased levels of inflammatory cytokines could up-regulate the expression of CFTR and CAII in the prostate, thereby enhancing HCO_3^- secretion and leading to the characteristic pH increase in prostatitis. Inhibition of CFTR function results in reduced bacterial killing both *in vitro* and *in vivo*. Moreover, we have elucidated that the CFTR-mediated HCO_3^- secretion has a direct role in bacteria killing. Therefore, in this study, we have revealed a previously undefined role of CFTR in host defense against bacterial infection in the prostate. Importantly, the present findings also suggest the possible role of the CFTR-mediated HCO_3^- secretion in anti-inflammatory process in nonbacterial prostatitis.

In addition to the role of CFTR in host defense in the prostate, CFTR and its mediated HCO_3^- secretion in the prostate may also be vital to the fertilizing capacity of sperm. Clinically, infertility has been associated with prostate diseases, such as prostatitis, indicating the abnormality in prostate fluid could account for male infertility

(Giamarellou H,1984; Leib Z, 1994; Cunningham KA,2008). Extracellular pH is an important factor in the regulation of sperm physiology. An acidic pH (Parrish JJ, 1989) and low concentration of bicarbonate (Visconti PE, 1999) favor a non-capacitated state preventing premature acrosomal reaction. On the contrary, high concentration of HCC_3^- in the prostatitis could result in premature acrosomal reaction in sperm which eventually leads to abnormal sperm function. In the present study, we demonstrate that during prostate infection, HCO_3^- secretion is enhanced due to upregulation of CFTR, which might be responsible for the hallmark increase in pH observed in prostatitis. Therefore, while the normal concentration of HCO_3^- is very important to the fertilizing capacity of sperm, the abnormal increased HCO_3^- secretion mediated by CFTR during prostate inflammation may play a role in infection-induced male infertility.

The function of CFTR in prostate diseases (prostate hyperplasia/ prostate cancer)

The present study shows that during aging, the expression of CFTR in the prostate is decreased. Our finding in chapter 4 indicates that loss of physiologic function of CFTR could be associated with certain diseases related to advancing age such as prostate hyperplasia and prostate cancer. The results presented here have demonstrated for the first time that CFTR functions as a tumor suppressor in the prostate cancer development. Our claim is based on the following findings. (1) The expression of CFTR is reduced in both prostate cancer cell lines and primary prostate cancer samples. (2) Our gain and loss of function studies demonstrates that inhibition of CFTR function leads to enhanced tumorigenic phenotype, whereas overexpression of CFTR inhibits the tumorigenic

phenotype both *in vitro* and *in vivo*. (3) Mechanistically, CFTR modulates apoptotic response through its ion channel function in prostate cancer cells and both genetic and epigenetic mechanisms, which have been implicated in cancer development, have been identified as CFTR targets.

Since CFTR mutations or hypermethylations have been reported in multiple cancers, we speculate a more general role of CFTR as a tumor suppressor in cancer. Therefore, besides prostate cancer, which is the main focus of this thesis, we have also studied the biological significance of CFTR in breast cancer (data not shown). Interestingly, our results reveal that CFTR also functions as a tumor suppressor in breast cancer. More importantly, the expression of CFTR transcript in breast tumor tissues is inversely correlated with prognosis (according to the 10 years follow up cohort study done by our project collaborator –The research group of Professor Jiang WG in Cardiff University). Of note, the issue of correlation between CFTR mutation and incidence of breast cancer is highly controversial. One previous study claimed that deregulated CFTR was responsible for elevated blood ATP concentrations, which inhibited breast cancer growth (Abraham EH, 1996). However, another contradictory study reported the unexpected data showing that breast cancers bearing ΔF508 CFTR mutation were poorly differentiated tumors (Southey MC, 1998). Our cell line study and clinical data support the notion that CFTR acts as a tumor suppressor in prostate cancer and breast cancer.

Of particular interest, in our study, we have demonstrated that overexpression of CFTR has therapeutic effects on prostate cancer, indicating the potential treatment strategy by manipulating CFTR expression and function. Genistein, one of the major soy isoflavone has been shown to suppress cancer through mediating Akt, NF-κB,

MMPs and Bax/Bcl-2 signaling which fulfills its promise as a chemopreventive and therapeutic agent against human cancers (Banerjee S, 2008). Interestingly, it was reported that genistein could also activate CFTR by a direct interaction, probably at a nucleotide binding site which lead to a higher open probability (Weinreich F, 1997) and it may be used as a potential drug in treatment of CF (Wegrzyn G, 2010), this led us to speculate that genistein could exert its antitumor effects by upregulation of CFTR. Currently, we are testing this hypothesis in the lab. If it is true, then it can further verify our finding about the role of CFTR in cancer development.

Therefore, from the present results, we have demonstrated that in addition to its well-established ion channel function, CFTR is predicted to be a tumor suppressor in cancer development. The insights provided by these studies will not only advance our understanding of the role of CFTR and its possible signaling pathways involved in human prostate cells and prostate cancer progression but may also shed light into the molecular mechanism underlying cancer development involving ion channels in general. The findings of the current studies may also provide grounds for possible development of clinically useful diagnosis and treatment targets for prostate cancer, and for other cancers as well since CFTR is expressed in a wide range of epithelial tissues.

Future studies:

The present findings have provided a framework of the study on different biological functions of CFTR in prostatitis and prostate cancer development. However, more in-

depth investigations on the underlying mechanisms leading to the observed phenotypes are required. There are several important questions remained to be answered.

Firstly, it seemed that some cytokines were also elevated in non-bacterial prostatitis, the most common form of prostatitis. Since cytokines can up regulate CFTR, which can subsequently increase HCO_3^- secretion, what is the physiological function of the increased CFTR-mediated HCO_3^- secretion then? Apart from the role of HCO_3^- in bacterial prostatitis, it remains unclear whether the elevated HCO_3^- content or alkaline pH would be of any physiological significance in non-bacterial prostatitis.

Secondly, how does loss or mutations of CFTR trigger its downstream signaling pathway in cancer cells? The results in chapter 4 suggested that CFTR could regulate the expression of miRNAs, however, the exact mechanisms by which CFTR regulates the transcription level of miR-34a and miR-193b and whether rescue the expression of these miRNAs in CFTR knockdown or overexpressed cells could reverse the biological phenotype in these cells require further studies. Moreover, it is still possible CFTR may communicate with other proteins or oncogene/tumor suppressor genes by other mechanisms. It would be interesting to study the molecular mechanisms leading to activation of CFTR-related signaling pathways.

Thirdly, we found that CFTR was down-regulated in most prostate carcinoma specimen. However, we noticed that in a few cases, CFTR is only mildly downregulated in some tumor cells. The question of whether the CFTR expression is associated with cancer cell differentiation state needs to be further investigated.

Finally, our data showed that overexpression of CFTR could remarkably down-regulate the transcription level of TWIST1 which had been shown to induce EMT and implicate in the regulation of metastasis. Further investigation of the relationship between CFTR and the well-known EMT signaling pathway such as TGF-β may provide some hints on the role of CFTR in cancer metastasis. It would also be interesting to know if CFTR is involved in more early steps of tumor formation, such as immortalization and transformation.

Conclusion:

To conclude, the present studies have demonstrated the biological functions of CFTR in prostate health and disease. The results suggest that CFTR participates in host defense against bacterial infection in prostatitis and acts as a tumor suppressor in prostate cancer development which may have clinical implications in the treatment of prostatitis and potential application in diagnosis and prognosis of cancer.

Reference List

1. Abraham EH, Vos P, Kahn J, Grubman SA, Jefferson DM, Ding I, Okunieff P.Cystic fibrosis hetero- and homozygosity is associated with inhibition of breast cancer growth. Nat Med. 1996 May;2(5):593-6.

2. Ajonuma LC, He Q, Sheung Chan PK, Yu Ng EH, Fok KL, Yan Wong CH, Tsang LL, Ho LS, Lau MC, Huang HY, Yang DZ, Rowlands DK, Tang XX, Zhang XH, Chung YW, Chan HC. Involvement of cystic fibrosis transmembrane conductance regulator in infection-induced edema. Cell Biol Int. 2008 Jul; 32(7):801-6. Epub 2008 Mar 29.

3. Ajonuma LC, Tsang LL, Zhang GH, Wong CH, Lau MC, Ho LS, Rowlands DK, Zhou CX, Ng CP, Chen J, Xu PH, Zhu JX, Chung YW, Chan HC. Estrogen-induced abnormally high cystic fibrosis transmembrane conductance regulator expression results in ovarian hyperstimulation syndrome. Mol Endocrinol. 2005 Dec;19(12):3038-44. Epub 2005 Jul 28.

4. Alexander RB, Ponniah S, Hasday J, Hebel JR. Elevated levels of proinflammatory cytokines in the semen of patients with chronic prostatitis/chronic pelvic pain syndrome. Urology. 1998 Nov; 52(5):744-9.

5. Anderson RU, Fair WR. Physical and chemical determinations of prostatic secretion in benign hyperplasia, prostatitis, and adenocarcinoma. Invest Urol. 1976 Sep;14(2):137-40.

6. Banerjee PP, Banerjee S, Tilly KI, Tilly JL, Brown TR, Zirkin BR. Lobe-specific apoptotic cell death in rat prostate after androgen ablation by castration. Endocrinology. 1995 Oct;136(10):4368-76.

7. Banerjee S, Li Y, Wang Z, Sarkar FH. Multi-targeted therapy of cancer by genistein. Cancer Lett. 2008 Oct 8;269(2):226-42. Epub 2008 May 19.

8. Barrière H, Poujeol C, Tauc M, Blasi JM, Counillon L, Poujeol P. CFTR modulates programmed cell death by decreasing intracellular pH in Chinese hamster lung fibroblasts. Am J Physiol Cell Physiol. 2001 Sep;281(3):C810-24.

9. Beeler JA, Tang WJ. Expression and purification of soluble adenylyl cyclase from Escherichia coli. Methods Mol Biol. 2004;237:39-53.

10. Bhattacharya A, Datta A. Effect of cyclic AMP on RNA and protein synthesis in Candida albicans. Biochem Biophys Res Commun. 1977 Aug 22; 77(4):1483-44. Biochemistry. 1979 May 29; 18(11):2210-8.

11. Bibikova M, Lin Z, Zhou L, Chudin E, Garcia EW, Wu B, Doucet D, Thomas NJ, Wang Y, Vollmer E, Goldmann T, Seifart C, Jiang W, Barker DL, Chee MS,

Floros J, Fan JB. High-throughput DNA methylation profiling using universal bead arrays. Genome Res. 2006 Mar;16(3):383-93. Epub 2006 Jan 31.

12. Bjerklund Johansen TE, Grüneberg RN, Guibert J, Hofstetter A, Lobel B, Naber KG, Palou Redorta J, van Cangh PJ.The role of antibiotics in the treatment of chronic prostatitis: a consensus statement. Eur Urol. 1998 Dec; 34(6):457-66. Review.

13. Blacklock NJ, Beavis JP. The response of prostatic fluid pH in inflammation. Br J Urol. 1974 Oct; 46(5):537-42.

14. Boat TF, Cheng PW. Epithelial cell dysfunction in cystic fibrosis: implications for airways disease. Acta Paediatr Scand Suppl. 1989;363:25-9; discussion 29-30. Review.

15. Boyle P, Maisonneuve P, Napalkov P. Incidence of prostate cancer will double by the year 2030: the argument for. Eur Urol. 1996;29 Suppl 2:3-9. Review.

16. Brahimi-Horn MC, Pouysségur J. Oxygen, a source of life and stress. FEBS Lett. 2007 Jul 31;581(19):3582-91. Epub 2007 Jun 19.

17. Brouillard F, Bouthier M, Leclerc T, Clement A, Baudouin-Legros M, Edelman A. NF-kappa B mediates up-regulation of CFTR gene expression in Calu-3 cells by interleukin-1beta. J Biol Chem. 2001 Mar 23;276(12):9486-91. Epub 2000 Dec 12.

18. Bruchovsky N, Wilson JD. The conversion of testosterone to 5-alpha-androstan-17-beta-ol-3-one by rat prostate in vivo and in vitro. J Biol Chem. 1968 Apr 25;243(8):2012-21.

19. Cafferata EG, González-Guerrico AM, Giordano L, Pivetta OH, Santa-Coloma TA. Interleukin-1beta regulates CFTR expression in human intestinal T84 cells. Biochim Biophys Acta. 2000 Feb 21;1500(2):241-8

20. Chan HC, Ruan YC, He Q, Chen MH, Chen H, Xu WM, Chen WY, Xie C, Zhang XH, Zhou Z. The cystic fibrosis transmembrane conductance regulator in reproductive health and disease. J Physiol. 2009 May 15;587(Pt 10):2187-95. Epub 2008 Nov 17. Review.

21. Chan HC, Shi QX, Zhou CX, Wang XF, Xu WM, Chen WY, Chen AJ, Ni Y, Yuan YY, Critical role of CFTR in uterine bicarbonate secretion and the fertilizing capacity of sperm. Mol Cell Endocrinol. 2006 May 16;250(1-2):106-13. Epub 2006 Jan 18. Review.

22. Chandiok S, Fisk PG, Riley VC.Prostatitis--clinical and bacterial studies. Int J STD AIDS. 1992 May-Jun;3(3):188-90.

23. Chapman HA. Plasminogen activators, integrins, and the coordinated regulation of cell adhesion and migration. Curr Opin Cell Biol. 1997 Oct;9(5):714-24. Review.

24. Chegwidden WR, Dodgson SJ, Spencer IM. The roles of carbonic anhydrase in metabolism, cell growth and cancer in animals. EXS. 2000;(90):343-63. Review.

25. Chen J, Feilotter HE, Paré GC, Zhang X, Pemberton JG, Garady C, Lai D, Yang X, Tron VA. MicroRNA-193b represses cell proliferation and regulates cyclin D1 in melanoma. Am J Pathol. 2010 May;176(5):2520-9. Epub 2010 Mar 19.

26. Chen J, Xu Z, Zhao H, Jiang X. Citrate in Expressed Prostatic Secretions Has the Feasibility to Be Used as a Useful Indicator for the Diagnosis of Category IIIB Prostatitis.Urol Int. 2007;78:230–234

27. Chen MH, Chen H, Zhou Z, Ruan YC, Wong HY, Lu YC, Guo JH, Chung YW, Huang PB, Huang HF, Zhou WL, Chan HC. Involvement of CFTR in oviductal HCO_3^- secretion and its effect on soluble adenylate cyclase-dependent early embryo development. 2010 Apr 20. Hum Reprod. 2010 Jul;25(7):1744-54. Epub 2010 Apr 20.

28. Chen WY, Xu WM, Chen ZH, Ni Y, Yuan YY, Zhou SC, Zhou WW, Tsang LL, Chung YW, Höglund P, Chan HC, Shi QX. Cl- is required for HCO_3^- entry necessary for sperm capacitation in guinea pig: involvement of a Cl-/HCO3-exchanger (SLC26A3) and CFTR. Biol Reprod. 2009 Jan;80(1):115-23. Epub 2008 Sep 10.

29. Chen Y, Cann MJ, Litvin TN, Iourgenko V, Sinclair ML, Levin LR, Buck J. Soluble adenylyl cyclase as an evolutionarily conserved bicarbonate sensor. Science. 2000 Jul 28;289(5479):625-8.

30. Chia SK, Wykoff CC, Watson PH, Han C, Leek RD, Pastorek J, Gatter KC, Ratcliffe P, Harris AL.Prognostic significance of a novel hypoxia-regulated marker, carbonic anhydrase IX, in invasive breast carcinoma. J Clin Oncol. 2001 Aug 15;19(16):3660-8.

31. Chiang WL, Chu SC, Yang SS, Li MC, Lai JC, Yang SF, Chiou HL, Hsieh YS. The aberrant expression of cytosolic carbonic anhydrase and its clinical significance in human non-small cell lung cancer. Cancer Lett. 2002 Dec 15;188(1-2):199-205.

32. Chiche J, Ilc K, Laferrière J, Trottier E, Dayan F, Mazure NM, Brahimi-Horn MC, Pouysségur J. Hypoxia-inducible carbonic anhydrase IX and XII promote tumor cell growth by counteracting acidosis through the regulation of the intracellular pH. Cancer Res. 2009 Jan 1;69(1):358-68.

33. Choi JY, Muallem D, Kiselyov K, Lee MG, Thomas PJ, Muallem S.Aberrant CFTR-dependent HCO_3^- transport in mutations associated with cystic fibrosis. Nature. 2001 Mar 1; 410(6824):94-7

34. Coakley RD, Grubb BR, Paradiso AM, Gatzy JT, Johnson LG, Kreda SM, O'Neal WK, Boucher RC. Abnormal surface liquid pH regulation by cultured cystic fibrosis bronchial epithelium. Proc Natl Acad Sci U S A. 2003 Dec 23;100(26):16083-8. Epub 2003 Dec 10.

35. Cohn JA, Friedman KJ, Noone PG, Knowles MR, Silverman LM, Jowell PS. Relation between mutations of the cystic fibrosis gene and idiopathic pancreatitis. N Engl J Med. 1998 Sep 3;339(10):653-8.

36. Cohn JA, Melhus O, Page LJ, Dittrich KL & Vigna SR. CFTR: development of high-affinity antibodies and localization in sweat gland. Biochem Biophys Res Commun.1991, 181, 36–43

37. Collins FS.Cystic fibrosis: molecular biology and therapeutic implications. Science. 1992 May 8;256(5058):774-9.

38. Corral LG, Post LS, Montville TJ. Antimicrobial activity of sodium bicarbonate. J Food Sci.1988, 53:981–982.

39. Craig, S. B., M. J. Concannon, G. A. McDonald and C. L. Puckett. "The antibacterial effects of tumescent liposuction fluid." Plast Reconstr Surg.1999, 103(2): 666-70.

40. Crawford I, Maloney PC, Zeitlin PL, Guggino WB, Hyde SC, Turley H, Gatter KC, Harris A, Higgins CF. Immunocytochemical localization of the cystic fibrosis gene product CFTR. Proc Natl Acad Sci U S A. 1991 Oct 15;88(20):9262-6.

41. Cummings HS, Hershey JW. Translation initiation factor IF1 is essential for cell viability in Escherichia coli. J Bacteriol. 1994 Jan;176(1):198-205.

42. Cunningham KA, Beagley KW. Male genital tract chlamydial infection: implications for pathology and infertility. Biology of Reproduction. 2008 Aug ,79(2):180-9.

43. Dass K, Ahmad A, Azmi AS, Sarkar SH, Sarkar FH.Evolving role of uPA/uPAR system in human cancers. Cancer Treat Rev. 2008 Apr;34(2):122-36. Epub 2007 Dec 26.

44. David G. Bostwick, Liang cheng, Urologic surgical pathology, ISBN-978-0-323-01970-5;

45. De la Rosette JJ, Hubregtse MR, Meuleman EJ, Stolk-Engelaar MV, Debruyne FM. Diagnosis and treatment of 409 patients with prostatitis syndromes. Urology. 1993 Apr;41(4):301-7.

46. De Marzo AM, Marchi VL, Epstein JI, Nelson WG. Proliferative inflammatory atrophy of the prostate: implications for prostatic carcinogenesis. Am J Pathol. 1999 Dec;155(6):1985-92.

47. De Marzo AM, Platz EA, Sutcliffe S, Xu J, Grönberg H, Drake CG, Nakai Y, Isaacs WB, Nelson WG. Inflammation in prostate carcinogenesis. Nat Rev Cancer. 2007 Apr;7(4):256-69. Review.

48. De Moor CH, Meijer H, Lissenden S. Mechanisms of translational control by the 3' UTR in development and differentiation. Semin Cell Dev Biol. 2005 Feb;16(1):49-58. Epub 2005 Jan 12.

49. Devor DC, Singh AK, Lambert LC, DeLuca A, Frizzell RA, Bridges RJ: Bicarbonate and chloride secretion in Calu-3 airway epithelial cells. J Gen Physiol 1999;113:743-760.

50. Ding S, Gong BD, Yu J, Gu J, Zhang HY, Shang ZB, Fei Q, Wang P, Zhu JD. Methylation profile of the promoter CpG islands of 14 "drug-resistance" genes in hepatocellular carcinoma. World J Gastroenterol. 2004 Dec 1;10(23):3433-40.

51. Discovery of glycine hydrazide pore-occluding CFTR inhibitors: mechanism, structure-activity analysis, and in vivo efficacy.J Gen Physiol. 2004 Aug;124(2):125-37.

52. Dorschner RA, Lopez-Garcia B, Peschel A, Kraus D, Morikawa K, Nizet V, Gallo RL. The mammalian ionic environment dictates microbial susceptibility to antimicrobial defense peptides. FASEB J. 2006 Jan;20(1):35-42.

53. Drake, D. R., K. Vargas, A. Cardenzana and R. Srikantha. "Enhanced bactericidal activity of Arm and Hammer Dental Care." Am J Dent. 1995,8(6): 308-12.

54. Elble RC, Pauli BU. Tumor suppression by a proapoptotic calcium-activated chloride channel in mammary epithelium. J Biol Chem. 2001 Nov 2;276(44):40510-7. Epub 2001 Aug 1.

55. Erdogan S, Aslantas O, Celik S, Atik E.The effects of increased cAMP content on inflammation, oxidative stress and PDE4 transcripts during Brucella melitensis infection. Res Vet Sci. 2008 Feb;84(1):18-25. Epub 2007 Mar 29.

56. Fair WR, Cordonnier JJ. The pH of prostatic fluid: a reappraisal and therapeutic implications. J Urol. 1978 Dec;120(6):695-8.

57. Fair WR, Couch J, Wehner N. Prostatic antibacterial factor. Identity and significance. Urology. 1976 Feb;7(2):169-77.

58. Foster CS, Dodson A, Karavana V, Smith PH, Ke Y. Prostatic stem cells. J Pathol. 2002 Jul;197(4):551-65.

59. Fuessel S, Sickert D, Meye A, Klenk U, Schmidt U, Schmitz M, Rost AK, Weigle B, Kiessling A, Wirth MP. Multiple tumor marker analyses (PSA, hK2, PSCA, trp-p8) in primary prostate cancers using quantitative RT-PCR. Int J Oncol. 2003 Jul;23(1):221-8.

60. Gallagher AM, Gottlieb RA. Proliferation, not apoptosis, alters epithelial cell migration in small intestine of CFTR null mice. Am J Physiol Gastrointest Liver Physiol. 2001 Sep;281(3):G681-7.

61. Garcia MA, Yang N, Quinton PM. Normal mouse intestinal mucus release requires cystic fibrosis transmembrane regulator-dependent bicarbonate secretion. J Clin Invest. 2009 Sep;119(9):2613-22. doi: 10.1172/JCI38662. Epub 2009 Aug 24.

62. Giamarellou H, Tympanidis K, Bitos NA, Leonidas E, Daikos GK. Infertility and chronic prostatitis. Andrologia. 1984 Sep-Oct;16(5):417-22.

63. Gohji K, Nakajima M, Boyd D, Dinney CP, Bucana CD, Kitazana S, Kamidono S, Fidler IJ. Organ-site dependence for the production of urokinase-type plasminogen activator and metastasis by human renal cell carcinoma cells. Am J Pathol. 1997 Dec;151(6):1655-61.

64. Gonzalgo ML, Isaacs WB. Molecular pathways to prostate cancer. J Urol. 2003 Dec;170(6 Pt 1):2444-52.

65. Gottlieb RA, Dosanjh A. Mutant cystic fibrosis transmembrane conductance regulator inhibits acidification and apoptosis in C127 cells: possible relevance to cystic fibrosis. Proc Natl Acad Sci U S A. 1996 Apr 16;93(8):3587-91.

66. Grant M. Baxter, Paul S. Sidhu, Ultrasound of the urogenital system. 10-ISBN 1-58890-237-4 (TNY)

67. Grill S, Moll I, Hasenöhrl D, Gualerzi CO, Bläsi U. Modulation of ribosomal recruitment to 5'-terminal start codons by translation initiation factors IF2 and IF3. FEBS Lett. 2001 Apr 27;495(3):167-71.

68. Gualerzi CO, Pon CL. Initiation of mRNA translation in prokaryotes. Biochemistry. 1990 Jun 26;29(25):5881-9. Review.

69. Guggino WB, Banks-Schlegel SP. Macromolecular interactions and ion transport in cystic fibrosis. Am J Respir Crit Care Med. 2004 Oct 1;170(7):815-20. Review.

70. Gupta GP, Massagué J. Cancer metastasis: building a framework. Cell. 2006 Nov 17;127(4):679-95.

71. Gurumurthy S, Vasudevan KM, Rangnekar VM. Regulation of apoptosis in prostate cancer. Cancer Metastasis Rev. 2001;20(3-4):225-43.

72. Hassan MI, Aijaz A, Ahmad F. Structural and functional analysis of human prostatic acid phosphatase. Expert Rev Anticancer Ther. 2010 Jul;10(7):1055-68.

73. He L, He X, Lowe SW, Hannon GJ. microRNAs join the p53 network--another piece in the tumour-suppression puzzle. Nat Rev Cancer. 2007 Nov;7(11):819-22. Review.

74. He L, Wang Y, Long Z, Jiang C. Clinical significance of IL-2, IL-10, and TNF-alpha in prostatic secretion of patients with chronic prostatitis. Urology. 2010 Mar;75(3):654-7. Epub 2009 Dec 6.

75. He Q, Tsang LL, Ajonuma LC, Chan HC. Abnormally up-regulated cystic fibrosis transmembrane conductance regulator expression and uterine fluid accumulation contribute to Chlamydia trachomatis-induced female infertility. Fertil Steril. 2010 May 15;93(8):2608-14. Epub 2010 Mar 15.

76. Heinert G, Tan Th, Thielen H, Kruger J, Wurth G, Essers L: Analysis of perioperative ofloxacin concentrations in serum and prostate tissue. Drugs 1993;45(suppl 3):358–359.

77. Helmlinger G, Yuan F, Dellian M, Jain RK. Interstitial pH and pO2 gradients in solid tumors in vivo: high-resolution measurements reveal a lack of correlation. Nat Med. 1997 Feb;3(2):177-82.

78. Hermeking H. The miR-34 family in cancer and apoptosis. Cell Death and Differentiation 2010, 17, 193-199

79. Hihnala S, Kujala M, Toppari J, Kere J, Holmberg C, Höglund P. Expression of SLC26A3, CFTR and NHE3 in the human male reproductive tract: role in male subfertility caused by congenital chloride diarrhoea. Mol Hum Reprod. 2006 Feb;12(2):107-11. Epub 2006 Jan 18.

80. Höglund P, Haila S, Socha J, Tomaszewski L, Saarialho-Kere U, Karjalainen-Lindsberg ML, Airola K, Holmberg C, de la Chapelle A, Kere J. Mutations of the Down-regulated in adenoma (DRA) gene cause congenital chloride diarrhoea. Nat Genet. 1996 Nov;14(3):316-9.

81. Houslay, M.D., Adams, D.R.. PDE4 cAMP phosphodiesterases: modular enzymes that orchestrate signalling cross-talk, desensitization and compartmentalization. Biochemical Journal. 2003.370, 1–18.

82. Hug MJ, Tamada T, Bridges RJ. CFTR and bicarbonate secretion by epithelial cells. News Physiol Sci. 2003 Feb;18:38-42

83. Hume JR, Wang GX, Yamazaki J, Ng LC, Duan D. CLC-3 chloride channels in the pulmonary vasculature. Adv Exp Med Biol. 2010;661:237-47. Review.

84. Ishiguro H, Steward M, Naruse S. Cystic fibrosis transmembrane conductance regulator and SLC26 transporters in HCO_3^- secretion by pancreatic duct cells. Sheng Li Xue Bao 2007; 59: 465-476.

85. Jang TL, Schaeffer AJ. The role of cytokines in prostatitis. World J Urol. 2003 Jun;21(2):95-9. Epub 2003 May 29. Review. Erratum in: World J Urol. 2003 Mar-Apr;70(2):223.

86. Jarvis GN, Fields MW, Adamovich DA, Arthurs CE, Russell JB. The mechanism of carbonate killing of Escherichia coli. Lett Appl Microbiol. 2001 Sep;33(3):196-200.

87. Jemal A, Siegel R, Ward E, Murray T, Xu J, Thun MJ. Cancer statistics, 2007. CA Cancer J Clin. 2007 Jan-Feb;57(1):43-66.

88. Jeroen Roelofs and Peter J. M. Van Haastert, Deducing the Origin of Soluble Adenylyl Cyclase, a Gene Lost in Multiple Lineages, Molecular Biology and Evolution .2002,19:2239-2246

89. Kaul R, Tao S, Wenman WM. Cyclic AMP inhibits protein synthesis in Chlamydia trachomatis at a transcriptional level. Biochim Biophys Acta. 1990 Jun 12;1053(1):106-12.

90. Kavanagh J. P., Darby C. and Costello C. B. The response of seven prostatic fluid components to prostatic disease. Int. J. Androl. 1982, 5, 487–496.

91. Kivelä A, Parkkila S, Saarnio J, Karttunen TJ, Kivelä J, Parkkila AK, Waheed A, Sly WS, Grubb JH, Shah G, Türeci O, Rajaniemi H.Expression of a novel transmembrane carbonic anhydrase isozyme XII in normal human gut and colorectal tumors. Am J Pathol. 2000 Feb;156(2):577-84.

92. Kloosterman WP and Plasterk RH. The diverse functions of microRNAs in animal development and disease. Dev Cell 2006; 11:441-450

93. Ko SB, Shcheynikov N, Choi JY, Luo X, Ishibashi K, Thomas PJ, Kim JY, Kim KH, Lee MG, Naruse S, Muallem S. A molecular mechanism for aberrant CFTR-dependent HCO(3)(-) transport in cystic fibrosis. EMBO J. 2002 Nov 1;21(21):5662-72.

94. Ko SB, Zeng W, Dorwart MR, Luo X, Kim KH, Millen L, Goto H, Naruse S, Soyombo A, Thomas PJ, Muallem S. Gating of CFTR by the STAS domain of SLC26 transporters. Nat Cell Biol. 2004 Apr;6(4):343-50. Epub 2004 Mar 28.

95. Kohnen PW, Drach GW. Patterns of inflammation in prostatic hyperplasia: a histologic and bacteriologic study. J Urol. 1979 Jun;121(6):755-60.

96. Kopelman H, Corey M, Gaskin K, Durie P, Weizman Z, Forstner G: Impaired chloride secretion, as well as bicarbonate secretion, underlies the fluid secretory defect in the cystic fibrosis pancreas. Gastroenterology 1988;118:1187-1196.

97. Kozliak EI, Fuchs JA, Guilloton MB, Anderson PM. Role of bicarbonate/CO2 in the inhibition of Escherichia coli growth by cyanate. J Bacteriol. 1995 Jun;177(11):3213-9.

98. Kumar S, Kasseckert S, Kostin S, Abdallah Y, Piper HM, Steinhoff G, Reusch HP & Ladilov Y. Importance of bicarbonate transport for ischaemia-induced apoptosis of coronary endothelial cells. J Cell Mol Med .2007, 11, 798-809.

99. Kumpulainen T and Nystrom SH, Immunohistochemical localization of carbonic anhydrase isoenzyme C in human brain. Brain Res. 1981, **220** pp. 220–225

100. Kurita T, Wang YZ, Donjacour AA, Zhao C, Lydon JP, O'Malley BW, Isaacs JT, Dahiya R, Cunha GR. Paracrine regulation of apoptosis by steroid hormones in the male and female reproductive system. Cell Death Differ. 2001 Feb;8(2):192-200.

101. Lagadic-Gossmann D, Huc L & Lecureur V. Alterations of intracellular pH homeostasis in apoptosis: origins and roles. Cell Death Differ. 2004, 11, 953-961.

102. Lang F, Föller M, Lang KS, Lang PA, Ritter M, Gulbins E, Vereninov A, Huber SM.Ion channels in cell proliferation and apoptotic cell death. J Membr Biol. 2005 Jun;205(3):147-57. Review.

103. Laniado ME, Fraser SP, Djamgoz MB. Voltage-gated K(+) channel activity in human prostate cancer cell lines of markedly different metastatic potential: distinguishing characteristics of PC-3 and LNCaP cells. Prostate. 2001 Mar 1;46(4):262-74.

104. Lee Y, Kim M, Han J, Yeom KH, Lee S, Baek SH, Kim VN. MicroRNA genes are transcribed by RNA polymerase II. EMBO J. 2004 Oct 13;23(20):4051-60. Epub 2004 Sep 16.

105. Lee MG,Choi JY,Luo X,Thomas PJ,Muallem S. Cystic fibrosis transmembrane conductance regulator regulates luminal Cl-/HCO-3 exchange in mouse submandibular and pancreatic ducts. J. Biol. Chem. 1999,274, 14670-14677.

106. Leib Z, Bartov B, Eltes F, Servadio C. Reduced semen quality caused by chronic abacterial prostatitis: an enigma or reality? Fertil Steril 1994; 66: 1109-16

107. Lemonnier L, Shuba Y, Crepin A, Roudbaraki M, Slomianny C, Mauroy B, Nilius B, Prevarskaya N, Skryma R. Bcl-2-dependent modulation of swelling-activated Cl- current and ClC-3 expression in human prostate cancer epithelial cells. Cancer Res. 2004 Jul 15;64(14):4841-8.

108. Li LC, Carroll PR, Dahiya R. Epigenetic changes in prostate cancer: implication for diagnosis and treatment. J Natl Cancer Inst. 2005 Jan 19;97(2):103-15. Review.

109. Li XF, Yan PJ, Shao ZM. Downregulation of miR-193b contributes to enhance urokinase-type plasminogen activator (uPA) expression and tumor progression and invasion in human breast cancer. Oncogene. 2009 Nov 5;28(44):3937-48. Epub 2009 Aug 24.

110. Li Y, Sun Z, Wu Y, Babovic-Vuksanovic D, Li Y, Cunningham JM, Pankratz VS, Yang P. Cystic fibrosis transmembrane conductance regulator gene mutation and lung cancer risk. Lung Cancer. 2010 Jan 28.

111. Lin SL, Chiang A, Chang D, Ying SY. Loss of mir-146a function in hormone-refractory prostate cancer. RNA. 2008 Mar;14(3):417-24. Epub 2008 Jan 3.

112. Lipsky BA, Byren I, Hoey CT. Treatment of bacterial prostatitis, Clin Infect Dis. 2010 Jun 15;50(12):1641-52.

113. Maestro R, Dei Tos AP, Hamamori Y, et al. Twist is potential oncogene that inhibits apoptosis. Genes Dev 1999;13: 2207-17

114. Maisonneuve P, FitzSimmons SC, Neglia JP, Campbell PW 3rd, Lowenfels AB. Cancer risk in nontransplanted and transplanted cystic fibrosis patients: a 10-year study. J Natl Cancer Inst. 2003 Mar 5;95(5):381-7.

115. Mariot P, Vanoverberghe K, Lalevee N, Rossier MF & Prevarskaya N. Overexpression of an alpha 1H (Cav3.2) T-type calcium channel during neuroendocrine differentiation of human prostate cancer cells. J Biol Chem. 2002, 277, 10824-10833.

116. Matthews RP, McKnight GS. Characterization of the cAMP response element of the cystic fibrosis transmembrane conductance regulator gene promoter. J Biol Chem. 1996 Dec 13;271(50):31869-77.

117. McCarthy VA, Harris A. The CFTR gene and regulation of its expression. Pediatr Pulmonol. 2005 Jul;40(1):1-8.

118. McNaughton Collins M, Barry MJ. Epidemiology of chronic prostatitis. Curr Opin Urol. 1998 Jan;8(1):33-7.

119. McNeal JE. The zonal anatomy of the prostate. Prostate. 1981;2(1):35-49.

120. McWilliams R, Highsmith WE, Rabe KG, de Andrade M, Tordsen LA, Holtegaard LM, Petersen GM. Cystic fibrosis transmembrane regulator gene carrier status is a risk factor for young onset pancreatic adenocarcinoma.Gut. 2005 Nov;54(11):1661-2.

121. Meares EM. Prostatitis. In: Chisholm GD, Fair WR, eds. Scientific Foundations of Urology, 3rd ed. London:Heinemann, 1990:373-378

122. Mishra DK, Chen Z, Wu Y, Sarkissyan M, Koeffler HP, Vadgama JV. Global methylation pattern of genes in androgen-sensitive and androgen-independent prostate cancer cells. Mol Cancer Ther. 2010 Jan;9(1):33-45. Epub 2010 Jan 6.

123. Mitsumori K, Terai A, Yamamoto S, Ishitoya S, Yoshida O. Virulence characteristics of Escherichia coli in acute bacterial prostatitis. J Infect Dis. 1999 Oct;180(4):1378-81

124. Mori M, Staniunas RJ, Barnard GF, Jessup JM, Steele GD and. Chen LB, The significance of carbonic anhydrase expression in human colorectal cancer. Gastroenterology 1993,**105,** pp. 820–826.

125. Muanprasat C, Sonawane ND, Salinas D, Taddei A, Galietta LJ, Verkman AS.

126. Narod SA, Dupont A, Cusan L, Diamond P, Gomez JL, Suburu R, Labrie F. The impact of family history on early detection of prostate cancer. Nat Med. 1995 Feb;1(2):99-101.

127. Neglia JP, FitzSimmons SC, Maisonneuve P, Schöni MH, Schöni-Affolter F, Corey M, Lowenfels AB. The risk of cancer among patients with cystic fibrosis. Cystic Fibrosis and Cancer Study Group. N Engl J Med. 1995 Feb 23;332(8):494-9.

128. Nickel JC. Prostatitis: diagnosis and classification. Curr Urol Rep. 2003 Aug;4(4):259-60

129. Noble RL.Production of Nb rat carcinoma of the dorsal prostate and response of estrogen-dependent transplants to sex hormones and tamoxifen. Cancer Res. 1980 Oct;40(10):3547-50.

130. Okada Y. Cell volume-sensitive chloride channels: phenotypic properties and molecular identity. Contrib Nephrol. 2006;152:9-24.

131. Padua RA, Warren N, Grimshaw D, Smith M, Lewis C, Whittaker J, Laidler P, Wright P, Douglas-Jones A, Fenaux P, Sharma A, Horgan K, West R. The cystic fibrosis delta F508 gene mutation and cancer. Hum Mutat. 1997;10(1):45-8.

132. Parekh AB, Putney Jr JW. Store-operated calcium channel. Physiol Rev 2005;85: 757-810

133. Parkkila AK, Herva R, Parkkila S, Rajaniemi H.Immunohistochemical demonstration of human carbonic anhydrase isoenzyme II in brain tumours. Histochem J. 1995 Dec;27(12):974-82.

134. Parkkila S, Parkkila AK, Juvonen T., Lehto V.P. and Rajaniemi H, Immunohistochemical demonstration of the carbonic anhydrase isoenzymes I and II in pancreatic tumours. Histochem. J. 1995,27, pp. 133–138.

135. Parrish JJ, Susko-Parrish JL, First NL: Capacitation of bovine sperm by heparin: inhibitory effect of glucose and role of intracellular pH. Biol Reprod. 1989; 41: 683-99.

136. Partin AW, Carter HB, Chan DW, Epstein JI, Oesterling JE, Rock RC, Weber JP, Walsh PC. Prostate specific antigen in the staging of localized prostate cancer: influence of tumor differentiation, tumor volume and benign hyperplasia. J Urol. 1990 Apr;143(4):747-52.

137. Pfau A, Perlberg S, Shapira A. The pH of the prostatic fluid in health and disease: implications of treatment in chronic bacterial prostatitis. J Urol. 1978 Mar; 119(3):384-7.

138. Pittman N, Shue G, LeLeiko NS, Walsh MJ. Transcription of cystic fibrosis transmembrane conductance regulator requires a CCAAT-like element for both basal and cAMP-mediated regulation. J Biol Chem. 1995 Dec 1;270(48):28848-57.

139. Porkka KP, Pfeiffer MJ, Waltering KK, Vessella RL, Tammela TL, Visakorpi T. MicroRNA expression profiling in prostate cancer. Cancer Res. 2007 Jul 1;67(13):6130-5.

140. Poulsen JH, Fischer H, Illek B, Machen TE.Bicarbonate conductance and pH regulatory capability of cystic fibrosis transmembrane conductance regulator. Proc Natl Acad Sci U S A. 1994, Jun 7;91(12):5340-4.

141. Poulsen KA, Andersen EC, Hansen CF, Klausen TK, Hougaard C, Lambert IH, Hoffmann EK. Deregulation of apoptotic volume decrease and ionic movements in multidrug-resistant tumor cells: role of chloride channels. Am J Physiol Cell Physiol. 2010 Jan;298(1):C14-25. Epub 2009 Oct 21.

142. Prevarskaya N, Skryma R, Bidaux G, Flourakis M, Shuba Y. Ion channels in death and differentiation of prostate cancer cells. Cell Death Differ. 2007 Jul;14(7):1295-304. Epub 2007 May 4. Review.

143. Qiao D, Yi L, Hua L, Xu Z, Ding Y, Shi D, Ni L, Song N, Wang Y, Wu H., Cystic fibrosis transmembrane conductance regulator (CFTR) gene 5T allele may protect against prostate cancer: a case-control study in Chinese Han population. J Cyst Fibros. 2008 May;7(3):210-4. Epub 2007 Aug 29.

144. Quinton PM. The neglected ion: HCO_3^-. Nat Med. 2001 Mar;7(3):292-3.

145. Quinton PM. Cystic fibrosis: impaired bicarbonate secretion and mucoviscidosis. Lancet. 2008 Aug 2;372(9636):415-7.

146. Raver-Shapira N, Marciano E, Meiri E, Spector Y, Rosenfeld N, Moskovits N, Bentwich Z, Oren M. Transcriptional activation of miR-34a contributes to p53-mediated apoptosis. Mol Cell. 2007 Jun 8;26(5):731-43. Epub 2007 May 31

147. Reddy MM, Quinton PM. Control of dynamic CFTR selectivity by glutamate and ATP in epithelial cells. Nature. 2003 Jun 12;423(6941):756-60.

148. Ridley AJ, Schwartz MA, Burridge K, Firtel RA, Ginsberg MH, Borisy G, Parsons JT, Horwitz AR.. Cell migration: integrating signals from front to back. Science 2003; **302**: 1704–9.

149. Riordan JR. CFTR function and prospects for therapy. Annu Rev Biochem. 2008;77:701-26. Review.

150. Rowe SM, Miller S, Sorscher EJ. Cystic fibrosis. N Engl J Med. 2005 May 12;352(19):1992-2001.

151. Rybalchenko V, Prevarskaya N, Van Coppenolle F, Legrand G, Lemonnier L, Le Bourhis X, Skryma R, Verapamil inhibits proliferation of LNCaP human prostate cancer cells influencing K+ channel gating. Mol Pharmacol. 2001 Jun;59(6):1376-87.

152. Saito Y, Liang G, Egger G, Friedman JM, Chuang JC, Coetzee GA, Jones PA. Specific activation of microRNA-127 with downregulation of the proto-oncogene BCL6 by chromatin-modifying drugs in human cancer cells. Cancer Cell. 2006 Jun;9(6):435-43.

153. Sampson N, Untergasser G, Plas E, Berger P. The ageing male reproductive tract. J Pathol. 2007 Jan;211(2):206-18. Review.

154. Santos AF, Huang H, Tindall DJ.The androgen receptor: a potential target for therapy of prostate cancer. Steroids. 2004 Feb;69(2):79-85. Review.

155. Sayner SL, Alexeyev M, Dessauer CW, Stevens T.Soluble adenylyl cyclase reveals the significance of cAMP compartmentation on pulmonary microvascular endothelial cell barrier. Circ Res. 2006 Mar 17;98(5):675-81. Epub 2006 Feb 9.

156. Schaeffer AJ, Wendel EF, Dunn JK, Grayhack JT. Prevalence and significance of prostatic inflammation. J Urol. 1981 Feb;125(2):215-9.

157. Scheckenbach KL, Losa D, Dudez T, Bacchetta M, O'Grady S, Crespin S, Chanson M. PGE2 Regulation of CFTR Activity and Air Surface Liquid Volume

Requires Gap Junctional Communication. Am J Respir Cell Mol Biol. 2010 Feb 18.

158. Shcheynikov N, Wang Y, Park M, Ko SB, Dorwart M, Naruse S, Thomas PJ, Muallem S.Coupling modes and stoichiometry of Cl-/HCO3- exchange by slc26a3 and slc26a6. J Gen Physiol. 2006 May;127(5):511-24. Epub 2006 Apr 10.

159. Sheldon CD, Hodson ME, Carpenter LM, Swerdlow AJ. A cohort study of cystic fibrosis and malignancy. Br J Cancer. 1993 Nov;68(5):1025-8.

160. Shen MR, Yang TP, Tang MJ. A novel function of Bcl-2 overexpression in regulatory volume decrease. Enhancing swelling-activated Ca(2+) entry and Cl(-) channel activity. J Biol Chem. 2002 May 3;277(18):15592-9. Epub 2002 Feb 22.

161. Shi XB, Tepper CG, White RW. MicroRNAs and prostate cancer. J Cell Mol Med. 2008 Sep-Oct;12(5A):1456-65. Epub 2008 Jul 8. Review.

162. Shi XB, Xue L, Yang J, Ma AH, Zhao J, Xu M, Tepper CG, Evans CP, Kung HJ, deVere White RW.An androgen-regulated miRNA suppresses Bak1 expression and induces androgen-independent growth of prostate cancer cells. Proc Natl Acad Sci U S A. 2007 Dec 11;104(50):19983-8. Epub 2007 Dec 3.

163. Skowron-zwarg M, Boland S, Caruso N, Coraux C, Marano F & Tournier F. Interleukin-13 interferes with CFTR and AQP5 expression and localization during human airway epithelial cell differentiation. Exp Cell Res. 2007, 313, 2695-2702

164. Snow DC, Shoskes DA. Pharmacotherapy of prostatitis. Expert Opin Pharmacother. 2010 Jun 23. 1-12

165. Southey MC, Batten L, Andersen CR, McCredie MR, Giles GG, Dite G, Hopper JL, Venter DJ. CFTR deltaF508 carrier status, risk of breast cancer before the age of 40 and histological grading in a population-based case-control study. Int J Cancer. 1998 Oct 23;79(5):487-9.

166. Stamey TA, Yang N, Hay AR, McNeal JE, Freiha FS, Redwine E. Prostate-specific antigen as a serum marker for adenocarcinoma of the prostate. N Engl J Med. 1987 Oct 8;317(15):909-16.

167. Strong TV, Boehm K, Collins FS.Localization of cystic fibrosis transmembrane conductance regulator mRNA in the human gastrointestinal tract by in situ hybridization. J Clin Invest. 1994 Jan; 93(1):347-54.

168. Swietach P, Patiar S, Supuran CT, Harris AL, Vaughan-Jones RD. The role of carbonic anhydrase 9 in regulating extracellular and intracellular ph in three-dimensional tumor cell growths. J Biol Chem. 2009 Jul 24;284(30):20299-310

169. Tajima Y, Okamura N, Sugita Y. The activating effects of bicarbonate on sperm motility and respiration at ejaculation. Biochim Biophys Acta 1987; 924(3): 519-529.

170. Taketa S, Nishi N, Takasuga H, Okutani T, Takenaka I, Wada F. Differences in growth requirements between epithelial and stromal cells derived from rat ventral prostate in serum-free primary culture. Prostate. 1990;17(3):207-18.

171. Tate S, MacGregor G, Davis M, Innes JA, Greening AP. Airways in cystic fibrosis are acidified: detection by exhaled breath condensate. Thorax. 2002 Nov;57(11):926-9.

172. Thebault S, Lemonnier L, Bidaux G, Flourakis M, Bavencoffe A, Gordienko D, Roudbaraki M, Delcourt P, Panchin Y, Shuba Y, Skryma R, Prevarskaya N. Novel role of cold/menthol-sensitive transient receptor potential melastatine family member 8 (TRPM8) in the activation of store-operated channels in LNCaP human prostate cancer epithelial cells. J Biol Chem. 2005 Nov 25;280(47):39423-35. Epub 2005 Sep 20.

173. Thin RN.The diagnosis of prostatitis: a review. Genitourin Med. 1991 Aug;67(4):279-83. Review.

174. Thomas JA, Buchsbaum RN, Zimniak A, Racker E.Intracellular pH measurements in Ehrlich ascites tumor cells utilizing spectroscopic probes generated in situ._Biochemistry. 1979, May 29;18(11):2210-8.

175. Thompson, K. D., S. Welykyj and M. C. Massa. Antibacterial activity of lidocaine in combination with a bicarbonate buffer. J Dermatol Surg Oncol.1993, 19(3): 216-20.

176. Trevani AS, Andonegui G, Giordano M, et al. Extracellular acidification induces human neutrophil activation. J Immunol 1999;162:4849-57.

177. Trezise AE, Linder CC, Grieger D, Thompson EW, Meunier H, Griswold MD, Buchwald M. CFTR expression is regulated during both the cycle of the seminiferous epithelium and the oestrous cycle of rodents. Nat Genet. 1993 Feb;3(2):157-64.

178. Vanden Abeele F, Shuba Y, Roudbaraki M, Lemonnier L, Vanoverberghe K, Mariot P, Skryma R & Prevarskaya N. Store-operated Ca2+ channels in prostate cancer epithelial cells: function, regulation, and role in carcinogenesis. Cell Calcium.2003, 33, 357-373.

179. Vermylen P, Roufosse C, Burny A, Verhest A, Bosschaerts T, Pastorekova S, Ninane V, Sculier JP. Carbonic anhydrase IX antigen differentiates between preneoplastic malignant lesions in non-small cell lung carcinoma. Eur Respir J. 1999 Oct;14(4):806-11.

180. Visconti PE, Stewart-Savage J, Blasco A, Battaglia L, Miranda P, Kopf GS, Tezon JG. Roles of bicarbonate, cAMP, and protein tyrosine phosphorylation on capacitation and the spontaneous acrosome reaction of hamster sperm. Biol Reprod 1999; 61: 76 84.

181. Wagenlehner FM, Weidner W, Sorgel F, Naber KG. The role of antibiotics in chronic bacterial prostatitis. Int J Antimicrob Agents 2005; 26:1–7.

182. Wai Kei Kwok,Ming-Tat Ling,Tak-Wing Lee, Tracy C.M. Lau,Chun Zhou, Xiaomeng Zhang, Chee Wai Chua, Kwok W. Chan,2Franky L. Chan, Carlotta Glackin, Yong-Chuan Wong, and Xianghong Wang. Up-regulation of TWIST in prostate cancer and its implication as a therapeutic target. Cancer Res June 15, 2005; 65: (12): 5153-5162

183. Walker J, Watson J, Holmes C, Edelman A, Banting G. Production and characterization of monoclonal and polyclonal antibodies to different regions of the cystic fibrosis transmembrane conductance regulator (CFTR): detection of immunologically related proteins. J Cell Sci, 1995 Jun: 108 (pt 6):2433-44

184. Wang XF, Zhou CX, Shi QX, Yuan YY, Yu MK, Ajonuma LC, Ho LS, Lo PS, Tsang LL, Liu Y, Lam SY, Chan LN, Zhao WC, Chung YW, Chan HC., Involvement of CFTR in uterine bicarbonate secretion and the fertilizing capacity of sperm. Nat Cell Biol. 2003 Oct;5(10):902-6. Epub 2003 Sep 28.

185. Warren N, Holmes JA, al-Jader L, West RR, Lewis DC, Padua RA. Frequency of carriers of cystic fibrosis gene among patients with myeloid malignancy and melanoma. BMJ. 1991 Mar 30;302(6779):760-1.

186. Wegrzyn G, Jakóbkiewicz-Banecka J, Gabig-Cimińska M, Piotrowska E, Narajczyk M, Kloska A, Malinowska M, Dziedzic D, Gołebiewska I, Moskot M, Wegrzyn A. Genistein: a natural isoflavone with a potential for treatment of genetic diseases. Biochem Soc Trans. 2010 Apr;38(2):695-701. Review.

187. Weidner W. Prostatitis--diagnostic criteria, classification of patients and recommendations for therapeutic trials. Infection. 1992;20 Suppl 3:S227-31; discussion S235.

188. Weinreich F, Wood PG, Riordan JR, Nagel G. Direct action of genistein on CFTR. Pflugers Arch. 1997 Aug;434(4):484-91.

189. Welsh MJ, Smith AE. Molecular mechanisms of CFTR chloride channel dysfunction in cystic fibrosis. Cell. 1993 Jul 2;73(7):1251-4. Review.

190. Wernert N, Seitz G, Achtstätter T.Immunohistochemical investigation of different cytokeratins and vimentin in the prostate from the fetal period up to adulthood and in prostate carcinoma. Pathol Res Pract. 1987 Oct;182(5):617-26.

191. White MA, Change in pH of expressed prostatic secretion during the course of prostatitis Proc. R. Soc. Med. 1975 Aug; 68(8),511-3

192. Wilschanski M, Durie PR. Patterns of GI disease in adulthood associated with mutations in the CFTR gene. Gut. 2007 Aug;56(8):1153-63. Epub 2007 Apr 19.

193. Winningham DG, Nemoy NJ, Stamey TA. Diffusion of antibiotics from plasma into prostatic fluid. Nature. 1968 Jul 13;219(5150):139-43.

194. Wolff H, Bezold G, Zebhauser M, Meurer M. Impact of clinically silent infammation on male genital tract organs as refected by biochemical markers in semen. J Androl 1991; 12: 331-4

195. Wong YC, Wang YZ. Growth factors and epithelial-stromal interactions in prostate cancer development. Int Rev Cytol. 2000;199:65-116.

196. Xie F, Garcia MA, Carlson AE, Schuh SM, Babcock DF, Jaiswal BS, Gossen JA, Esposito G, van Duin M, Conti M. Soluble adenylyl cyclase (sAC) is indispensable for sperm function and fertilization. Dev Biol. 2006 Aug 15;296(2):353-62. Epub 2006 Jun 7.

197. Xue Y, Smedts F, Debruyne FM, de la Rosette JJ, Schalken JA. Identification of intermediate cell types by keratin expression in the developing human prostate. Prostate. 1998 Mar 1;34(4):292-301.

198. Yang J, Mani SA, Donaher JL, Ramaswamy S, Itzykson RA, Come C, Savagner P, Gitelman I, Richardson A, Weinberg RA. Twist, a master regulator of morphogenesis, plays an essential role in tumor metastasis. Cell. 2004 Jun 25;117(7):927-39.

199. Yang MH, Wu KJ.TWIST activation by hypoxia inducible factor-1 (HIF-1): implications in metastasis and development. Cell Cycle. 2008 Jul 15;7(14):2090-6. Epub 2008 May 21.

200. Zhan Q, Jin S, Ng B, Plisket J, Shangary S, Rathi A, Brown KD, Baskaran R.Caspase-3 mediated cleavage of BRCA1 during UV-induced apoptosis. Oncogene. 2002 Aug 8;21(34):5335-45.

201. Zheng W, Kuhlicke J, Jäckel K, Eltzschig HK, Singh A, Sjöblom M, Riederer B, Weinhold C, Seidler U, Colgan SP, Karhausen J. Hypoxia inducible factor-1 (HIF-1)-mediated repression of cystic fibrosis transmembrane conductance regulator (CFTR) in the intestinal epithelium. FASEB J. 2009 Jan;23(1):204-13. Epub 2008 Sep 8.

202. Zhou CX, Wang XF, Chan HC. Bicarbonate secretion by the female reproductive tract and its impact on sperm fertilizing capacity. Sheng Li Xue Bao. 2005 Apr 25;57(2):115-24.

203. Zielenski J, Tsui LC. Cystic fibrosis: genotypic and phenotypic variations. Annu Rev Genet. 1995;29:777-807. Review.

204. Zumoff B, Strain GW, Kream J, O'Connor J, Rosenfeld RS, Levin J, Fukushima DK. Age variation of the 24-hour mean plasma concentrations of androgens, estrogens, and gonadotropins in normal adult men. J Clin Endocrinol Metab. 1982 Mar;54(3):534-8